Cone metrics on the sphere and Livné's lattices

John R. Parker
Department of Mathematical Sciences,
University of Durham,
South Road, Durham DH1 3LE,
England.
e-mail: J.R.Parker@durham.ac.uk

December 21, 2005

Abstract

We give an explicit construction of a family of lattices in $\mathrm{PU}(1,2)$ originally constructed by Livné. Following Thurston, we construct these lattices as the modular group of certain Euclidean cone metrics on the sphere. We give connections between these groups and other groups of complex hyperbolic isometries.

1 Introduction

In his thesis [12] Ron Livné constructed an interesting family of lattices in $\mathrm{PU}(1,2)$. To do this, Livné used techniques from algebraic geometry; see also Section 3.2 of Hirzebruch [9]. Livné's lattices are contained in Mostow's list [15] of monodromy groups of hypergeometric functions; see Chapter 16 of Deligne and Mostow [3]. An alternative construction of these monodromy groups was given by Thurston [21] who described them as the modular group of certain Euclidean cone-metrics on the sphere; see also Weber [22]. Livné's groups have many remarkable properties. For example, Kapovich has shown [11] that certain (well chosen) subgroups of Livné's groups are finitely generated but infinitely presented. Also, Livné's groups give equality in the version of Jørgensen's inequality for groups with boundary elliptic elements; see Section 5 of [10]. This indicates that the quotient of complex hyperbolic 2-space by Livné's groups are orbifolds of small volume; see [18] where Sauter computes volumes of these orbifolds.

In this paper we use Thurston's method to give a geometrical construction of Livné's lattices. Namely, we consider Euclidean cone metrics on the sphere with five cone points and certain prescribed cone angles, Section 2. These cone angles correspond to Mostow's ball 5-tuples. We may cut our sphere along a piecewise linear path running through the cone points to obtain a Euclidean polygon with a certain set of side identifications. The key observation of Thurston is that the Euclidean area of such a polygon (that is the area of the sphere with the cone metric) gives rise to a Hermitian form of signature $(1,2)$. Thus such a polygon corresponds to a positive vector in $\mathbb{C}^{1,2}$. Also, any automorphism of the cone metric (or the polygon) gives rise to a unitary matrix in $\mathrm{U}(1,2)$. Each similarity class of cone metrics corresponds to a positive point in $\mathbb{P}(\mathbb{C}^{1,2})$, that is a point in complex hyperbolic space. Automorphisms of similarity classes correspond to complex hyperbolic isometries in $\mathrm{PU}(1,2)$. We construct two kinds of automorphism. The first arises from changing the piecewise linear cut to obtain different polygons corresponding to the same cone metric. This is done by interchanging two cone points with the same cone angle. Such an automorphism could be realised by performing a Dehn twist along a simple closed curve through our two cone points and which does not separate the other three cone points. The second automorphism is an example of one of Thurston's butterfly moves. As described in [21], the moduli space of cone metrics does not form a complete subset of complex hyperbolic space. To get around this, Thurston uses formal automorphisms, which he calls butterfly moves, to extend the moduli space to points corresponding to non-simple polygons which are not fundamental polygons for a cone metric. We consider the group generated by these automorphisms which, a priori, are only subgroups of Livné's groups.

We go on to consider how the automorphisms described above act on complex hyperbolic space. In particular, we construct a complex hyperbolic polyhedron D, Section 3, and use Poincaré's polyhedron theorem to show that our automorphisms generate a lattice with fundamental domain D, Section 4. Poincaré's theorem also gives a presentation for the groups and we show that this presentation is the same as that given by Livné in Lemma 3 on page 108 of [12]. Thus the groups are isomorphic and so, by Mostow rigidity, they are conjugate. As is well known, there are no totally geodesic real hypersurfaces in complex hyperbolic space and so, when constructing polyhedra, one has to make a choice of hypersurfaces containing the sides. Our polyhedron D has eight sides, each of which is contained in a bisector. Thus it is remarkably simple (compare [4], [7], [19]).

In the final sections we give further links between Livné's groups and other interesting groups, namely the Eisenstein-Picard modular group [7], Mostow groups [13], [4] and triangle groups [20], [17]. In particular, Livné groups have (non-faithful) triangle groups as normal subgroups. These are either a lattice (compare [5]) or geometrically infinite, Corollary 7.4. Moreover, these triangle groups give a counterexample to a conjecture of Schwartz [20], Proposition 7.5. The corresponding quotient groups are faithful triangle groups.

There are two major aspects of this paper that are new. First, Thurston's construction of complex hyperbolic lattices has not previously been combined with Poincaré's polyhedron theorem in a completely explicit way, although this is what is going on behind the scenes in Thurston's work. It should be possible to extend the construction of this paper to many, possibly to all, the groups on the Mostow-Thurston list. Secondly, no fundamental domain for the Livné groups was known previously, and hence no explicit analysis of the geometry of their action on complex hyperbolic space was possible. This is important for two reasons. First, they are a particularly interesting family of lattices and, secondly, they provide a family of lattices with fairly simple explicit fundamental polyhedra. Since there are very few examples of complex hyperbolic lattices known, and even fewer that have be analysed geometrically, this will aid the formulation of general results about complex hyperbolic lattices. Furthermore, calculations in complex hyperbolic geometry have a tendency to become extremely complicated, which means explicit constructions are rather difficult to obtain. Thus it is quite remarkable that the polyhedra we construct are so simple.

Part of the novelty of this paper is to provide new proofs of results that were known previously. Therefore we keep our treatment as self contained as possible. We choose to give simple, explicit geometrical arguments wherever possible, and we are able to make a good choice of coordinates in order to do so. However, sometimes we are forced to resort to algebraic manipulation and this somewhat obscures the geometry. We also try to emphasise the connection with and the links between earlier results. There are further links that we could have explored, for example from our description we can demonstrate that all the Livné groups are arithmetic except the one with $n = 9$ which is not arithmetic. We shall give the details elsewhere and not discuss arithmeticity here.

Acknowledgements: While writing this paper I have had useful discussions with Martin Deraux, Elisha Falbel, Bill Goldman, Nikolay Gusevskii, Norbert Peyerimhoff and Rich Schwartz. I would like to thank each of them for the different kinds of help they have given me. I would also like to thank the referee for his/her many helpful and insightful comments.

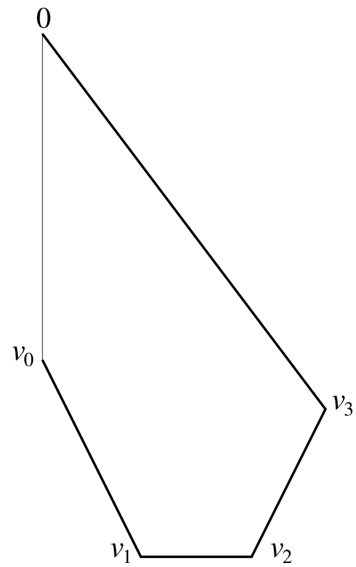

Figure 1: *The doubled pentagon. Cutting along the heavy line gives the octagon in Figure 2.*

2 Cone metrics on the sphere

A cone singularity of a manifold is an isolated point where the total angle is different from 2π. This angle is called the *cone angle*. A Euclidean cone metric on the sphere is a metric that is locally isometric to the standard metric on $\mathbb{R}^2$ but with finitely many cone singularities. For example, a cube is a Euclidean cone metric on the sphere with eight cone singularities, each with cone angle $3\pi/2$. A simple family of examples of Euclidean cone metrics on the sphere is obtained by taking two copies of the same plane Euclidean polygon and identifying them along their boundary. This is called the *double* of the polygon. The cone angles are then twice the corresponding internal angles of the polygon. We will be interested in what happens when we fix certain cone angles, but allow the cone singularities to move around the sphere. For example, the double of a square (a "pillow case") and a regular tetrahedron both have four cone singularities, each with cone angle π. By moving the cone singularities around, one may transform one of these into the other.

2.1 A family of Euclidean cone metrics

In this section we take a Euclidean cone metric on the sphere with five cone points with cone angles $(2\pi-\theta,\ \pi+\theta,\ \pi+\theta,\ \pi+\theta,\ \pi-2\theta)$ where $\theta = 2\pi/n$. By cutting the sphere open along a path through the five cone points we obtain a Euclidean polygon Π. Conversely, after gluing the sides of Π together, we can reconstruct our cone metric on the sphere. We give an explicit parametrisation of such polygons by three complex numbers and we show that, in terms of these parameters, the area of the polygon gives a Hermitian form of signature $(1,2)$. Different ways of doing this are described in Thurston [21] and Weber [22]. Our method is different from theirs.

For simplicity, we first consider the situation where the cone manifold is the double of a Euclidean pentagon. We cut this pentagon open along four of its sides; see Figure 1. The first point on our cut is the cone point 0 with angle $\pi-2\theta$, then we go around the boundary of the pentagon through the three cone points v_3, v_2 and v_1 with cone angle $\pi+\theta$ and finish at the cone point v_0 with cone angle $2\pi-\theta$. Cutting the doubled pentagon open in this way yields an octagon, which we call Π. This octagon has a reflection symmetry. Using this symmetry to identify boundary points

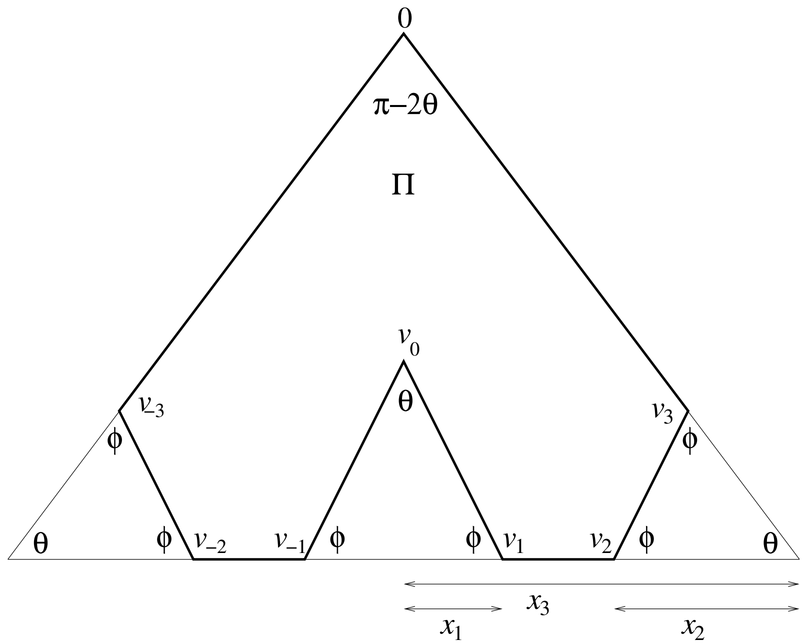

Figure 2: *The polygon* Π *with real parameters* x_1, x_2, x_3. *Here* $\phi = (\pi - \theta)/2$.

exactly reconstructs the doubled pentagon with which we began.

We now show how to construct Π geometrically in terms of three real parameters x_1, x_2 and x_3; see Figure 2 which should be compare to Figure 2 of [21]. Let x_1, x_2 and x_3 be positive real numbers. Let T_1, T_2 and T_3 be three isosceles triangles. The triangle T_1 has base length $2x_1$ and apex angle θ; T_2 has two sides of length x_2 and apex angle θ and T_3 has base length $2x_3$ and two internal angles θ. We form an octagon Π by first removing from T_3 a copy of T_1 whose base is centred on the base of T_3 and then removing two copies of T_2 whose apexes lie in the base corners of T_3; see Figure 2. The octagon is simple (that is the interiors of its edges are disjoint) provided T_1 and T_2 are disjoint and their interiors are contained in the interior of T_3. In other words, provided $x_1 + x_2 < x_3$ and $x_1 < x_3(1 - \cos\theta)/\cos\theta = x_3 \tan\theta \tan(\theta/2)$.

We now make this precise by adopting coordinates as follows. We place T_3 in the complex plane so that its apex is at the origin and its base is parallel to the real axis. The vertices of the triangles are given in the following table (where T_2' is the second copy of T_2):

Triangle	Vertices		
T_1 :	$x_1 i \cot(\theta/2) - x_3 i \tan(\theta)$	$x_1 - x_3 i \tan\theta$	$-x_1 - x_3 i \tan\theta$
T_2 :	$-x_2(\cos\theta - i\sin\theta) + x_3(1 - i\tan\theta)$	$x_3(1 - i\tan\theta)$	$-x_2 + x_3(1 - i\tan\theta)$
T_2' :	$x_2(\cos\theta + i\sin\theta) - x_3(1 + i\tan\theta)$	$-x_3(1 + i\tan\theta)$	$x_2 - x_3(1 + i\tan\theta)$
T_3 :	0	$x_3(1 - i\tan\theta)$	$-x_3(1 + i\tan\theta)$

The resulting octagon is preserved by reflection in the imaginary axis and we label its vertices so that this reflection interchanges v_j and v_{-j}. Moreover, gluing points of the boundary of Π to their image under this reflection reconstructs the doubled pentagon we started with. The vertices are given in the following table; see Figure 2:

$v_0 = x_1 i \cot(\theta/2) - x_3 i \tan\theta$,	0,
$v_1 = x_1 - x_3 i \tan\theta$,	$v_{-1} = -x_1 - x_3 i \tan\theta$,
$v_2 = -x_2 + x_3(1 - i\tan\theta)$,	$v_{-2} = x_2 - x_3(1 + i\tan\theta)$,
$v_3 = -x_2(\cos\theta - i\sin\theta) + x_3(1 - i\tan\theta)$,	$v_{-3} = x_2(\cos\theta + i\sin\theta) - x_3(1 + i\tan\theta)$.

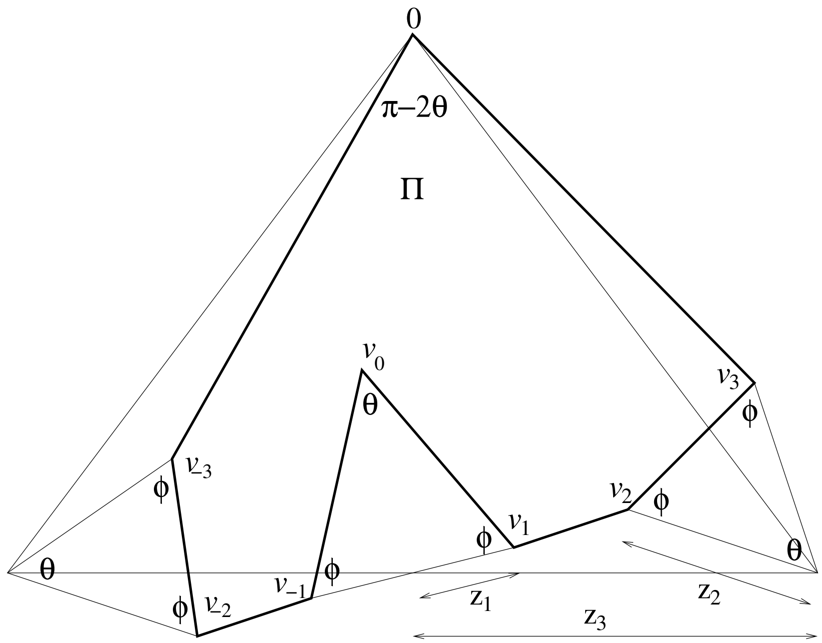

Figure 3: *The polygon* Π *with complex parameters* z_1, z_2, z_3. *Again* $\phi = (\pi - \theta)/2$.

The area of Π may be obtained by subtracting the area of T_1 and twice the area of T_2 from the area of T_3 (compare equation (1) of [21]). The areas of the triangles are

$$\begin{aligned} Area(T_1) &= x_1 x_1 \cot(\theta/2) = \frac{\sin\theta}{1-\cos\theta} {x_1}^2, \\ Area(T_2) &= x_2 \cos(\theta/2) x_2 \sin(\theta/2) = \frac{\sin\theta}{2} {x_2}^2, \\ Area(T_3) &= x_3 x_3 \tan\theta = \frac{\sin\theta}{\cos\theta} {x_3}^2. \end{aligned}$$

Hence

$$Area(\Pi) = \sin\theta \left(\frac{-1}{1-\cos\theta} {x_1}^2 - {x_2}^2 + \frac{1}{\cos\theta} {x_3}^2 \right).$$

We may now allow the variables x_j to be complex and we write them as z_j. We still have triangles T_1, T_2 and T_3 but now $2z_1$ and $2z_3$ are vectors along the bases of T_1 and T_3 respectively, and z_2 is a vector along a side of T_2. Once again, we place the centre of the base of T_1 in the centre of the base of T_3 and the apexes of T_2 and T_2' at the base vertices of T_3. However, when z_1 and z_2 are not real multiples of z_3 then the corresponding edges no longer line up. The vertices of the resulting octagon are the corresponding vertices of the triangles and are still labelled v_j, but in general there will no longer be any edges contained in edges of T_3; see Figure 3. The vertices are now:

$v_0 = z_1 i \cot(\theta/2) - z_3 i \tan\theta$,	0,
$v_1 = z_1 - z_3 i \tan(\theta)$,	$v_{-1} = -z_1 - z_3 i \tan\theta$,
$v_2 = -z_2 + z_3(1 - i\tan\theta)$,	$v_{-2} = z_2 - z_3(1 + i\tan\theta)$,
$v_3 = -z_2(\cos\theta - i\sin\theta) + z_3(1 - i\tan\theta)$,	$v_{-3} = z_2(\cos\theta + i\sin\theta) - z_3(1 + i\tan\theta)$.

We can use cut and paste on this octagon (see Figure 3) to see that it has the same area as the

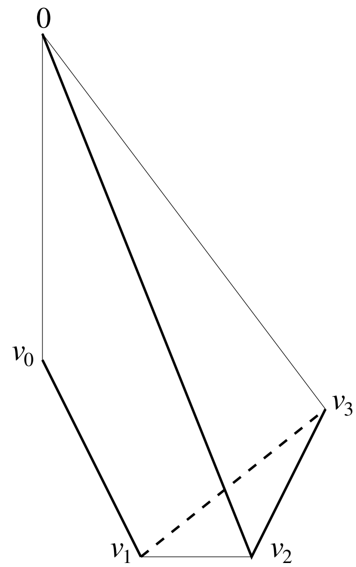

Figure 4: *The doubled pentagon from Figure 1 with the new cut associated to the move R_1.*

triangle T_3 less the area of one copy of T_1 and two copies of T_2. Thus it has area

$$Area(\Pi) = \sin\theta \left(\frac{-1}{1-\cos\theta}|z_1|^2 - |z_2|^2 + \frac{1}{\cos\theta}|z_3|^2 \right). \tag{1}$$

The area gives a Hermitian form of signature $(1, 2)$ on $\mathbb{C}^3$. This is the key observation that leads to a complex hyperbolic structure on the moduli space of such polygons. This is a special case of Proposition 3.3 of Thurston [21] (see also Lemma 4.3 of [22]).

There is a natural way to construct a particular Euclidean cone manifold from Π. Consider the following edge pairing maps of Π. These maps σ_j will be orientation preserving Euclidean isometries and so are completely determined on each edge by their value on the vertices v_j, v_{j+1}. The maps are

$$\begin{aligned} \sigma_1(0) &= 0, & \sigma_1(v_3) &= v_{-3}; & \sigma_2(v_3) &= v_{-3}, & \sigma_1(v_2) &= v_{-2}; \\ \sigma_3(v_2) &= v_{-2}, & \sigma_3(v_1) &= v_{-1}; & \sigma_4(v_1) &= v_{-1}, & \sigma_4(v_0) &= v_0. \end{aligned}$$

Let M be the Euclidean cone manifold given by identifying the edges of Π using the maps σ_j. It is clear that M is homeomorphic to a sphere and has five cone points corresponding to 0, v_0, $v_{\pm 1}$, $v_{\pm 2}$, $v_{\pm 3}$ with cone angles $\pi - 2\theta$, $2\pi - \theta$, $\pi + \theta$, $\pi + \theta$, $\pi + \theta$ respectively. These are examples of the cone manifolds studied by Thurston in [21] and the cone angles correspond to the ball 5-tuples studied by Mostow [15].

2.2 Moves on the cone structure

In the spirit of [21], we define various "moves" on such polygons. First, observe that complex conjugating all three of z_1, z_2 and z_3 is the same as reflecting in the imaginary axis. (If z_3 is real, this line passes through 0 and the midpoint of the base of T_3.) Thus complex conjugation is an automorphism.

Other automorphisms may be defined as follows. The cone manifold has five cone points, one each with cone angle $\pi - 2\theta$ and $2\pi - \theta$, corresponding to the vertex 0 and the vertex v_0 respectively,

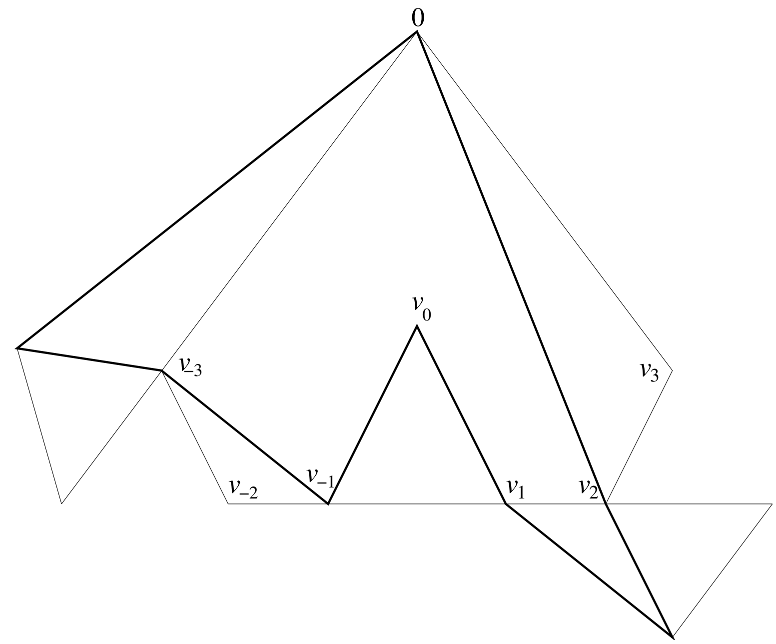

Figure 5: *The move corresponding to R_1 applied to the polygon from Figure 2.*

and three with cone angle $\pi + \theta$, corresponding to identifying $v_{\pm 1}$, $v_{\pm 2}$, $v_{\pm 3}$ respectively. When we make our cut in the cone manifold there is no canonical ordering of the three cone points with angle $\pi + \theta$ and so our first moves on the cone structure correspond to taking these cone points in a different order when making the cut.

First, there is a move R_1 fixing 0, v_0 and $v_{\pm 1}$ and interchanging the vertices $v_{\pm 2}$ and $v_{\pm 3}$. From the mapping class point of view, this is a Dehn twist about a simple closed curve on the sphere that passes through these two cone points and does not separate the others. When cutting open the cone manifold to form the polygon Π one must now cut from 0 directly to $v_{\pm 2}$, then to $v_{\pm 3}$, and then on to $v_{\pm 1}$ and v_0 as before; see Figure 4. After we make this cut we can open the pentagon out to make the octagon, shown in Figure 5.

We now show how to construct the new octagon from the old one by cut and paste. First, the cut goes from 0 directly to v_2. Hence the triangle 0, v_2, v_3 must be glued back on along the edge 0, v_{-3} according to the side identification σ_1. Likewise, the triangle v_{-1}, v_{-2}, v_{-3} must be glued by σ_3^{-1} to the side v_1, v_2. This is illustrated in Figure 5.

Having found the new polygon we must find the new parameters w_1, w_2, w_3. It is not hard to see that the large triangle T_3 corresponding to z_3 is unchanged, as is the small central triangle T_1 corresponding to z_1. However, the triangles T_2 and T_2' have each been rotated anti-clockwise through an angle θ about their apex. Therefore the new coordinates are z_1, $z_2 e^{i\theta}$ and z_3. The new variables are given in terms of the old by the matrix

$$R_1 = \begin{bmatrix} 1 & 0 & 0 \\ 0 & e^{i\theta} & 0 \\ 0 & 0 & 1 \end{bmatrix}. \qquad (2)$$

Observe that complex conjugation followed by R_1 is an involution.

We now demonstrate an alternative way to find these new coordinates by analysing the vertices.

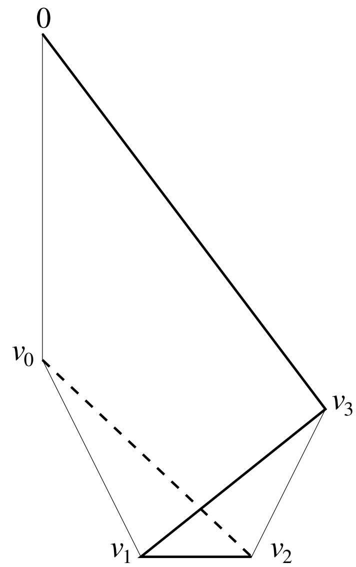

Figure 6: *The doubled pentagon from Figure 1 with the new cut associated to the move* R_2*.*

We write the new vertices as v_j'. Then:

$$\begin{aligned} w_1 i\cot(\theta/2) - w_3 i\tan\theta &= v_0' = v_0 = z_1 i\cot(\theta/2) - z_3 i\tan\theta, \\ w_1 - w_3 i\tan\theta &= v_1' = v_1 = z_1 - z_3 i\tan\theta, \\ -w_2(\cos\theta - i\sin\theta) + w_3(1 - i\tan\theta) &= v_3' = v_2 = -z_2 + z_3(1 - i\tan\theta). \end{aligned}$$

These equations may be solved to give:

$$w_1 = z_1, \qquad w_2 = e^{i\theta} z_2, \qquad w_3 = z_3.$$

Secondly, there is a move R_2 fixing 0, v_0 and v_3 but interchanging $v_{\pm 1}$ and $v_{\pm 2}$. Again this corresponds to a Dehn twist along a simple closed curve through $v_{\pm 1}$ and $v_{\pm 2}$ that does not separate the other cone points. This time we obtain the octagon Π by cutting from 0 to $v_{\pm 3}$, then to $v_{\pm 1}$, $v_{\pm 2}$ and finally to v_0; see Figure 6.

The cut and paste procedure is similar to that giving R_1. The slit now goes from 0 to v_3 and then directly to v_1. Hence the triangle v_1, v_2, v_3 must be glued by σ_2 to v_{-2}, v_{-3}. Likewise, the triangle v_0, v_{-1}, v_{-2} is glued using σ_4^{-1} to v_0, v_1. This is illustrated in Figure 7. It can be seen that all three triangles have been changed and we must be careful when finding w_1, w_2, w_3.

The easiest way to find the new coordinates is to analyse the vertices:

$$\begin{aligned} w_1 i\cot(\theta/2) - w_3 i\tan\theta &= v_0' = v_0 = z_1 i\cot(\theta/2) - z_3 i\tan\theta, \\ -w_2 + w_3(1 - i\tan\theta) &= v_2' = v_1 = z_1 - z_3 i\tan\theta, \\ -w_2(\cos\theta - i\sin\theta) + w_3(1 - i\tan\theta) &= v_3' = v_3 = -z_2(\cos\theta - i\sin\theta) + z_3(1 - i\tan\theta). \end{aligned}$$

Solving for w_1, w_2 and w_3 we find that

$$\begin{aligned} (1-\cos\theta + i\sin\theta)w_1 &= i\sin\theta\, z_1 - (1-\cos\theta)z_2 + (1-\cos\theta)z_3, \\ (1-\cos\theta + i\sin\theta)w_2 &= -z_1 - (\cos\theta - i\sin\theta)z_2 + z_3, \\ (1-\cos\theta + i\sin\theta)w_3 &= -\cos\theta\, z_1 - \cos\theta\, z_2 + (1 + i\sin\theta)z_3. \end{aligned}$$

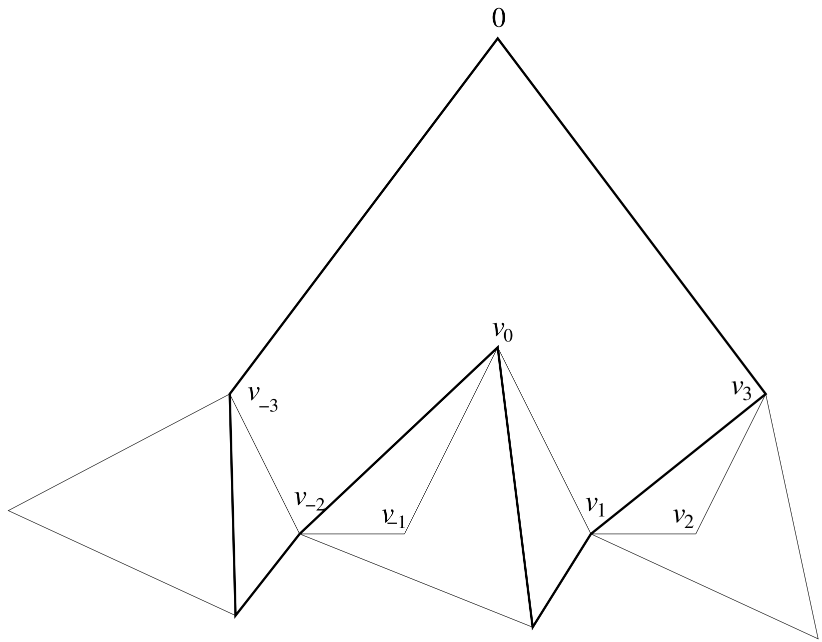

Figure 7: *The move corresponding to R_2 applied to the polygon from Figure 2.*

The new variables are given in terms of the old by the matrix

$$R_2 = \frac{1}{1-\cos\theta + i\sin\theta}\begin{bmatrix} i\sin\theta & -1+\cos\theta & 1-\cos\theta \\ -1 & -e^{-i\theta} & 1 \\ -\cos\theta & -\cos\theta & 1+i\sin\theta \end{bmatrix}. \tag{3}$$

Note that $\det(R_2) = e^{i\theta}$ and that complex conjugation followed by R_2 is an involution.

We remark that R_1 and R_2 each correspond to interchanging a pair of cone points and so the corresponding mapping class on the five times punctured sphere is a Dehn twist along a curve through these two points. This leads us to expect that R_1 and R_2 should satisfy the braid relation $R_1R_2R_1 = R_2R_1R_2$, and in Theorem 5.1 (iii) we verify that this is indeed the case.

We show in the next section that, after projectivising, the points $(z_1, z_2, z_3) \in \mathbb{C}^3$ corresponding to simple polygons form a non-complete region inside complex hyperbolic space; compare Thurston [21]. In order to extend this region to the whole of complex hyperbolic space we must consider triples (z_1, z_2, z_3) that do not correspond to simple polygons, but which formally share many properties with those that do. Following Thurston, we allow the boundary of Π to intersect itself and keep track of a signed area. It turns out that we only need to consider one more move on the cone structure, denoted I_1, and following Thurston we call it a *butterfly move*; see Figure 5 of [21] for an explanation of the name. Specifically, the automorphism I_1 is constructed by rotating the triangle T_1 through angle π. This is equivalent to sending z_1 to $-z_1$ while keeping z_2 and z_3 the same. That is I_1 is given by applying the matrix:

$$I_1 = \begin{bmatrix} -1 & 0 & 0 \\ 0 & 1 & 0 \\ 0 & 0 & 1 \end{bmatrix}. \tag{4}$$

Observe that I_1 is an involution as is complex conjugation followed by I_1. Moreover, I_1 commutes with R_1. This may be seen either by considering the matrices or by the geometrical action on the polygons.

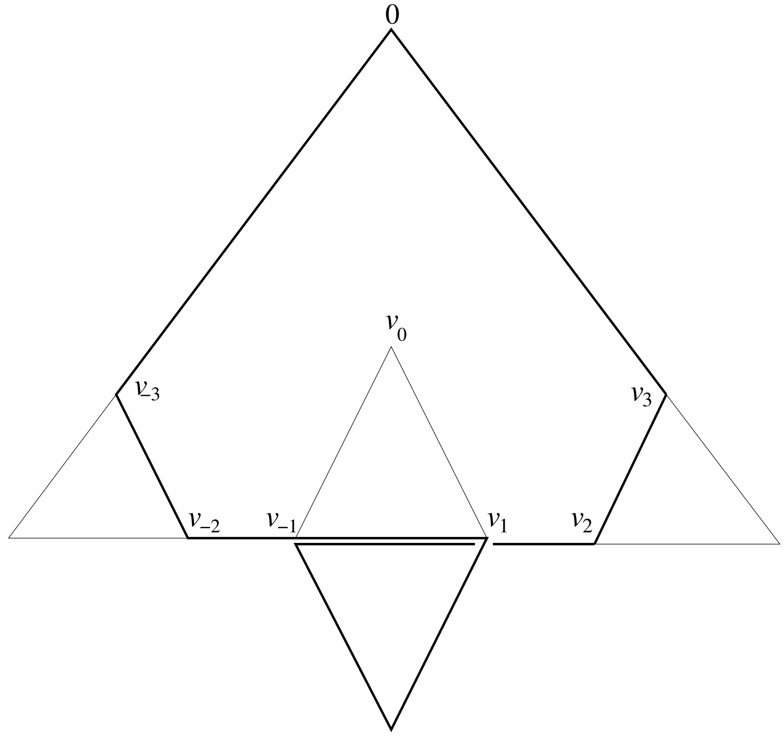

Figure 8: *The butterfly move corresponding to I_1 applied to the polygon from Figure 2.*

As indicated in Figure 8, making z_1 real and negative forces the triangle T_1 to points downwards and makes the boundary of Π intersect itself. When traversing the boundary of Π we must now go around ∂T_1 with the opposite orientation from that which we use on ∂T_3. Hence the area of T_1 is now negative. Therefore the area of the new polygon is still given by (1).

All three of these moves preserve the (signed) area of Π. In other words, from (1) the matrices are unitary with respect to the Hermitian form given by $\langle \mathbf{z}, \mathbf{w} \rangle = \mathbf{w}^* H \mathbf{z}$ where $\mathbf{w}^*$ is the Hermitian conjugate of $\mathbf{w}$ and H is given by

$$H = -\sin\theta \begin{bmatrix} 1/(1-\cos\theta) & 0 & 0 \\ 0 & 1 & 0 \\ 0 & 0 & -1/\cos\theta \end{bmatrix}. \tag{5}$$

We are going to consider the group of unitary matrices Γ generated by these three moves, namely

$$\Gamma = \langle R_1,\, R_2,\, I_1 \rangle$$

where $\theta = 2\pi/n$ for $n = 5, 6, 7, 8, 9, 10, 12$ and 18. For these values of n we will show that the group Γ is discrete and is isomorphic to one of the *Livné groups*. When $n = 4$ the group is elementary and for all other values of $n \geq 5$ not on this list the cone angles violate Mostow's criterion, hence these groups are not discrete. In fact, for all such n the group Γ may be shown to be non-discrete using Jørgensen's inequality; see [10]. We will give the details elsewhere. Also observe that, since complex conjugation followed by any of R_1, R_2, I_1 is an involution, Γ is an index two subgroup of a group containing antiholomorphic automorphisms.

Finally, we remark that by examining the cone angles, we see that Γ is in the list of 94 groups constructed by Mostow, pages 584–586 of [15], and Thurston, pages 548–549 of [21]. For reference we give the corresponding numbers in their respective lists

n	5	6	7	8	9	10	12	18
Mostow	58	49	76	53	80	57	62	79
Thurston	52	40	76	45	80	49	57	79

3 The polyhedron D

In this section we show how that collection of cone metrics on the sphere, or equivalently polygons Π, may be parametrised by a subset of complex hyperbolic space. It will immediately follow that the automorphisms act as complex hyperbolic isometries. It is really the geometry of the action of these isometries that will be of most interest to us. We construct a polyhedron D in complex hyperbolic space whose sides are contained in bisectors and whose vertices correspond to certain degenerate cone metrics obtained either from the collision of three cone points or from the collision of two pairs of cone points. Once we have constructed D we will cease to be interested in the cone metrics but, rather, will concentrate on the complex hyperbolic geometry of the polyhedron. Specifically, we will analyse how the sides of D intersect. Some of the more routine calculations involved in this are relegated to the appendices. There is a difference between the three cases $n = 5$, $n = 6$ and $n \geq 7$. In this section we concentrate on the case $n \geq 7$ and in Section 6 we discuss the other two cases.

3.1 Complex hyperbolic space

From now on we concentrate on those points z_1, z_2, z_3 for which the area of Π is positive. Since the area (1) is given in terms of the Hermitian form H from (5), the area of Π being positive is equivalent to:

$$-\sin\theta \begin{bmatrix} \overline{z}_1 & \overline{z}_2 & \overline{z}_3 \end{bmatrix} \begin{bmatrix} 1/(1-\cos\theta) & 0 & 0 \\ 0 & 1 & 0 \\ 0 & 0 & -1/\cos\theta \end{bmatrix} \begin{bmatrix} z_1 \\ z_2 \\ z_3 \end{bmatrix} = \mathbf{z}^* H \mathbf{z} = \langle \mathbf{z}, \mathbf{z} \rangle > 0.$$

Multiplying each z_j by a non-zero complex number μ preserves the the polygon up to similarity and scales the area by $|\mu|^2 > 0$. Thus it is natural to consider similarity classes of polygons by applying the canonical projection from $\mathbb{C}^3$ to $\mathbb{CP}^2$. Since the area is positive we must have $z_3 \neq 0$ and we may take a section by restricting to the affine plane where $z_3 = 1$.

Thus, in what follows we consider complex hyperbolic space to be those points in $\mathbb{CP}^2$ for which the Hermitian form H given by (5) is positive. That is:

$$\mathbf{H}^2_{\mathbb{C}} = \left\{ \mathbf{z} = \begin{bmatrix} z_1 \\ z_2 \\ 1 \end{bmatrix} \ : \ \langle \mathbf{z}, \mathbf{z} \rangle = \mathbf{z}^* H \mathbf{z} = \frac{-|z_1|^2 \sin\theta}{1-\cos\theta} - |z_2|^2 \sin\theta + \frac{\sin\theta}{\cos\theta} > 0 \right\}. \tag{6}$$

We have already seen that the moves on the the cone structure I_1, R_1, R_2 and their products correspond to unitary matrices with respect to the Hermitian form H. These act projectively on $\mathbf{H}^2_{\mathbb{C}}$, and so lie in $\mathrm{PU}(1,2)$, the holomorphic isometry group of $\mathbf{H}^2_{\mathbb{C}}$. Likewise complex conjugation is an antiholomorphic isometry of $\mathbf{H}^2_{\mathbb{C}}$.

It will be convenient to introduce a second set of coordinates on $\mathbf{H}^2_{\mathbb{C}}$. Just as for the groups considered in [7] and [19], there is a particular element of the group, which we call P, that will play an important role in our construction (it is also called P in [7] and is called K in [19]). In particular P is a side pairing of our fundamental domain D and images of D under powers of P form a cylinder or a torus with a repeating pattern of faces. Algebraically, this corresponds to the fact that I_1 and its conjugates by powers of P generate a triangle group; see Section 7 and, in particular compare Lemma 7.1 with Lemma 3.1 of [19]. Our second set of coordinates will be the preimage of the first under P. To this end we define $P = R_1R_2$, and we write it as a matrix:

$$P = \frac{1}{1-\cos\theta + i\sin\theta}\begin{bmatrix} i\sin\theta & -(1-\cos\theta) & 1-\cos\theta \\ -e^{i\theta} & -1 & e^{i\theta} \\ -\cos\theta & -\cos\theta & 1+i\sin\theta \end{bmatrix}. \tag{7}$$

We will want to keep track of coordinates, which we denote by $\mathbf{w}$, given by

$$\mathbf{w} = \begin{bmatrix} w_1 \\ w_2 \\ 1 \end{bmatrix} = \left[P^{-1}(\mathbf{z})\right] = \frac{1}{1-\cos\theta - i\sin\theta}\begin{bmatrix} -i\sin\theta & -(1-\cos\theta)e^{-i\theta} & 1-\cos\theta \\ -1 & -1 & 1 \\ -\cos\theta & -\cos\theta e^{-i\theta} & 1-i\sin\theta \end{bmatrix}\begin{bmatrix} z_1 \\ z_2 \\ 1 \end{bmatrix}. \tag{8}$$

In other words

$$w_1 = \frac{-z_1 i\sin\theta - z_2e^{-i\theta}(1-\cos\theta) + (1-\cos\theta)}{-z_1\cos\theta - z_2e^{-i\theta}\cos\theta + 1 - i\sin\theta}, \tag{9}$$

$$w_2 = \frac{-z_1 - z_2 + 1}{-z_1\cos\theta - z_2e^{-i\theta}\cos\theta + 1 - i\sin\theta}. \tag{10}$$

Likewise

$$\mathbf{z} = \begin{bmatrix} z_1 \\ z_2 \\ 1 \end{bmatrix} = \left[P(\mathbf{w})\right] = \frac{1}{1-\cos\theta + i\sin\theta}\begin{bmatrix} i\sin\theta & -(1-\cos\theta) & 1-\cos\theta \\ -e^{i\theta} & -1 & e^{i\theta} \\ -\cos\theta & -\cos\theta & 1+i\sin\theta \end{bmatrix}\begin{bmatrix} w_1 \\ w_2 \\ 1 \end{bmatrix}.$$

Hence

$$z_1 = \frac{w_1 i\sin\theta - w_2(1-\cos\theta) + (1-\cos\theta)}{-w_1\cos\theta - w_2\cos\theta + 1 + i\sin\theta}, \tag{11}$$

$$z_2 = \frac{-w_1e^{i\theta} - w_2 + e^{i\theta}}{-w_1\cos\theta - w_2\cos\theta + 1 + i\sin\theta}. \tag{12}$$

The reason for keeping track of two sets of coordinates is that it gives a simple description of the polyhedron D in terms of the arguments of z_1, z_2, w_1 and w_2; see (17) below.

3.2 The vertices of D

We identify some distinguished points of $\mathbf{H}^2_{\mathbb{C}}$ which will be the vertices of our polyhedron. Writing $\mathbf{w} = P^{-1}(\mathbf{z})$ as in (8), it will be useful to have our points in $\mathbf{w}$-coordinates as well as $\mathbf{z}$-coordinates. In all cases these distinguished cone structures are obtained by letting some of the cone points approach each other until in the limit they coalesce, and hence result in a new cone point. The complementary angle of this new cone point (that is 2π minus the cone angle) is the sum of the complementary angles of the cone points that have coalesced. See Thurston's discussion in [21] Section 3, in particular Figure 11, for a more detailed discussion of this process. From the point of view of the octagon Π discussed in Section 2, this process is the same as either expanding or contracting the triangles T_1 and T_2 until some of the vertices become the same point. If such vertices are adjacent then the edge between them has degenerated to a point.

In Propositions 3.5 of [21] Thurston discusses what happens when two cone points collide. He shows that this occurs along a stratum S of codimension 1 and gives a formula for $\gamma(S)$, the cone angle around this stratum. In our setting the moduli space is an orbifold and so in each case

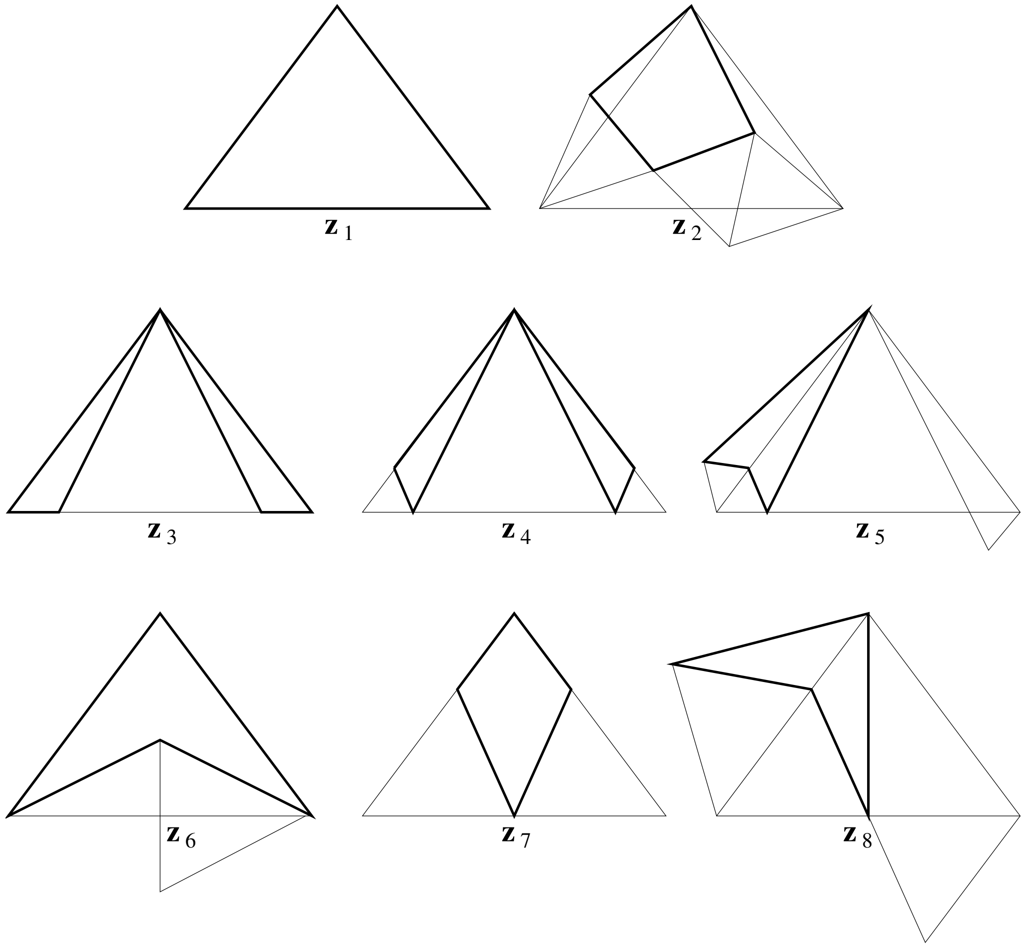

Figure 9: *Polygons corresponding to vertices of D.*

$2\pi/\gamma(S)$ is an integer. The stabiliser of the stratum S is then a subgroup of Γ of order $2\pi/\gamma(S)$. Suppose that the two cone points have cone angles ϕ_1 and ϕ_2 then Proposition 3.5 of [21] shows that if $\phi_1 \neq \phi_2$ then $\gamma(S) = \phi_1 + \phi_2 - 2\pi$ and if $\phi_1 = \phi_2$ then $\gamma(S) = \phi_1 - \pi$. We now indicate the strata associated to various collisions of pairs cone points and give the appropriate subgroups of Γ.

Cone points	Stratum S	$\gamma(S)$	Subgroup
$v_0,\ v_{\pm 1}$	$z_1 = 0$	$\pi = (2\pi - \theta) + (\pi + \theta) - 2\pi$	$\langle I_1 \rangle$
$v_0,\ v_{\pm 3}$	$w_1 = 0$	$\pi = (2\pi - \theta) + (\pi + \theta) - 2\pi$	$\langle P I_1 P^{-1} \rangle$
$v_{\pm 2},\ v_{\pm 3}$	$z_2 = 0$	$\theta = (\pi + \theta) - \pi$	$\langle R_1 \rangle$
$v_{\pm 1},\ v_{\pm 2}$	$w_2 = 0$	$\theta = (\pi + \theta) - \pi$	$\langle R_2 \rangle$
$0,\ v_0$	$z_1 = (1 - \cos\theta)/\cos\theta$	$\pi - 3\theta = (\pi - 2\theta) + (2\pi - \theta) - 2\pi$	$\langle P^3 \rangle$

We can check that in each case the generator of the group in the last column is a complex reflection of order $2\pi/\gamma(S)$. This indicates, but does not prove, that our group is indeed the same as Thurston's group.

We now discuss the cone structures that will be the vertices of our polyhedron. The point $\mathbf{z}_1$ will be fixed by R_1 and I_1. It is the origin in the $\mathbf{z}$ coordinates. Since z_1 and z_2 are both zero, the triangles T_1 and T_2 discussed in Section 2 have both degenerated to a point. Thus the octagon Π has degenerated to become the simply the triangle T_3. In terms of the cone manifolds, $z_1 = 0$

corresponds to the cone points corresponding to v_0 and $v_{\pm 1}$ coalescing to give a new cone point with cone angle π; and $z_2 = 0$ corresponds to the cone points corresponding to $v_{\pm 2}$ and $v_{\pm 3}$ coalescing to give a new cone point with cone angle 2θ. The polygon Π corresponding to $\mathbf{z}_1$ is given in the top row of Figure 9. The corresponding point where $w_1 = w_2 = 0$, which is fixed by R_2, is denoted $\mathbf{z}_2$. This is the origin in the $\mathbf{w}$ coordinates. Here the cone points v_0 and $v_{\pm 3}$ coalesce as do $v_{\pm 1}$ and $v_{\pm 2}$. Hence the base of T_2 has become one of the sides of T_1.

There are three points $\mathbf{z}_3$, $\mathbf{z}_4$, $\mathbf{z}_5$ with $z_1 = (1 - \cos\theta)/\cos\theta$. This condition corresponds to T_1 and T_3 having their bases parallel (recall that we have taken $z_3 = 1$ and in this case z_1 is real) and the apex of T_1 at 0, which is also the apex of T_3. This configuration only works in the cases where $n \geq 7$. The cone points corresponding to 0 and v_0 have coalesced to give a new cone point with cone angle $\pi - 3\theta$. For $\mathbf{z}_3$ we have $z_2 = 0$, and so, as above, $v_{\pm 2}$ and $v_{\pm 3}$ have coalesced to give a new cone point with cone angle 2θ. This is shown on the left of the middle row of Figure 9. For $\mathbf{z}_4$ we have z_2 real and $z_1 + z_2 = 1$. This means that the cone points $v_{\pm 1}$ and $v_{\pm 2}$ have coalesced to give a new cone point with cone angle 2θ. As shown in the middle of the middle row of Figure 9, the corresponding polygon can be obtained from Figure 2 by first allowing T_1 to be as large as possible, but with its interior still inside T_3, and then allowing T_2 and T_2' to be as large as possible, but with their interiors inside T_3 but outside T_1. The vertex $\mathbf{z}_5$ is the image of $\mathbf{z}_4$ under R_1. This means that the cone points $v_{\pm 1}$ and $v_{\pm 3}$ have coalesced to give a new cone point with cone angle 2θ. As shown on the right of the middle row of Figure 9, this is the limit of Figure 5 as T_1, T_2 and T_2' each become as large as possible.

In this section we are only interested in the cases where $n \geq 7$, but for completeness we now indicated what happens when $n = 5$ and $n = 6$; see Section 6 for more details. When $n = 5$ or 6 the three vertices $\mathbf{z}_3$, $\mathbf{z}_4$ and $\mathbf{z}_5$ are replaced with a single vertex where $z_1 = 1$ and $z_2 = 0$ (and so also $w_1 = 1$ and $w_2 = 0$). When $n = 6$ the angles $\pi - 2\theta$ and θ are the same. In this case, when z_1 is real, the sides (v_0, v_1) and $(0, v_3)$ are parallel. Thus as v_0 tends to 0 we must also have v_1, v_2, v_3 coalescing and likewise v_{-1}, v_{-2} and v_{-3}. Hence the polygon degenerates to a figure with zero area. This limiting configuration corresponds to a point on the boundary of complex hyperbolic space, which is a cusp of the lattice. When $n = 5$, the configuration with $z_1 = 1$ and $z_2 = 0$ corresponds to a point in the interior of complex hyperbolic space and involves the cone points corresponding to $v_{\pm 1}$, $v_{\pm 2}$ and $v_{\pm 3}$ all coalescing to give a new cone point with cone angle $3\theta - \pi = \pi/5$.

Finally, we will discuss the vertices $\mathbf{z}_6$, $\mathbf{z}_7$ and $\mathbf{z}_8$. First, $\mathbf{z}_6$ has z_1 purely imaginary. This means that the base of T_1 is orthogonal to the base of T_3. Furthermore the apex of T_1 is one of the base vertices of T_3 and also, as $z_2 = 0$, the triangle T_2 has degenerated to a point. In this configuration the cone points corresponding to v_0, $v_{\pm 2}$ and $v_{\pm 3}$ have all coalesced to give a new cone point with cone angle θ. Next for $\mathbf{z}_7$ the cone points corresponding to v_0, $v_{\pm 1}$ and $v_{\pm 2}$ have coalesced to give a new cone point with cone angle θ. As shown in the middle of the bottom row of Figure 9, this is the limit of the polygon from Figure 2 as T_1 shrinks to a point and T_2 and T_2' become as large as possible, but with disjoint interiors. Finally, $\mathbf{z}_8$ is the image of $\mathbf{z}_7$ under R_1. Here the cone points v_0, $v_{\pm 1}$ and $v_{\pm 3}$ have all coalesced, again giving a new cone point with cone angle θ. This polygon is again the limit of that shown in Figure 5.

We summarise the above discussion with the following table relating the points $\mathbf{z}_j$ and the cone points that have coalesced.

Point	Cone points	Angle	Cone points	Angle
$\mathbf{z}_1$	$v_0,\ v_{\pm1}$	π	$v_{\pm2},\ v_{\pm3}$	2θ
$\mathbf{z}_2$	$v_0,\ v_{\pm3}$	π	$v_{\pm1},\ v_{\pm2}$	2θ
$\mathbf{z}_3$	$0,\ v_0$	$\pi-3\theta$	$v_{\pm2},\ v_{\pm3}$	2θ
$\mathbf{z}_4$	$0,\ v_0$	$\pi-3\theta$	$v_{\pm1},\ v_{\pm2}$	2θ
$\mathbf{z}_5$	$0,\ v_0$	$\pi-3\theta$	$v_{\pm1},\ v_{\pm3}$	2θ
$\mathbf{z}_6$	$v_0,\ v_{\pm2},\ v_{\pm3}$	θ		
$\mathbf{z}_7$	$v_0,\ v_{\pm1},\ v_{\pm2}$	θ		
$\mathbf{z}_8$	$v_0,\ v_{\pm1},\ v_{\pm3}$	θ		

In Proposition 3.6 of [21] Thurston shows that j cone points with cone angles $\phi_1,\ldots,\phi_j$ collide in a stratum S of codimension $j-1$. The resulting cone angle of the moduli space is $\gamma(S)=\bigl(\phi_1+\cdots+\phi_j-2\pi(j-1)\bigr)$. Furthermore the order of the stabiliser of S is $N\bigl(2\pi/\gamma(S)\bigr)^{j-1}$ where N is the order of the subgroup of the symmetric group preserving the angles. By combining this information we can also find the stabiliser of each vertex and compute the corresponding cone angles. We again see that our group is consistent with Thurston. For example, the vertex $\mathbf{z}_7$ is stabilised by the group $\langle I_1,\,R_2\rangle$. We claim that it will follow from results of Section 7 that this group has order $2n^2$. We now sketch a proof of this claim. Cyclically permuting the indices in (36) we see that $R_2I_1R_2^{-1}=I_3$ and $R_2I_3R_2^{-1}=I_3I_1I_3$ (where I_3 is as defined as in Section 7). Thus $\langle I_1,\,I_3\rangle$ is a normal subgroup of $\langle I_1,\,R_2\rangle$ with quotient group $\langle R_2\rangle$. Since $\langle I_1,\,I_3\rangle$ is dihedral group of order $2n$ (see Proposition 7.3) and $\langle R_2\rangle$ is cyclic of order n we immediately see that $\langle I_1,\,R_2\rangle$ has order $2n^2$ as claimed. The fact that these orbifold singularities have the same order as Thurston's is a strong indication that these groups are indeed isomorphic to Livné's lattices. In Theorem 5.1 we show the two groups have the same presentation and hence, by Mostow rigidity, they are conjugate.

The table below gives both the $\mathbf{z}$ and $\mathbf{w}$ coordinates of the eight vertices $\mathbf{z}_1,\ldots,\mathbf{z}_8$. This enables us to transform our geometrical problem concerning cone structures into an algebraic problem about the action of a certain matrix group. From now on, we shall not consider cone metrics any more, but will concentrate on the action of this matrix group on complex hyperbolic space. We analyse this with a combination of geometry (bisectors) and linear algebra.

Point	z_1	z_2	w_1	w_2
$\mathbf{z}_1$	0	0	$1-e^{-i\theta}/(1-i\sin\theta)$	$1/(1-i\sin\theta)$
$\mathbf{z}_2$	$1-e^{i\theta}/(1+i\sin\theta)$	$e^{i\theta}/(1+i\sin\theta)$	0	0
$\mathbf{z}_3$	$(1-\cos\theta)/\cos\theta$	0	$(1-\cos\theta)/\cos\theta$	$e^{i\theta}(2\cos\theta-1)/\cos\theta$
$\mathbf{z}_4$	$(1-\cos\theta)/\cos\theta$	$(2\cos\theta-1)/\cos\theta$	$(1-\cos\theta)/\cos\theta$	0
$\mathbf{z}_5$	$(1-\cos\theta)/\cos\theta$	$e^{i\theta}(2\cos\theta-1)/\cos\theta$	$(1-\cos\theta)/\cos\theta$	$(2\cos\theta-1)/\cos\theta$
$\mathbf{z}_6$	$-i(1-\cos\theta)/\sin\theta$	0	0	$e^{i\theta}$
$\mathbf{z}_7$	0	1	$i(1-\cos\theta)/\sin\theta$	0
$\mathbf{z}_8$	0	$e^{i\theta}$	0	1

Before we finish this section we show that the collection of vertices described above is symmetrical with respect to an involution. The polyhedron D will also have this symmetry which will simplify matters later on. Consider the antiholomorphic isometry ι given by $\iota(\mathbf{z})=R_1R_2R_1\bigl(\overline{\mathbf{z}}\bigr)$. In other words

$$\iota\begin{bmatrix}z_1\\ z_2\\ 1\end{bmatrix}=\frac{1}{1-\cos\theta+i\sin\theta}\begin{bmatrix}i\sin\theta & -e^{i\theta}(1-\cos\theta) & 1-\cos\theta\\ -e^{i\theta} & -e^{i\theta} & e^{i\theta}\\ -\cos\theta & -e^{i\theta}\cos\theta & 1+i\sin\theta\end{bmatrix}\begin{bmatrix}\overline{z}_1\\ \overline{z}_2\\ 1\end{bmatrix}\sim\begin{bmatrix}\overline{w}_1\\ \overline{w}_2e^{i\theta}\\ 1\end{bmatrix}. \tag{13}$$

(Here $\sim$ denotes projective equality.) The following lemma is easy to verify using (13) and the table above.

Lemma 3.1 *The isometry ι has order 2 and acts on the $\mathbf{z}_j$ by*

$$\iota(\mathbf{z}_1) = \mathbf{z}_2, \qquad \iota(\mathbf{z}_3) = \mathbf{z}_4, \qquad \iota(\mathbf{z}_5) = \mathbf{z}_5, \qquad \iota(\mathbf{z}_6) = \mathbf{z}_7, \qquad \iota(\mathbf{z}_8) = \mathbf{z}_8.$$

3.3 The polyhedron D

The faces of the polyhedron D will be contained in bisectors. We now give a brief summary of the properties of bisectors that we will need; see [8] or [13] for more details. A bisector is the locus of points in complex hyperbolic space equidistant from a given, pair of points in complex hyperbolic space, say $\mathbf{z}_j$ and $\mathbf{z}_k$. Using the standard formula for the distance function (see (3.4) of Goldman for example) we see that $\mathbf{z} \in D$ if and only if

$$\frac{\langle \mathbf{z}, \mathbf{z}_j\rangle\langle \mathbf{z}_j, \mathbf{z}\rangle}{\langle \mathbf{z}, \mathbf{z}\rangle\langle \mathbf{z}_j, \mathbf{z}_j\rangle} = \cosh^2\left(\frac{\rho(\mathbf{z}, \mathbf{z}_j)}{2}\right) = \cosh^2\left(\frac{\rho(\mathbf{z}, \mathbf{z}_k)}{2}\right) = \frac{\langle \mathbf{z}, \mathbf{z}_k\rangle\langle \mathbf{z}_k, \mathbf{z}\rangle}{\langle \mathbf{z}, \mathbf{z}\rangle\langle \mathbf{z}_k, \mathbf{z}_k\rangle}.$$

If $\mathbf{z}_j$ and $\mathbf{z}_k$ have the same norm, that is $\langle \mathbf{z}_j, \mathbf{z}_j\rangle = \langle \mathbf{z}_k, \mathbf{z}_k\rangle$, then this is equivalent to

$$B = \left\{\mathbf{z} \in \mathbf{H}^2_{\mathbb{C}} \ : \ \left|\langle \mathbf{z}, \mathbf{z}_j\rangle\right| = \left|\langle \mathbf{z}, \mathbf{z}_k\rangle\right|.\right\} \tag{14}$$

In Lemma 4.6 we will use this characterisation of bisectors. In fact, this definition of a bisector only depends on $\langle \mathbf{z}_j, \mathbf{z}_j\rangle = \langle \mathbf{z}_k, \mathbf{z}_k\rangle$ and not on whether this quantity is positive, negative or zero. That is, the points $\mathbf{z}_j$ and $\mathbf{z}_k$ may be on the boundary of complex hyperbolic space or outside; see Lemma 4.4.

The points $\mathbf{z}_j$ and $\mathbf{z}_k$ lie in a unique complex line L, called the *complex spine* of the bisector B. There is a geodesic γ in L that is equidistant from our pair of points with respect to the natural Poincaré metric on L. This geodesic is called the *spine*. This still makes sense when $\mathbf{z}_j$ and $\mathbf{z}_k$ lie on the boundary of $\mathbf{H}^2_{\mathbb{C}}$ or lie outside: For any anti-holomorphic involution interchanging $\mathbf{z}_j$ and $\mathbf{z}_k$ we may define the spine as the locus of points in L fixed by this involution. It is easy to check that this definition of the spine is independent of the chosen antiholomorphic involution. Bisectors are not totally geodesic (there are no totally geodesic real hypersurfaces in complex hyperbolic space), but are foliated by totally geodesic subspaces in two different ways. First there are the slices; see [13]. Let Π_L denote orthogonal projection onto L, then the bisector is the pre-image of γ under Π_L. Each fibre of this map, that is each complex line that is the pre-image of a point of γ, is a *slice* of our bisector. Secondly, there are the meridians; see [8]. Each *meridian* is a Lagrangian plane that contains the spine γ, and is the fixed point set of one of the antiholomorphic involutions that swaps $\mathbf{z}_j$ and $\mathbf{z}_k$. Every Lagrangian plane containing γ is a meridian and the bisector is the union of all its meridians.

We now define the bisectors containing the sides of our polyhedron D. The spine of each bisector will be the geodesic passing through a pair of the points defined in Section 3.2. By inspection this leads to a definition in terms of the argument of one of z_1, z_2, w_1 or w_2. In Lemmas 4.4 and 4.6 we will also characterise the bisectors using (14), that is as the locus of points equidistant from a given pair of points. We now define the eight bisectors in question. Their label reflects the pair of vertices in the spine.

Bisector	Definition	Points on spine		Other points			
B_{13}	$\mathrm{Im}\,(z_1) = 0$	$\mathbf{z}_1,$	$\mathbf{z}_3$	$\mathbf{z}_4,$	$\mathbf{z}_5,$	$\mathbf{z}_7,$	$\mathbf{z}_8$
B_{24}	$\mathrm{Im}\,(w_1) = 0$	$\mathbf{z}_2,$	$\mathbf{z}_4$	$\mathbf{z}_3,$	$\mathbf{z}_5,$	$\mathbf{z}_6,$	$\mathbf{z}_8$
B_{16}	$\mathrm{Re}\,(z_1) = 0$	$\mathbf{z}_1,$	$\mathbf{z}_6$	$\mathbf{z}_7,$	$\mathbf{z}_8$		
B_{27}	$\mathrm{Re}\,(w_1) = 0$	$\mathbf{z}_2,$	$\mathbf{z}_7$	$\mathbf{z}_6,$	$\mathbf{z}_8$		
B_{17}	$\mathrm{Im}\,(z_2) = 0$	$\mathbf{z}_1,$	$\mathbf{z}_7$	$\mathbf{z}_3,$	$\mathbf{z}_4,$	$\mathbf{z}_6$	
B_{26}	$\mathrm{Im}\,(w_2 e^{-i\theta}) = 0$	$\mathbf{z}_2,$	$\mathbf{z}_6$	$\mathbf{z}_3,$	$\mathbf{z}_4,$	$\mathbf{z}_7$	
B_{18}	$\mathrm{Im}\,(z_2 e^{-i\theta}) = 0$	$\mathbf{z}_1,$	$\mathbf{z}_8$	$\mathbf{z}_3,$	$\mathbf{z}_5,$	$\mathbf{z}_6$	
B_{28}	$\mathrm{Im}\,(w_2) = 0$	$\mathbf{z}_2,$	$\mathbf{z}_8$	$\mathbf{z}_4,$	$\mathbf{z}_5,$	$\mathbf{z}_7$	

(15)

The following lemma follows immediately from this table and Lemma 3.1.

Lemma 3.2 *Let ι be the involution defined by (13). Then*

$$\iota(B_{13}) = B_{24}, \qquad \iota(B_{16}) = B_{27}, \qquad \iota(B_{17}) = B_{26}, \qquad \iota(B_{18}) = B_{28}.$$

The spines of B_{13}, B_{16}, B_{17} and B_{18} all pass through the point $\mathbf{z}_1$, which is the origin in the $\mathbf{z}$ coordinates. Observe that I_1 maps each of the bisectors B_{1j} to itself. Similarly, R_1 preserves B_{13} and B_{16} and sends B_{17} to B_{18}. The four bisectors B_{13}, B_{16}, B_{17} and B_{18} bound a *wedge* W_1. Writing $\mathbf{z}$ as in (6), this wedge is given by

$$W_1 = \Big\{\mathbf{z} \ : \ \arg(z_1) \in (-\pi/2, 0),\ \arg(z_2) \in (0, \theta)\Big\}. \tag{16}$$

Lemma 3.3 *The wedge W_1 is homeomorphic to a half space in $\mathbb{R}^4$ and this homeomorphism extends to a homeomorphism from ∂W_1 to $\mathbb{R}^3$.*

Proof: In order to see this, first apply the conformal homeomorphism $\Phi : (z_1, z_2) \longmapsto (z_1^2, z_2^{n/2})$. Using $\theta = 2\pi/n$, we see that $\Phi(W_1)$ is the product of two half planes:

$$\Phi(W_1) = \Big\{(x_1 + iy_1,\, x_2 + iy_2) \ : \ y_1 < 0,\, y_2 > 0\Big\}$$

The boundary of this set comprises those points where $y_1 = 0$ or $y_2 = 0$ (or both).

Secondly, apply the following homeomorphism from $\Phi(W_1)$ to a halfspace in $\mathbb{R}^4$:

$$\Psi : (x_1 + iy_1,\, x_2 + iy_2) \longmapsto (x_1,\, x_2,\, y_1 + y_2,\, y_1 y_2).$$

The restriction of Ψ to $\Phi(\partial W_1)$ is

$$\Psi : (x_1 + iy_1,\, x_2 + iy_2) \longmapsto \begin{cases} (x_1,\, x_2,\, y_1,\, 0) & \text{if } y_2 = 0, \\ (x_1,\, x_2,\, y_2,\, 0) & \text{if } y_1 = 0. \end{cases}$$

The image of the boundary $\Psi\Phi(\partial W_1)$ is clearly the whole of $\mathbb{R}^3$ as claimed. □

Similarly, the spines of B_{24}, B_{26}, B_{27} and B_{28} all pass through $\mathbf{z}_2$, the origin in the $\mathbf{w}$ coordinates; see (8) . Moreover, R_2 preserves B_{24} and B_{27} and sends B_{28} to B_{26}. The four bisectors bound a wedge $W_2 = P(W_1)$, where P is given by (7). Writing $\mathbf{w}$ as in (8) this wedge is given by

$$W_2 = \Big\{\mathbf{w} \ : \ \arg(w_1) \in (0, \pi/2),\ \arg(w_2) \in (0, \theta)\Big\}.$$

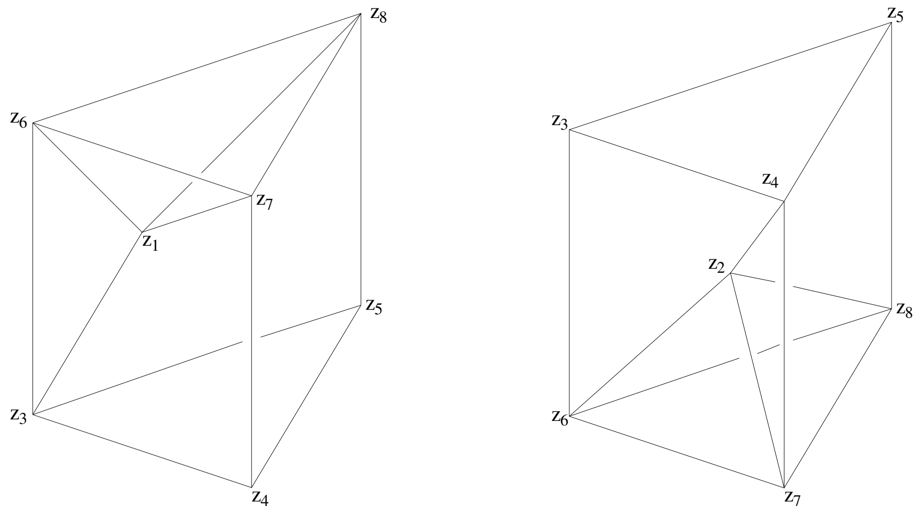

Figure 10: *The sides in each wedge W_1 and W_2.*

Since P is a homeomorphism, using Lemma 3.3 we immediately see that W_2 is homeomorphic to a half-space in $\mathbb{R}^4$ and this homeomorphism extends to a homeomorphism from ∂W_2 to $\mathbb{R}^3$.

We define the polyhedron D to be the intersection of the wedges W_1 and W_2 (compare [4]):

$$D = W_1 \cap W_2 = \left\{ \mathbf{z} = P(\mathbf{w}) \ : \ \begin{array}{ll} \arg(z_1) \in (-\pi/2, 0), & \arg(z_2) \in (0, \theta), \\ \arg(w_1) \in (0, \pi/2), & \arg(w_2) \in (0, \theta) \end{array} \right\}. \tag{17}$$

We define the side S_{1j} or S_{2j} of D to be the intersection of $\overline{D}$ with the bisector B_{1j} or B_{2j}, respectively. Below we give each side in terms of $\mathbf{z}$ and $\mathbf{w}$, in particular the arguments of their entries.

Side	$\arg(z_1)$	$\arg(z_2)$	$\arg(w_1)$	$\arg(w_2)$
S_{13}	$-\pi/2$	$[0,\theta]$	$[0,\pi/2]$	$[0,\theta]$
S_{24}	$[-\pi/2,0]$	$[0,\theta]$	$\pi/2$	$[0,\theta]$
S_{16}	0	$[0,\theta]$	$[0,\pi/2]$	$[0,\theta]$
S_{27}	$[-\pi/2,0]$	$[0,\theta]$	0	$[0,\theta]$
S_{17}	$[-\pi/2,0]$	0	$[0,\pi/2]$	$[0,\theta]$
S_{26}	$[-\pi/2,0]$	$[0,\theta]$	$[0,\pi/2]$	θ
S_{18}	$[-\pi/2,0]$	θ	$[0,\pi/2]$	$[0,\theta]$
S_{28}	$[-\pi/2,0]$	$[0,\theta]$	$[0,\pi/2]$	0

(18)

The vertices of each side are precisely the points listed in the table of bisectors (15). In Figure 10 the sides containing $\mathbf{z}_1$ and those containing $\mathbf{z}_2$ are shown. These collections of sides form open subsets of ∂W_1 and ∂W_2 respectively. Below we show that each two dimensional face of each side is homeomorphic to a disc. Gluing these discs together, we can see that the outer boundary of the collection of sides containing Π_1, respectively $\mathbf{z}_2$, is homeomorphic to a sphere. There is a obvious contraction of this sphere down to $\mathbf{z}_1$ or $\mathbf{z}_2$ and so we see, using Lemma 3.3, the collection of sides containing $\mathbf{z}_1$ and those containing $\mathbf{z}_2$ are each homeomorphic to a 3-ball. Gluing the boundaries together gives a 3-sphere, which is ∂D.

We now consider the 1-skeleton of D. This consists of arcs joining pairs of vertices of D, called *edges*. Let $\gamma_{jk} = \gamma_{kj}$ denote the edge of D with endpoints the vertices $\mathbf{z}_j$ and $\mathbf{z}_k$. We claim that each γ_{jk} is a geodesic arc. The reason for this is because each pair of vertices is in the common intersection of either a slice of one bisector and a meridian of another or in the intersection of meridians of two bisectors. We now list each edge, the pair of bisectors and the slices (S) or meridians (M).

Edge	Bisectors		Coordinates	Bisectors		Coordinates
γ_{13}	$B_{13} \cap B_{17}$	M	$\mathrm{Im}\,(z_1) = \mathrm{Im}\,(z_2) = 0$	$B_{13} \cap B_{18}$	M	$\mathrm{Im}\,(z_1) = \mathrm{Im}\,(z_2 e^{-i\theta}) = 0$
γ_{16}	$B_{16} \cap B_{17}$	M	$\mathrm{Re}\,(z_1) = \mathrm{Im}\,(z_2) = 0$	$B_{16} \cap B_{18}$	M	$\mathrm{Re}\,(z_1) = \mathrm{Im}\,(z_2 e^{-i\theta}) = 0$
γ_{17}	$B_{17} \cap B_{13}$	M	$\mathrm{Im}\,(z_1) = \mathrm{Im}\,(z_2) = 0$	$B_{17} \cap B_{16}$	M	$\mathrm{Re}\,(z_1) = \mathrm{Im}\,(z_2) = 0$
γ_{18}	$B_{18} \cap B_{13}$	M	$\mathrm{Im}\,(z_1) = \mathrm{Im}\,(z_2 e^{-i\theta}) = 0$	$B_{18} \cap B_{16}$	M	$\mathrm{Re}\,(z_1) = \mathrm{Im}\,(z_2 e^{-i\theta}) = 0$
γ_{24}	$B_{24} \cap B_{26}$	M	$\mathrm{Im}\,(w_1) = \mathrm{Im}\,(w_2 e^{-i\theta}) = 0$	$B_{24} \cap B_{28}$	M	$\mathrm{Im}\,(w_1) = \mathrm{Im}\,(w_2) = 0$
γ_{27}	$B_{27} \cap B_{26}$	M	$\mathrm{Re}\,(w_1) = \mathrm{Im}\,(w_2 e^{-i\theta}) = 0$	$B_{27} \cap B_{28}$	M	$\mathrm{Re}\,(w_1) = \mathrm{Im}\,(w_2) = 0$
γ_{26}	$B_{26} \cap B_{24}$	M	$\mathrm{Im}\,(w_1) = \mathrm{Im}\,(w_2 e^{-i\theta}) = 0$	$B_{26} \cap B_{27}$	M	$\mathrm{Re}\,(w_1) = \mathrm{Im}\,(w_2 e^{-i\theta}) = 0$
γ_{28}	$B_{28} \cap B_{24}$	M	$\mathrm{Im}\,(w_1) = \mathrm{Im}\,(w_2) = 0$	$B_{28} \cap B_{27}$	M	$\mathrm{Re}\,(w_1) = \mathrm{Im}\,(w_2) = 0$
γ_{34}	$B_{13} \cap B_{17}$	M	$\mathrm{Im}\,(z_1) = \mathrm{Im}\,(z_2) = 0$	$B_{24} \cap B_{26}$	M	$\mathrm{Im}\,(w_1) = \mathrm{Im}\,(w_2 e^{-i\theta}) = 0$
γ_{45}	$B_{13} \cap B_{24}$	S	$z_1 = w_1 = (1 - \cos\theta)/\cos\theta$	$B_{24} \cap B_{28}$	M	$\mathrm{Im}\,(w_1) = \mathrm{Im}\,(w_2) = 0$
γ_{53}	$B_{13} \cap B_{24}$	S	$z_1 = w_1 = (1 - \cos\theta)/\cos\theta$	$B_{13} \cap B_{18}$	M	$\mathrm{Im}\,(z_1) = \mathrm{Im}\,(z_2 e^{-i\theta}) = 0$
γ_{36}	$B_{17} \cap B_{18}$	S	$z_2 = 0$	$B_{24} \cap B_{26}$	M	$\mathrm{Im}\,(w_2) = \mathrm{Im}\,(w_2 e^{-i\theta}) = 0$
γ_{47}	$B_{26} \cap B_{28}$	S	$w_2 = 0$	$B_{13} \cap B_{17}$	M	$\mathrm{Im}\,(z_1) = \mathrm{Im}\,(z_2) = 0$
γ_{58}	$B_{13} \cap B_{18}$	M	$\mathrm{Im}\,(z_1) = \mathrm{Im}\,(z_2 e^{-i\theta}) = 0$	$B_{24} \cap B_{28}$	M	$\mathrm{Im}\,(w_1) = \mathrm{Im}\,(w_2) = 0$
γ_{67}	$B_{16} \cap B_{17}$	M	$\mathrm{Re}\,(z_1) = \mathrm{Im}\,(z_2) = 0$	$B_{26} \cap B_{27}$	M	$\mathrm{Re}\,(w_1) = \mathrm{Im}\,(w_2 e^{-i\theta}) = 0$
γ_{78}	$B_{13} \cap B_{16}$	S	$z_1 = 0$	$B_{27} \cap B_{28}$	M	$\mathrm{Re}\,(w_1) = \mathrm{Im}\,(w_2) = 0$
γ_{86}	$B_{24} \cap B_{27}$	S	$w_1 = 0$	$B_{16} \cap B_{18}$	M	$\mathrm{Re}\,(z_1) = \mathrm{Im}\,(z_2 e^{-i\theta}) = 0$

The combinatorics of these edges can be seen in Figure 10. Namely, there are nine edges not involving $\mathbf{z}_1$ or $\mathbf{z}_2$ arranged in a graph that is the boundary of a triangular prism. The other eight edges are obtained by joining four of the vertices of the prism to $\mathbf{z}_1$ and four to $\mathbf{z}_2$.

The following lemma follows immediately from Lemma 3.1 and the fact that the edges are geodesic arcs.

Lemma 3.4 *Let ι be the involution defined by (13). Then*

$$\begin{array}{lllll} \iota(\gamma_{13}) = \gamma_{24}, & \iota(\gamma_{16}) = \gamma_{27}, & \iota(\gamma_{17}) = \gamma_{26}, & \iota(\gamma_{18}) = \gamma_{28}, & \iota(\gamma_{34}) = \gamma_{34}, \\ \iota(\gamma_{45}) = \gamma_{35}, & \iota(\gamma_{36}) = \gamma_{47}, & \iota(\gamma_{58}) = \gamma_{58}, & \iota(\gamma_{67}) = \gamma_{67}, & \iota(\gamma_{78}) = \gamma_{68}. \end{array}$$

3.4 The faces of D

We have now defined the zero, one, and three-dimensional cells in the boundary of D. It remains to consider the two-dimensional cells. In this section we discuss all the two dimensional intersections among pairs of sides of D. We call these two-dimensional cells the *faces* of D and we denote them by F_{ijk} or F_{ijkl} where i, j, k, l are the indices of the vertices of the face. First we need to examine how pairs of bisectors intersect. It is clear that for each choice of distinct j, $k \in \{3, 6, 7, 8\}$ the bisectors B_{1j} and B_{1k} either have a common slice or a common meridian. Likewise for B_{2j} and B_{2k} for j, $k \in \{4, 6, 7, 8\}$. In Appendix A we give the general form for points in the intersection of pairs of bisectors B_{1j} and B_{2k}. Here we will find exactly which pairs of bisectors give faces of D. In Appendix B we will show that the remaining intersections among pairs of sides intersect D only in its 1-skeleton, that is along the edges. As a consequence of our analysis, we prove the following result, which is the major goal of this section:

Proposition 3.5 *The interior of each face F of D is homeomorphic to an open ball in $\mathbb{R}^2$ and the boundary of F is made up of edges on the list above.*

By construction, complex hyperbolic space, as defined by (6), is a bounded subset of $\mathbb{C}^2$. We now give explicit bounds for the coordinates (6) or (8).

Lemma 3.6 *If* $\mathbf{z}$ *is in* $\mathbf{H}^2_{\mathbb{C}}$ *as given in (6), and* $\mathbf{w}$ *is written in terms of* $\mathbf{z}$ *by (8), then*

$$|z_1| < \frac{\sin\theta}{\cos\theta}, \qquad |z_2| < \frac{1}{\cos\theta}, \qquad |w_1| < \frac{\sin\theta}{\cos\theta}, \qquad |w_2| < \frac{1}{\cos\theta}.$$

Furthermore, when $n \geq 7$ *we also have*

$$|z_1| < 1, \qquad |w_1| < 1.$$

PROOF: We have

$$\frac{|z_1|^2}{1-\cos\theta} + |z_2|^2 - \frac{1}{\cos\theta} < 0.$$

Thus

$$\begin{aligned} |z_1|^2 &< \frac{1-\cos\theta}{\cos\theta} < \frac{\sin^2\theta}{\cos^2\theta}, \\ |z_2|^2 &< \frac{1}{\cos\theta} < \frac{1}{\cos^2\theta}. \end{aligned}$$

Also, when $n \geq 7$,

$$|z_1|^2 < \frac{1-\cos\theta}{\cos\theta} < 1 - \frac{2\cos\theta - 1}{\cos\theta} < 1.$$

Similarly for w_1 and w_2. □

First we discuss faces of D contained in $S_{1j} \cap S_{1k}$ or $S_{2j} \cap S_{2k}$. These are all contained in complex lines or Lagrangian planes. For example, the face $F_{178} = S_{13} \cap S_{16}$ with vertices $\mathbf{z}_1$, $\mathbf{z}_7$, $\mathbf{z}_8$ is contained in the complex line $z_1 = 0$; or $F_{1347} = S_{13} \cap S_{17}$ with vertices $\mathbf{z}_1$, $\mathbf{z}_3$, $\mathbf{z}_4$ and $\mathbf{z}_7$ is contained in the Lagrangian plane with $\mathrm{Im}\,(z_1) = \mathrm{Im}\,(z_2) = 0$. These faces are each plane hyperbolic polygons (either triangles or quadrilaterals) whose boundary comprises the geodesic arcs joining the vertices. As these geodesic arcs only intersect in their endpoints, each face is obviously homeomorphic to a disc.

Similarly, for $n \geq 7$, there is the face $F_{345} = S_{13} \cap S_{24}$ contained in the complex line where $z_1 = (1-\cos\theta)/\cos\theta$. With its natural (Poincaré) hyperbolic metric, this face is the geodesic triangle with vertices $\mathbf{z}_3$, $\mathbf{z}_4$, $\mathbf{z}_5$ and internal angles (θ, θ, θ).

These faces are given in the following table

Face	Vertices	Sides	Coordinates
F_{178}	$\mathbf{z}_1,\ \mathbf{z}_7,\ \mathbf{z}_8$	$S_{13},\ S_{16}$	$z_1 = 0$
F_{268}	$\mathbf{z}_2,\ \mathbf{z}_6,\ \mathbf{z}_8$	$S_{24},\ S_{27}$	$w_1 = 0$
F_{136}	$\mathbf{z}_1,\ \mathbf{z}_3,\ \mathbf{z}_6$	$S_{17},\ S_{18}$	$z_2 = 0$
F_{247}	$\mathbf{z}_2,\ \mathbf{z}_4,\ \mathbf{z}_7$	$S_{26},\ S_{28}$	$w_2 = 0$
F_{345}	$\mathbf{z}_3,\ \mathbf{z}_4,\ \mathbf{z}_5$	$S_{13},\ S_{24}$	$z_1 = w_1 = (1-\cos\theta)/\cos\theta$
F_{1347}	$\mathbf{z}_1,\ \mathbf{z}_3,\ \mathbf{z}_4,\ \mathbf{z}_7$	$S_{13},\ S_{17}$	$\mathrm{Im}\,(z_1) = \mathrm{Im}\,(z_2) = 0$
F_{2436}	$\mathbf{z}_2,\ \mathbf{z}_4,\ \mathbf{z}_3,\ \mathbf{z}_6$	$S_{24},\ S_{26}$	$\mathrm{Im}\,(w_1) = \mathrm{Im}\,(w_2 e^{-i\theta}) = 0$
F_{1358}	$\mathbf{z}_1,\ \mathbf{z}_3,\ \mathbf{z}_5,\ \mathbf{z}_8$	$S_{13},\ S_{18}$	$\mathrm{Im}\,(z_1) = \mathrm{Im}\,(z_2 e^{-i\theta}) = 0$
F_{2458}	$\mathbf{z}_2,\ \mathbf{z}_4,\ \mathbf{z}_5,\ \mathbf{z}_8$	$S_{24},\ S_{28}$	$\mathrm{Im}\,(w_1) = \mathrm{Im}\,(w_2) = 0$
F_{167}	$\mathbf{z}_1,\ \mathbf{z}_6,\ \mathbf{z}_7$	$S_{16},\ S_{17}$	$\mathrm{Re}\,(z_1) = \mathrm{Im}\,(z_2) = 0$
F_{276}	$\mathbf{z}_2,\ \mathbf{z}_7,\ \mathbf{z}_6$	$S_{27},\ S_{26}$	$\mathrm{Re}\,(w_1) = \mathrm{Im}\,(w_2 e^{-i\theta}) = 0$
F_{168}	$\mathbf{z}_1,\ \mathbf{z}_6,\ \mathbf{z}_8$	$S_{16},\ S_{18}$	$\mathrm{Re}\,(z_1) = \mathrm{Im}\,(z_2 e^{-i\theta}) = 0$
F_{278}	$\mathbf{z}_2,\ \mathbf{z}_7,\ \mathbf{z}_8$	$S_{27},\ S_{28}$	$\mathrm{Re}\,(w_1) = \mathrm{Im}\,(w_2) = 0$

We now discuss the other faces one by one.

Proposition 3.7 *The point* $\mathbf{z}$ *lies in* $S_{13} \cap S_{28}$ *if and only if* $z_1 = x$ *and* $w_2 = u$ *where* $0 \le u \le 1-x$ *and* $0 \le x \le (1-\cos\theta)/\cos\theta$. *Furthermore, if* $\mathbf{z} \in S_{13} \cap S_{28}$ *then* $\mathrm{Re}\,(w_1) \le (1-\cos\theta)/\cos\theta$.

PROOF: Using table (18) we see that, by definition, $\mathbf{z} \in S_{13} \cap S_{28}$ if and only if $\arg(z_1) = 0$, $\arg(z_2) \in [0,\theta]$, $\arg(w_1) \in [0,\pi/2]$ and $\arg(w_2) = 0$. Thus we can write $z_1 = x$ and $w_2 = u$ where $x \ge 0$ and $u \ge 0$. From Lemma 3.6 we also have $u < 1/\cos\theta$. We can use Proposition A.6 to write z_2 and w_1 in terms of x and u:

$$\begin{aligned} z_2 &= e^{i\theta}\,\frac{1-x-u+xu\cos\theta+ui\sin\theta}{\cos\theta-u\cos\theta+i\sin\theta}, \\ w_1 &= \frac{1-\cos\theta-x-u(1-\cos\theta)+xu\cos\theta-xi\sin\theta}{-i\sin\theta-x\cos\theta}. \end{aligned}$$

In order to guarantee that $\mathbf{z} \in S_{13} \cap S_{28}$ we must find conditions on x and u so that $\arg(z_2) \in [0,\theta]$ and $\arg(w_1) \in [0,\pi/2]$, or equivalently so that $\mathrm{Im}\,(z_2) \ge 0$, $\mathrm{Im}\,(z_2 e^{-i\theta}) \le 0$, $\mathrm{Re}\,(w_1) \ge 0$ and $\mathrm{Im}\,(w_1) \ge 0$.

First we have

$$\begin{aligned} \mathrm{Im}\,(z_2) &= \frac{u\sin\theta\big((1-\cos\theta)(1+u\cos\theta)+x\cos\theta(1-u\cos\theta)\big)}{(1-u)^2\cos^2\theta+\sin^2\theta}, \\ \mathrm{Re}\,(w_1) &= \frac{x\big((1-\cos\theta)(1+u\cos\theta)+x\cos\theta(1-u\cos\theta)\big)}{x^2\cos^2\theta+\sin^2\theta}. \end{aligned}$$

Since $x \ge 0$, $u \ge 0$ and $1-u\cos\theta > 0$ we have

$$(1-\cos\theta)(1+u\cos\theta)+x\cos\theta(1-u\cos\theta) > 0.$$

This implies $\mathrm{Im}\,(z_2) \ge 0$ and $\mathrm{Re}\,(w_1) \ge 0$ and so these two conditions require no extra hypotheses on x and u.

Secondly,

$$\mathrm{Im}\,(z_2 e^{-i\theta}) = \frac{-\sin\theta(1-x-u)(1-u\cos\theta)}{(1-u)^2\cos^2\theta+\sin^2\theta}.$$

Thus $\mathrm{Im}\,(z_2 e^{-i\theta}) \le 0$ if and only if $1-x-u \ge 0$ (we have again used $1-u\cos\theta > 0$). Likewise

$$\mathrm{Im}\,(w_1) = \frac{\sin\theta(1-x-u)(1-\cos\theta-x\cos\theta)}{x^2\cos^2\theta+\sin^2\theta}.$$

Therefore when $\mathrm{Im}\,(z_2 e^{-i\theta}) \le 0$ we also have $\mathrm{Im}\,(w_1) \ge 0$ if and only if $x \le (1-\cos\theta)/\cos\theta$. This gives the first part of the result.

Finally, we must show that $\mathrm{Re}\,(w_1) - (1-\cos\theta)/\cos\theta \le 0$.

$$\mathrm{Re}\,(w_1) - \frac{1-\cos\theta}{\cos\theta} = \frac{-(1-\cos\theta-x\cos\theta)(\sin^2\theta+x(1-u)\cos^2\theta)}{\cos\theta(x^2\cos^2\theta+\sin^2\theta)}.$$

Since $\sin^2\theta + x(1-u)\cos^2\theta > 0$ we see that $x \le (1-\cos\theta)/\cos\theta$ implies $\mathrm{Re}\,(w_1) \le (1-\cos\theta)/\cos\theta$.
□

Corollary 3.8 *The intersection of S_{13} and S_{28} is a face F_{4587} homeomorphic to a disc. The boundary of F_{4587} is $\gamma_{45} \cup \gamma_{58} \cup \gamma_{78} \cup \gamma_{47}$.*

PROOF: It is clear that the region in the (x, u)-plane where $0 \le x \le (1 - \cos\theta)/\cos\theta < 1$ and $0 \le u \le 1 - x$ is a quadrilateral. From Proposition 3.7 there is a homeomorphism from this quadrilateral to $S_{13} \cap S_{28}$.

This homeomorphism extends to the boundary. We now show that its image is the union of the four edges claimed. When $x = 0$ we have $z_1 = 0$ and $\mathrm{Re}\,(w_1) = 0$. Thus $\mathbf{z} \in B_{16} \cap B_{27}$ and so it is in γ_{78}. When $u = 0$ we have $\mathrm{Im}\,(z_2) = 0$ and $w_2 = 0$. Thus $\mathbf{z} \in B_{17} \cap B_{26}$ and so is in γ_{47}. When $x = (1 - \cos\theta)/\cos\theta$ we have $w_1 = 0$. Thus $\mathbf{z} \in B_{24}$ and so is in γ_{45}. Finally, when $x + u = 1$ we have $\mathrm{Im}\,(z_2 e^{-i\theta}) = \mathrm{Im}\,(w_1) = 0$. Hence $\mathbf{z} \in B_{18} \cap B_{24}$ and so is in γ_{58}. □

Applying ι gives:

Corollary 3.9 *The intersection of S_{18} and S_{24} is a face F_{3586} homeomorphic to a disc. The boundary of F_{3586} is $\gamma_{35} \cup \gamma_{58} \cup \gamma_{86} \cup \gamma_{36}$.*

Next, we have

Proposition 3.10 *The point $\mathbf{z}$ lies in $S_{16} \cap S_{27}$ if and only if $z_1 = iy$ and $w_1 = iv$ where $y \le 0$, $v \ge 0$ and*

$$(1-\cos\theta)^2 + y\sin\theta(1-\cos\theta) - v\sin\theta(1-\cos\theta) + yv\cos^2\theta \ge 0.$$

PROOF: This proof is similar to that of Proposition 3.7. If $\mathbf{z} \in S_{16} \cap S_{27}$ then, using table (18), we must have $\arg(z_1) = -\pi/2$, $\arg(z_2) \in [0, \theta]$, $\arg(w_1) = \pi/2$ and $\arg(w_2) \in [0, \theta]$. Thus we can write $z_1 = iy$ and $w_1 = iv$ where $y \le 0$ and $v \ge 0$. From Lemma 3.6 we may also suppose $y > -\sin\theta/\cos\theta$ and $v < \sin\theta/\cos\theta$. Now we use Proposition A.4 to write z_2 and w_2 in terms of y and v:

$$\begin{aligned} z_2 &= e^{i\theta}\,\frac{1-\cos\theta + y\sin\theta - v\sin\theta - yv\cos\theta - iv}{1-\cos\theta - iv\cos\theta}, \\ w_2 &= \frac{1-\cos\theta + y\sin\theta - v\sin\theta - yv\cos\theta - iy}{1-\cos\theta - iy\cos\theta}. \end{aligned}$$

In order for $\mathbf{z} \in S_{16} \cap S_{27}$ we must find conditions on y and v equivalent to $\mathrm{Im}\,(z_2) \ge 0$, $\mathrm{Im}\,(z_2 e^{-i\theta}) \le 0$, $\mathrm{Im}\,(w_2) \ge 0$ and $\mathrm{Im}\,(w_2 e^{-i\theta}) \le 0$.

First we have

$$\begin{aligned} \mathrm{Im}\,(z_2 e^{i\theta}) &= \frac{-v(1-\cos\theta)^2 + yv\cos\theta(\sin\theta - v\cos\theta) - v^2\cos\theta\sin\theta}{(1-\cos\theta)^2 + v^2\cos^2\theta}, \\ \mathrm{Im}\,(w_2) &= \frac{-y(1-\cos\theta)^2 - yv\cos\theta(\sin\theta + y\cos\theta) + y^2\cos\theta\sin\theta}{(1-\cos\theta)^2 + y^2\cos^2\theta}. \end{aligned}$$

Using $\sin\theta - v\cos\theta > 0$ and $\sin\theta + y\cos\theta > 0$, it is easy to see that if $y \le 0$ and $v \ge 0$ then $\mathrm{Im}\,(z_2 e^{-i\theta}) \le 0$ and $\mathrm{Im}\,(w_2) \ge 0$. Thus these two conditions require no extra hypotheses on y and v.

Secondly we have

$$\begin{aligned} \mathrm{Im}\,(z_2) &= \frac{(\sin\theta - v\cos\theta)\big((1-\cos\theta)^2 + y\sin\theta(1-\cos\theta) - v\sin\theta(1-\cos\theta) + yv\cos^2\theta\big)}{(1-\cos\theta)^2 + v^2\cos^2\theta}, \\ \mathrm{Im}\,(w_2 e^{-i\theta}) &= \frac{-(\sin\theta + y\cos\theta)\big((1-\cos\theta)^2 + y\sin\theta(1-\cos\theta) - v\sin\theta(1-\cos\theta) + yv\cos^2\theta\big)}{(1-\cos\theta)^2 + y^2\cos^2\theta}. \end{aligned}$$

Therefore both $\mathrm{Im}\,(z_2) \geq 0$ and $\mathrm{Im}\,(w_2 e^{-i\theta}) \leq 0$ if and only if

$$(1-\cos\theta)^2 + y\sin\theta(1-\cos\theta) - v\sin\theta(1-\cos\theta) + yv\cos^2\theta \geq 0.$$

(We have used $\sin\theta - v\cos\theta > 0$ and $\sin\theta + y\cos\theta > 0$ again.) This gives the result. □

Corollary 3.11 *The intersection of S_{16} and S_{27} is a face F_{678} homeomorphic to a disc. The boundary of F_{678} is $\gamma_{67} \cup \gamma_{78} \cup \gamma_{86}$.*

PROOF: This is similar to the proof of Corollary 3.8, but is slightly more tricky as we do not have a nice simple shape like a Euclidean quadrilateral.

The curve $(1-\cos\theta)^2 + y\sin\theta(1-\cos\theta) - v\sin\theta(1-\cos\theta) + yv\cos^2\theta = 0$ in the (y,v)-plane cuts the y-axis exactly once at $y = -(1-\cos\theta)/\sin\theta < 0$ and cuts the v-axis exactly once at $v = (1-\cos\theta)/\sin\theta > 0$. Thus, this curve, the y-axis and the v-axis bound a triangular region contained in the quadrant where $y \leq 0$ and $v \geq 0$. Proposition 3.10 gives a homeomorphism from this triangular region to $S_{16} \cap S_{27}$.

This homeomorphism extends to the boundary and we now show that the boundary is the union of the three edges claimed. If $(1-\cos\theta)^2 + y\sin\theta(1-\cos\theta) - v\sin\theta(1-\cos\theta) + yv\cos^2\theta = 0$ we have $\mathrm{Im}\,(z_2) = \mathrm{Im}\,(w_2 e^{-i\theta})$ and so $\mathbf{z} \in B_{17} \cap B_{26}$. Thus, by inspection from our table of edges, we have $\mathbf{z} \in \gamma_{67}$.

When $y = 0$ we have $z_1 = 0$ and $\mathrm{Im}\,(w_2) = 0$. Hence $\mathbf{z} \in B_{13} \cap B_{28}$ and so, again by inspection of the table of edges, $\mathbf{z} \in \gamma_{78}$. Finally, when $v = 0$ we have $w_1 = 0$ and $\mathrm{Im}\,(z_2 e^{-i\theta}) = 0$. Thus $\mathbf{z} \in B_{24} \cap B_{18}$ and so it lies in γ_{86}. □

Finally,

Proposition 3.12 *The point $\mathbf{z}$ lies in $S_{17} \cap S_{26}$ if and only if $z_2 = x$ and $w_2 = ue^{i\theta}$ where $x \geq 0$, $u \geq 0$,*

$$\begin{aligned} 1 - x - u + xu\cos^2\theta &\geq 0, \\ 2\cos\theta - 1 - x\cos\theta - u\cos\theta + xu\cos^2\theta &\leq 0. \end{aligned}$$

Furthermore, if $\mathbf{z} \in S_{17} \cap S_{26}$ then $\mathrm{Re}\,(z_1) \leq (1-\cos\theta)/\cos\theta$ and $\mathrm{Re}\,(w_1) \leq (1-\cos\theta)/\cos\theta$.

PROOF: This again is similar to the proof of Proposition 3.7. Write $z_2 = x$ and $w_2 = ue^{i\theta}$ where $0 \leq x < 1/\cos\theta$ and $0 \leq u < 1/\cos\theta$. Then from Proposition A.13, we have

$$\begin{aligned} z_1 &= \frac{1 - x - ue^{i\theta} + xu\cos\theta + iue^{i\theta}\sin\theta}{1 - ue^{i\theta}\cos\theta}, \\ w_1 &= \frac{1 - u - xe^{-i\theta} + xu\cos\theta - ixe^{-i\theta}\sin\theta}{1 - xe^{-i\theta}\cos\theta}. \end{aligned}$$

We must show that $\arg(z_1) \in [-\pi/2, 0]$ and $\arg(w_1) \in [0, \pi/2]$, or equivalently that $\mathrm{Re}\,(z_1) \geq 0$, $\mathrm{Im}\,(z_1) \leq 0$, $\mathrm{Re}\,(w_1) \geq 0$ and $\mathrm{Im}\,(w_1) \geq 0$. First:

$$\begin{aligned} \mathrm{Re}\,(z_1) &= \frac{(1-u\cos\theta)(1-x-u+xu\cos^2\theta)}{(1-u)^2\cos^2\theta + \sin^2\theta}, \\ \mathrm{Re}\,(w_1) &= \frac{(1-x\cos\theta)(1-x-u+xu\cos^2\theta)}{(1-x)^2\cos^2\theta + \sin^2\theta}. \end{aligned}$$

Thus $\mathrm{Re}\,(z_1) \geq 0$ and $\mathrm{Re}\,(w_1) \geq 0$ if and only if $1 - x - u + xu\cos^2\theta \geq 0$.

Secondly:

$$\begin{aligned} \mathrm{Im}\,(z_1) &= \frac{u\sin\theta(2\cos\theta - 1 - x\cos\theta - u\cos\theta + xu\cos^2\theta)}{(1-u)^2\cos^2\theta + \sin^2\theta}, \\ \mathrm{Im}\,(w_1) &= \frac{-x\sin\theta(2\cos\theta - 1 - x\cos\theta - u\cos\theta + xu\cos^2\theta)}{(1-x)^2\cos^2\theta + \sin^2\theta}. \end{aligned}$$

Thus $\mathrm{Im}\,(z_1) \leq 0$ and $\mathrm{Im}\,(w_1) \geq 0$ if and only if $2\cos\theta - 1 - x\cos\theta - u\cos\theta + xu\cos^2\theta \leq 0$.

This proves the first part of the result. For the second, observe that

$$\begin{aligned} \mathrm{Re}\,(z_1) - \frac{1-\cos\theta}{\cos\theta} &= \frac{(1-u\cos^2\theta)(2\cos\theta - 1 - x\cos\theta - u\cos\theta + xu\cos^2\theta)}{\cos\theta\big((1-u)^2\cos^2\theta + \sin^2\theta\big)}, \\ \mathrm{Re}\,(w_1) - \frac{1-\cos\theta}{\cos\theta} &= \frac{(1-x\cos^2\theta)(2\cos\theta - 1 - x\cos\theta - u\cos\theta + xu\cos^2\theta)}{\cos\theta\big((1-x)^2\cos^2\theta + \sin^2\theta\big)}. \end{aligned}$$

Therefore if $2\cos\theta - 1 - x\cos\theta - u\cos\theta + xu\cos^2\theta \leq 0$ we have $\mathrm{Re}\,(z_1) \leq (1-\cos\theta)/\cos\theta$ and $\mathrm{Re}\,(w_1) \leq (1-\cos\theta)/\cos\theta$. □

Corollary 3.13 *The intersection of S_{17} and S_{26} is a face F_{3476} homeomorphic to a disc. The boundary of F_{3476} is $\gamma_{34} \cup \gamma_{47} \cup \gamma_{67} \cup \gamma_{36}$.*

PROOF: This proof is similar to the proof of Corollary 3.11. We leave the details to the reader. The curve $1 - x - u + xu\cos^2\theta = 0$ intersects the x-axis at $x = 1$ and the u-axis at $u = 1$. Likewise, the curve $2\cos\theta - 1 - x\cos\theta - u\cos\theta + xu\cos\theta = 0$ intersects the x-axis at $x = (2\cos\theta - 1)/\cos\theta \in (0,1)$ and the u axis at $u = (2\cos\theta - 1)/\cos\theta$. We claim that these two curves do not intersect. Rearranging, we see that the curves are

$$u = \frac{1-x}{1-x\cos^2\theta}, \qquad u = \frac{2\cos\theta - 1 - x\cos\theta}{\cos\theta - x\cos^2\theta}.$$

Equating these two expressions gives $0 = (1-\cos\theta)\big((1-x)^2\cos^2\theta + \sin^2\theta\big)$. This is a contradiction. (The reader may check the cases where $x = 1/\cos^2\theta$ and $x = 1/\cos\theta$.) Thus it is straightforward to check that these two curves and the two axes bound a quadrilateral. Proposition 3.12 gives a homeomorphism to $S_{17} \cap S_{26}$ that extends to the boundary. As before, we can check that the boundary is the union of the four geodesics claimed. □

The following result is another consequence of the results from this section. It will be used when we are verifying the images of D under Γ tessellate $\mathbf{H}^2_{\mathbb{C}}$; see Lemma 4.14 below, for example.

Proposition 3.14 *If $\mathbf{z} \in \overline{D}$ then $\mathrm{Re}\,(z_1) \leq (1-\cos\theta)/\cos\theta$ and $\mathrm{Re}\,(w_1) \leq (1-\cos\theta)/\cos\theta$.*

PROOF: First consider the faces contained in complex lines or Lagrangian planes. These subspaces are totally geodesic and so, by convexity, we only need to check that the vertices all satisfy this condition. That is clear by inspection. Next consider the other faces we have constructed. From Propositions 3.7, 3.10, 3.12 we see that the faces F_{4587}, F_{3586}, F_{678} and F_{3476} all satisfy this condition. In Appendix B we shall show that all other bisector intersections only contribute to the 1-skeleton of D. Thus the whole of ∂D satisfies the conditions. By continuity we see that the interior points also satisfy these conditions and we are done. □

We remark that there is a subtle point here. Consider the geodesic where $z_1 = w_1 = x$ and $e^{-i\theta}z_2 = w_2 = 1 - x$ for $x \in \mathbb{R}$. All points in $\mathbf{H}^2_{\mathbb{C}}$ on this geodesic for which $x \geq 0$ have $\arg(z_1) = \arg(w_1) = \arg(w_2) = 0$ and $\arg(z_2) = \theta$. Hence if we had used closed intervals when defining D in (17) we would have included all of this (semi-infinite) geodesic arc. However, Proposition 3.14 shows that only those points with $x \leq (1 - \cos\theta)/\cos\theta$ lie in $\overline{D}$.

4 Discreteness of Γ

Our goal is to use Poincaré's polyhedron theorem to show that the group Γ generated by R_1, R_2 and I_1 is discrete and to find a presentation. The discreteness of Γ could be shown by applying Theorem 0.2 of [21]. However, this would not give us a presentation and only yields limited information about the geometry of the action of Γ on complex hyperbolic space. We will prove:

Theorem 4.1 *Suppose that the ordered pair (n, d) is in the following list*

$$(5, -10), \quad (6, \infty), \quad (7, 14), \quad (8, 8), \quad (9, 6), \quad (10, 5), \quad (12, 4), \quad (18, 3),$$

that is $d = 2n/(n - 6)$. Then writing $\theta = 2\pi/n$, the group Γ generated by the side pairings of D is a discrete subgroup of PU(1, 2) *with fundamental domain D and presentation:*

$$\Gamma = \left\langle J,\, P,\, R_1,\, R_2 \;:\; \begin{array}{c} J^3 = P^{3d} = R_1^n = R_2^n = (P^{-1}J)^2 = I, \\ R_2 = PR_1P^{-1} = JR_1J^{-1}, \qquad P = R_1R_2 \end{array} \right\rangle. \tag{19}$$

We prove this theorem using Poincaré's polyhedron theorem. First we discuss this theorem and then we prove Theorem 4.1 for the cases where $n \geq 7$. In Section 6 will discuss the two remaining cases of $n = 5$ and $n = 6$.

4.1 Poincaré's polyhedron theorem

In order to show that Γ is discrete with fundamental polyhedron D we need to use Poincaré's polyhedron theorem. We will follow the formulation given by Mostow in [13]; see also [4] or [7]. In the case of constant curvature, Epstein and Petronio [6] give a very careful treatment of Poincaré's theorem.

A *combinatorial polyhedron* is a cellular space homeomorphic to a compact polytope, in particular each of its codimension-2 cells, called a *face*, is contained in exactly two codimension-1 cells, called *sides*. A *polyhedron* D is the realisation of a combinatorial polyhedron as a cell complex in a manifold X. We use the convention that D is open. A polyhedron is *smooth* if its cells are smooth. In our case X will be complex hyperbolic space and the sides of the polyhedron D will all be contained in bisectors and D will be smooth.

A *Poincaré polyhedron* is a smooth polyhedron D in X with sides S_j and *side pairing maps* $T_j \in \mathrm{Isom}(X)$ satisfying:

(S.1) For each side S_j of D there is a side S_k of D and a side pairing map T_j so that $T_j(S_j) = S_k$.

(S.2) If $T_j(S_j) = S_k$ then $T_k = T_j^{-1}$. In particular, if $j = k$ then T_j^2 is the identity.

(S.3) $T_j^{-1}(D) \cap D = \emptyset$.

(S.4) $T_j^{-1}(\overline{D}) \cap \overline{D} = S_j$.

(S.5) The polyhedron D has only finitely many sides and each side has only finitely many faces.

(S.6) There exists a number $\delta > 0$ so that each pair of disjoint sides is a distance at least δ apart.

The relation coming from (S.2) is called a *reflection relation*.

In addition to the side-pairing conditions (S.1) to (S.6) there are some face conditions. Let S_1 be a side (codimension-1 cell) of D and F be a face (codimension-2 cell) in the boundary of S_1. Let T_1 be the side pairing map associated to S_1 and consider $T_1(F)$. By hypothesis each face is contained in the boundary of exactly two sides. Thus $T_1(F)$ is contained in the boundary of $T_1(S_1)$ and another side, which we call S_2. Let T_2 be the side pairing map associated to S_2 and consider $T_2 \circ T_1(F)$. Continuing in this way we obtain a sequence of faces, a sequence of sides S_j and a sequence of side pairing maps T_j. As the polyhedron has finitely many sides and faces, these sequences must be periodic. Let k be the smallest integer so that all three sequences are periodic with period k. Then we have $T_k \circ \cdots \circ T_2 \circ T_1(F) = F$ and we denote $T_k \circ \cdots \circ T_2 \circ T_1$ by T. Then T is called the *cycle transformation* at the face F.

Given a cycle transformation $T = T_k \circ \cdots \circ T_2 \circ T_1$ and a positive integer m, define transformations $U_0, \ldots, U_{mk-1}$ by

$$\begin{array}{llll}
U_0 = 1, & U_1 = T_1, & \cdots & U_{k-1} = T_{k-1} \circ \cdots T_2 \circ T_1, \\
U_k = T, & U_{k+1} = T_1 \circ T, & \cdots & U_{2k-1} = T_{k-1} \circ \cdots T_2 \circ T_1 \circ T, \\
\vdots & \vdots & & \vdots \\
U_{mk-k} = T^{m-1}, & U_{mk-k+1} = T_1 \circ T^{m-1}, & \cdots & U_{mk-1} = T_{k-1} \circ \cdots T_2 \circ T_1 \circ T^{m-1}.
\end{array}$$

Then the face conditions are

(F.1) Every face is a submanifold of X homeomorphic to a codimension-2 ball.

(F.2) For each face F with cycle transformation T there is an integer l so that the restriction of T^l to F is the identity.

(F.3) For each face F with cycle transformation T there is an integer m so that $T^{lm} = (T^l)^m$ is the identity on the whole space X. Furthermore, the polyhedra $U_j^{-1}(D)$ for $d = 0, \ldots, mlk - 1$ are disjoint and their closures $U_j^{-1}(\overline{D})$ cover a neighbourhood of the interior of F, that is D and its images *tessellate* a neighbourhood of F.

The relations $T^{lm} = 1$ from (F.3) are called the *cycle relations*.

Then Poincaré's polyhedron theorem states that

Theorem 4.2 *Let D be a Poincaré polyhedron with side-pairing transformations $T_j \in \Sigma$ satisfying side pairing conditions (S.1) to (S.6) and face conditions (F.1), (F.2) and (F.3). Then the group Γ generated by the side pairing transformations is a discrete subgroup of $Isom(X)$ and D a fundamental domain. A presentation is given by*

$$\Gamma = \langle \Sigma \mid \textit{reflection relations, cycle relations} \rangle$$

4.2 The side pairing maps

Let J be the move on the cone structure defined by $J = PI_1 = R_1R_2I_1$. That is

$$J = \frac{1}{1-\cos\theta + i\sin\theta}\begin{bmatrix} -i\sin\theta & -(1-\cos\theta) & 1-\cos\theta \\ e^{i\theta} & -1 & e^{i\theta} \\ \cos\theta & -\cos\theta & 1+i\sin\theta \end{bmatrix}. \tag{20}$$

Observe that $\mathrm{tr}\,(J)=0$ and so (as an element of $\mathrm{PU}(1,2)$) J has order 3. In fact one may easily check that $\det(J) = -e^{2i\theta}$ and so $J^3 = -e^{6i\theta}I$.

Let J, P, R_1 and R_2 be given by (20), (7), (2) and (3) respectively. In this section we show that the maps J, P, R_1, R_2 pair the sides of D, and they satisfy the conditions of Poincaré's theorem. These maps pair the sides of D as follows; see Figure 11:

$$\begin{array}{llll} P: S_{13} \longrightarrow S_{24}, & J: S_{16} \longrightarrow S_{27}, & R_1: S_{17} \longrightarrow S_{18}, & R_2: S_{28} \longrightarrow S_{26}, \\ P^{-1}: S_{24} \longrightarrow S_{13}, & J^{-1}: S_{27} \longrightarrow S_{16}, & R_1^{-1}: S_{18} \longrightarrow S_{17}, & R_2^{-1}: S_{26} \longrightarrow S_{28}. \end{array}$$

Observe that the side pairings are consistent with the antiholomorphic involution ι which maps D to itself. Specifically, one may easily check that $J\iota = \iota J^{-1}$, $P\iota = \iota P^{-1}$, $R_1\iota = \iota R_2^{-1}$ and $R_2\iota = \iota R_1^{-1}$. Each of the sides S_{1j} contains the vertex $\mathbf{z}_1$ in its 0-skeleton, and this vertex lies on the intersection of three faces. In each case, two of these faces are contained in meridians and the third in a slice of the bisector. This means that one of the edges incident to $\mathbf{z}_1$ is contained in the spine of S_{1j} for each $j = 3, 6, 7, 8$. Applying ι, we see that one of the edges incident to $\mathbf{z}_2$ is contained in the spine of S_{2j} for each $j = 4, 6, 7, 8$. In both cases, this edge has been indicated on Figure 11 with a bold line.

Then Theorem 4.1 will follow immediately once we show that Γ satisfies the hypotheses of Poincaré's theorem and that the relations in (19) are each cycle relations associated to a face cycle of D. These relations will follow from Propositions 4.5, 4.7, 4.8, 4.9, 4.10, 4.11, 4.12 and 4.13. We give the proof in detail for $n = 7$, 8, 9, 10, 12 and 18 and we will discuss the cases of $n = 5$ and $n = 6$ in Section 6.

It is clear that the side pairing maps satisfy conditions (S.1) and (S.2) and that D satisfies (S.5). As each pair of sides intersect we see that condition (S.6) is vacuous. Also the face condition (F.1) follows from Corollary 3.5.

We now verify conditions (S.3) and (S.4) for each side.

Lemma 4.3 *If T is one of J, P, R_1 or R_2 then $T^{-1}(D)\cap D = T(D)\cap D = \emptyset$. Also*

$$\begin{array}{llll} P^{-1}(\overline{D})\cap\overline{D} = S_{13}, & J^{-1}(\overline{D})\cap\overline{D} = S_{16}, & R_1^{-1}(\overline{D})\cap\overline{D} = S_{17}, & R_2^{-1}(\overline{D})\cap\overline{D} = S_{28}, \\ P(\overline{D})\cap\overline{D} = S_{24}, & J(\overline{D})\cap\overline{D} = S_{27}, & R_1(\overline{D})\cap\overline{D} = S_{18}, & R_2(\overline{D})\cap\overline{D} = S_{26}. \end{array}$$

Proof: Consider the side S_{13}. If $\mathbf{z}\in\overline{D}$ then $\mathrm{Im}\,(z_1)\le 0$ with equality only only when $\mathbf{z}\in S_{13}$. Likewise, if $\mathbf{z} = P(\mathbf{w})\in\overline{D}$ then $\mathrm{Im}\,(w_1)\ge 0$ with equality only when $\mathbf{z}\in S_{24}$. Hence if $P(\mathbf{z})\in D$, or equivalently $\mathbf{z}\in P^{-1}(D)$, then $\mathrm{Im}\,(z_1)\ge 0$ with equality if and only if $\mathbf{z}\in S_{13} = P^{-1}(S_{24})$. Thus (S.3) and (S.4) hold for this side and applying P also for S_{24}.

The other parts follow similarly. □

In the following sections we find the cycle transformation T of each face F. We will also give the integers l and m from conditions (F.2) and (F.3). In each case T^l will either be the identity or else F will be contained in a complex line L and the T^l will be a complex reflection of order

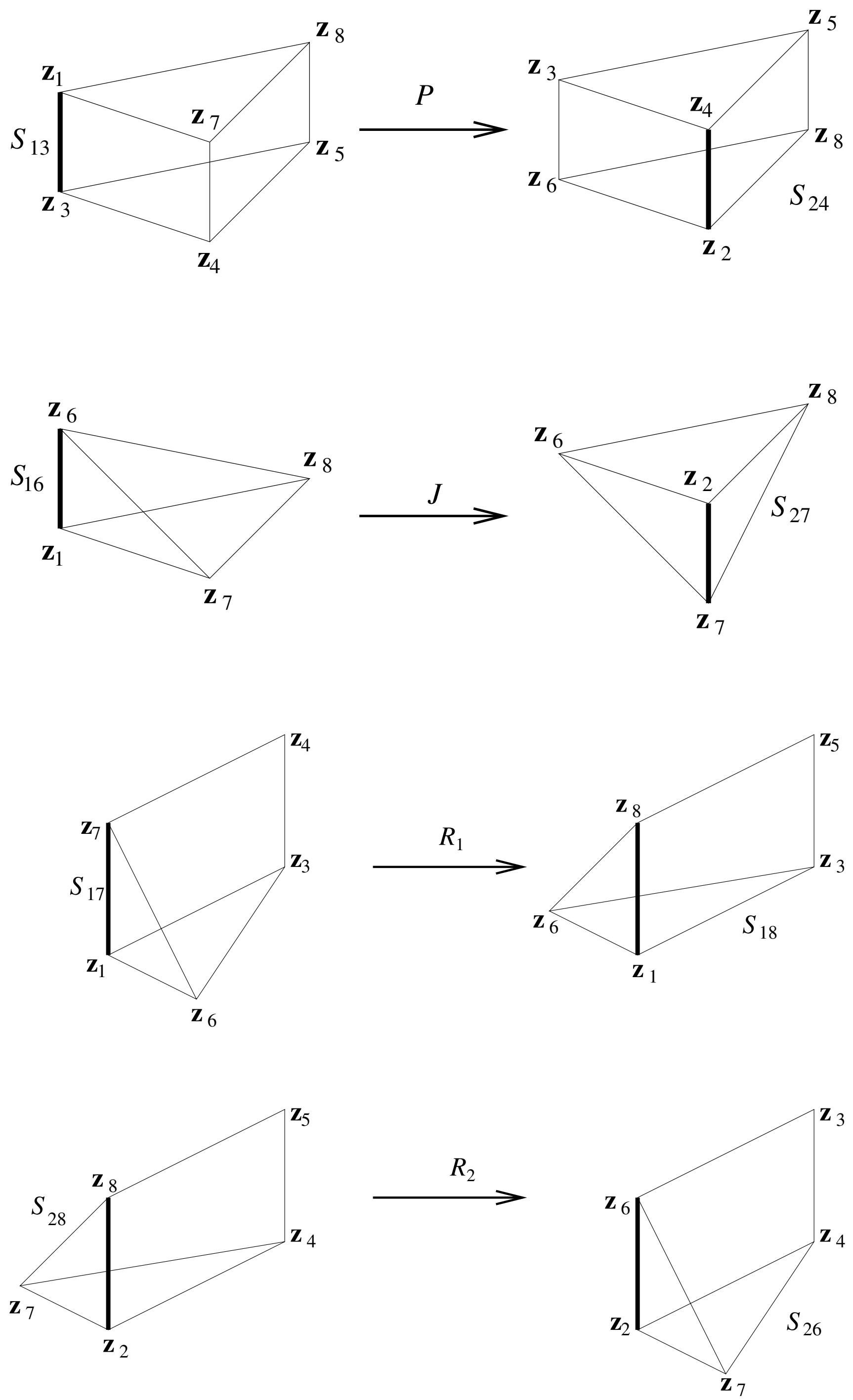

Figure 11: *The sides of the polyhedron and side pairings. The bold lines denote the spines of the bisectors.*

m that fixes L. This will verify condition (F.2) of Poincaré's theorem. We will also verify that the images of D tessellate around the faces formed by intersecting pairs of sides, that is conditions (F.3) are satisfied. As we go through this, we will generate a list of cycle relations. This will verify the presentation (19).

We conclude this section by describing our method of proving the tessellation conditions. We show that the (open) polyhedron D is disjoint from its image under the relevant side pairings and that the interior of each face has a neighbourhood covered by images of $\overline{D}$. Recall that D is defined as the intersection of eight halfspaces defined by bisectors. Each face is contained in two bisectors and so D is contained in the intersection of the corresponding two halfspaces. Each image of D under suitable side pairing maps is contained in the intersection of two halfspaces that are the image of one of the original pairs under this map. We must first show that each of these intersections is disjoint. Secondly, we choose a neighbourhood U of the interior of the face that is small enough that it does not meet any of the bisectors defining D except the two we are interested in. We then consider the closures of the halfspace intersections considered above and show that they cover U. It will be easier for us to use linear algebra to codify this picture, but we will always keep the underlying geometry in mind.

4.3 Tessellation around generic faces

In this section we consider the faces of D that are neither contained in a complex line nor in a Lagrangian plane. For each bisector B containing such a face of D we find points $\mathbf{z}_j$ and $\mathbf{z}_k$ so that B is equidistant from $\mathbf{z}_j$ and $\mathbf{z}_k$. We may express this geometric statement using the Hermitian form via equation (14). The open and closed halfspaces defined by this bisector may be described by replacing the equality of (14) with an inequality, Lemmas 4.4 and 4.6. Since the generators of Γ preserve the Hermitian form, we can use this method to also describe the halfspaces defining the images of D.

Let $\mathbf{z}_0$ the polar vector to the complex line L_{345} through $\mathbf{z}_3$, $\mathbf{z}_4$, $\mathbf{z}_5$:

$$\mathbf{z}_0 = \begin{bmatrix} 1 \\ 0 \\ 1 \end{bmatrix}. \tag{21}$$

Lemma 4.4 *Let $\mathbf{z}_0$ be given by (21). Then*

(i) $\big|\langle \mathbf{z}, \mathbf{z}_0\rangle\big| < \big|\langle \mathbf{z}, J^{-1}(\mathbf{z}_0)\rangle\big|$ *if and only if* $\mathrm{Re}\,(z_1) > 0$*;*

(ii) $\big|\langle \mathbf{z}, \mathbf{z}_0\rangle\big| < \big|\langle \mathbf{z}, J(\mathbf{z}_0)\rangle\big|$ *if and only if* $\mathrm{Re}\,(w_1) > 0$.

PROOF: Observe that $P(\mathbf{z}_0) = \mathbf{z}_0$. Using $J = PI_1$ we see that $I_1(\mathbf{z}_0) = I_1P^{-1}(\mathbf{z}_0) = J^{-1}(\mathbf{z}_0)$. In other words,

$$J^{-1}(\mathbf{z}_0) = \begin{bmatrix} -1 \\ 0 \\ 1 \end{bmatrix}.$$

Thus $\big|\langle \mathbf{z}, \mathbf{z}_0\rangle\big| < \big|\langle \mathbf{z}, I_1(\mathbf{z}_0)\rangle\big|$ if and only if

$$\left|\frac{z_1}{1-\cos\theta} - \frac{1}{\cos\theta}\right| < \left|-\frac{z_1}{1-\cos\theta} - \frac{1}{\cos\theta}\right|.$$

This is true if and only if $\mathrm{Re}\,(z_1) > 0$, proving (i). Part (ii) then follows by applying ι. □

Geometrically, this lemma says that B_{16} is the locus of points equidistant from the complex lines L_{345} and $J(L_{345})$. Similarly B_{27} is the locus of points equidistant from L_{345} and $J^{-1}(L_{345})$.

Proposition 4.5 *The polyhedron D and its images under J and J^{-1} tessellate around the face $F_{678} = S_{16} \cap S_{27}$. Moreover, the cycle transformation corresponding to this face is J and $l = 3$, $m = 1$. This gives the cycle relation $J^3 = I$.*

PROOF: By definition (17), if $\mathbf{z} \in D$ then $\mathrm{Re}\,(z_1) > 0$ and $\mathrm{Re}\,(w_1) > 0$. Hence, using Lemma 4.4 we see that

$$D \subset \Big\{ \mathbf{z} \in \mathbf{H}^2_{\mathbb{C}} \;:\; \big|\langle \mathbf{z}, \mathbf{z}_0 \rangle\big| < \big|\langle \mathbf{z}, J(\mathbf{z}_0)\rangle\big|, \quad \big|\langle \mathbf{z}, \mathbf{z}_0 \rangle\big| < \big|\langle \mathbf{z}, J^{-1}(\mathbf{z}_0)\rangle\big| \Big\}.$$

If $\mathbf{z} \in J^{\pm 1}(D)$ then $J^{\mp 1}(\mathbf{z}) \in D$. Hence

$$\big|\langle J^{\mp 1}(\mathbf{z}), \mathbf{z}_0 \rangle\big| < \big|\langle J^{\mp 1}(\mathbf{z}), J(\mathbf{z}_0)\rangle\big|, \qquad \big|\langle J^{\mp 1}(\mathbf{z}), \mathbf{z}_0 \rangle\big| < \big|\langle J^{\mp 1}(\mathbf{z}), J^{-1}(\mathbf{z}_0)\rangle\big|.$$

Applying $J^{\pm 1}$ to each point and using $J^3 = 1$, we obtain

$$J^{\pm 1}(D) \subset \Big\{ \mathbf{z} \in \mathbf{H}^2_{\mathbb{C}} \;:\; \big|\langle \mathbf{z}, J^{\pm 1}(\mathbf{z}_0) \rangle\big| < \big|\langle \mathbf{z}, \mathbf{z}_0\rangle\big|, \quad \big|\langle \mathbf{z}, J^{\pm 1}(\mathbf{z}_0) \rangle\big| < \big|\langle \mathbf{z}, J^{\mp 1}(\mathbf{z}_0)\rangle\big| \Big\}.$$

We immediately see that D, $J(D)$ and $J^{-1}(D)$ are disjoint.

We know, Proposition 3.10, that the face F_{678} comprises points where $\mathrm{Re}\,(z_1) = \mathrm{Re}\,(w_1) = 0$. Thus it is mapped to itself by J and J^{-1}. Let U be a neighbourhood of the interior of this face. By shrinking U if necessary, assume that for all points of U we have

$$\arg(z_1) \in (-\pi, 0), \qquad \arg(z_2) \in (0, \theta), \qquad \arg(w_1) \in (-\pi, 0), \qquad \arg(w_2) \in (0, \theta).$$

Then a point of U is in $\overline{D}$ if and only if both $\mathrm{Re}\,(z_1) \geq 0$ and $\mathrm{Re}\,(w_1) \geq 0$; or equivalently both $\big|\langle \mathbf{z}, \mathbf{z}_0 \rangle\big| \leq \big|\langle \mathbf{z}, J^{-1}(\mathbf{z}_0)\rangle\big|$ and $\big|\langle \mathbf{z}, \mathbf{z}_0 \rangle\big| \leq \big|\langle \mathbf{z}, J(\mathbf{z}_0)\rangle\big|$. From this it is easy to see that $\overline{D}$, $J(\overline{D})$ and $J^{-1}(\overline{D})$ cover U. □

Lemma 4.6 *Let $\mathbf{z}_6$, $\mathbf{z}_7$, $\mathbf{z}_8$ be as given in Section 3.2. Then:*

(i) $\big|\langle \mathbf{z}, \mathbf{z}_6 \rangle\big| < \big|\langle \mathbf{z}, P^{-1}(\mathbf{z}_7)\rangle\big|$ *if and only if* $\mathrm{Im}\,(z_1) < 0$;

(ii) $\big|\langle \mathbf{z}, \mathbf{z}_8 \rangle\big| < \big|\langle \mathbf{z}, R_1^{-1}(\mathbf{z}_7)\rangle\big|$ *if and only if* $\mathrm{Im}\,(z_2) > 0$;

(iii) $\big|\langle \mathbf{z}, \mathbf{z}_7 \rangle\big| < \big|\langle \mathbf{z}, R_1(\mathbf{z}_8)\rangle\big|$ *if and only if* $\mathrm{Im}\,(z_2 e^{-i\theta}) < 0$;

(iv) $\big|\langle \mathbf{z}, \mathbf{z}_7 \rangle\big| < \big|\langle \mathbf{z}, P(\mathbf{z}_6)\rangle\big|$ *if and only if* $\mathrm{Im}\,(w_1) > 0$;

(v) $\big|\langle \mathbf{z}, \mathbf{z}_8 \rangle\big| < \big|\langle \mathbf{z}, R_2(\mathbf{z}_6)\rangle\big|$ *if and only if* $\mathrm{Im}\,(w_2 e^{-i\theta}) < 0$.

(vi) $\big|\langle \mathbf{z}, \mathbf{z}_6 \rangle\big| < \big|\langle \mathbf{z}, R_2^{-1}(\mathbf{z}_8)\rangle\big|$ *if and only if* $\mathrm{Im}\,(w_2) > 0$;

PROOF: This is similar to the proof of Lemma 4.4. We will only give the proof for (i). All other parts are similar. Parts (iv), (v) and (vi) follow by applying ι to (i), (ii) and (iii).

We have

$$\mathbf{z}_6 = \begin{bmatrix} -i(1-\cos\theta)/\sin\theta \\ 0 \\ 1 \end{bmatrix}, \qquad P^{-1}(\mathbf{z}_7) = \begin{bmatrix} i(1-\cos\theta)/\sin\theta \\ 0 \\ 1 \end{bmatrix}.$$

Hence $\left|\langle \mathbf{z}, \mathbf{z}_6\rangle\right| < \left|\langle \mathbf{z}, P^{-1}(\mathbf{z}_7)\rangle\right|$ if and only if

$$\left|\frac{z_1 i}{\sin\theta} - \frac{1}{\cos\theta}\right| < \left|-\frac{z_1 i}{\sin\theta} - \frac{1}{\cos\theta}\right|.$$

This is true if and only if $\mathrm{Im}\,(z_1) < 0$, giving (i). □

Using the description in Section 3.3, this lemma gives the bisectors B_{13}, B_{17}, B_{18}, B_{27}, B_{26} and B_{28}, respectively, as the locus of points equidistant from a pair of points in $\mathbf{H}^2_{\mathbb{C}}$.

Proposition 4.7 *The polyhedron D and its images under R_1^{-1} and R_2 tessellate around the face $S_{3476} = S_{17} \cap S_{26}$. Moreover, the corresponding cycle transformation is $R_2 P^{-1} R_1$ and $l = m = 1$. This gives the cycle relation $R_2 P^{-1} R_1 = 1$*

Proof: Observe that if $\mathbf{z} \in D$ then $\mathbf{z}$ satisfies all six conditions of Lemma 4.6. Using Lemma 4.6 (ii), (v) we obtain

$$D \subset \left\{ \mathbf{z} \in \mathbf{H}^2_{\mathbb{C}} \ : \ \left|\langle \mathbf{z}, \mathbf{z}_8\rangle\right| < \left|\langle \mathbf{z}, R_1^{-1}(\mathbf{z}_7)\rangle\right|, \quad \left|\langle \mathbf{z}, \mathbf{z}_8\rangle\right| < \left|\langle \mathbf{z}, R_2(\mathbf{z}_6)\rangle\right| \right\}. \tag{22}$$

We now characterise $R_1^{-1}(D)$. First observe that $\mathbf{z} \in R_1^{-1}(D)$ if and only if $R_1(\mathbf{z}) \in D$. Thus $R_1(\mathbf{z})$ satisfies the conditions of (17). From Lemma 4.6 (iii), (iv) we obtain

$$\left|\langle R_1(\mathbf{z}), \mathbf{z}_7\rangle\right| < \left|\langle R_1(\mathbf{z}), R_1(\mathbf{z}_8)\rangle\right|, \qquad \left|\langle R_1(\mathbf{z}), \mathbf{z}_7\rangle\right| < \left|\langle R_1(\mathbf{z}), R_1 R_2(\mathbf{z}_6)\rangle\right|,$$

where we have written $P = R_1 R_2$. Thus

$$R_1^{-1}(D) \subset \left\{ \mathbf{z} \in \mathbf{H}^2_{\mathbb{C}} \ : \ \left|\langle \mathbf{z}, R_1^{-1}(\mathbf{z}_7)\rangle\right| < \left|\langle \mathbf{z}, \mathbf{z}_8)\rangle\right|, \quad \left|\langle \mathbf{z}, R_1^{-1}(\mathbf{z}_7)\rangle\right| < \left|\langle \mathbf{z}, R_2(\mathbf{z}_6)\rangle\right| \right\}. \tag{23}$$

Similarly, applying R_2 to Lemma 4.6 (vi), (i) we obtain:

$$R_2(D) \subset \left\{ \mathbf{z} \in \mathbf{H}^2_{\mathbb{C}} \ : \ \left|\langle \mathbf{z}, R_2(\mathbf{z}_6)\rangle\right| < \left|\langle \mathbf{z}, \mathbf{z}_{,8}\, \rangle\right|, \quad \left|\langle \mathbf{z}, R_2(\mathbf{z}_6)\rangle\right| < \left|\langle \mathbf{z}, R_1^{-1}(\mathbf{z}_7)\rangle\right| \right\}. \tag{24}$$

Comparing equations (22), (23) and (24) we see that D, $R_1^{-1}(D)$ and $R_2(D)$ are all disjoint. The second part of the result is proved in a similar manner to the second part of Proposition 4.5. The cycle transformation follows by observing that

$$S_{17} \cap S_{26} \xrightarrow{R_1} S_{24} \cap S_{18} \xrightarrow{P^{-1}} S_{28} \cap S_{13} \xrightarrow{R_2} S_{17} \cap S_{26}.$$

□

By applying $R_2^{-1} = P^{-1} R_1$ and R_1 respectively to Proposition 4.7 we see that D and its images under R_2^{-1} and P^{-1} tessellate around the face $F_{4587} = S_{12} \cap S_{28}$ and that D and its images under R_1 and P tessellate around the face $F_{3586} = S_{18} \cap S_{24}$. Alternatively, one could follow a direct argument analogous to that given above. In both cases the cycle relation is a cyclic permutation of $R_2 P^{-1} R_1 = I$.

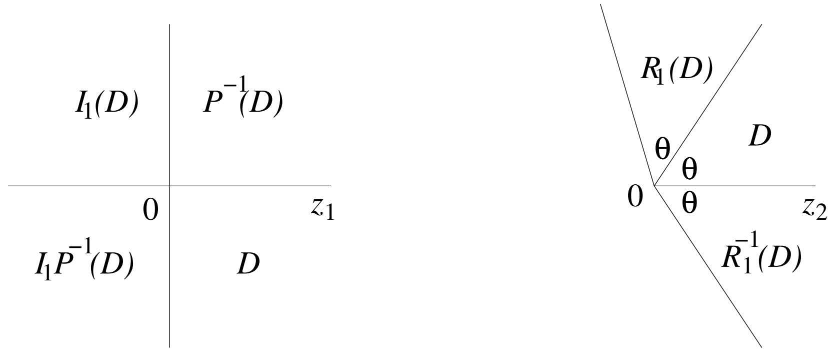

Figure 12: *The z_1 and z_2 planes close to 0 showing how their arguments vary in images of D.*

4.4 Tessellation around faces in totally geodesic planes

In this section we show that D and appropriate images tessellate around those faces of D containing either the vertex $\mathbf{z}_1$ or the vertex $\mathbf{z}_2$. Each of these faces is contained in a complex line or a Lagrangian plane. We focus on the faces containing $\mathbf{z}_1$. Then the result for those faces containing $\mathbf{z}_2$ will follow by applying ι.

We could have used the method of the previous section and described the halfspaces containing D in terms of the Hermitian form, as in (14). However, the bisectors in question are given solely in terms of the arguments of z_1 and z_2. Hence the halfspaces they determine are also given in terms of the arguments. In fact, the intersection of all four of these halfspaces is the wedge W_1 which we defined solely in terms of arguments (16). Thus to show that one the halfspace intersections is disjoint from the images of another we have to show that either the argument of z_1 or the argument of z_2 (or both) is different.

Recall from (17) that if $\mathbf{z} \in D$ then $\arg(z_1) \in (-\pi/2, 0)$ and $\arg(z_2) \in (0, \theta)$. Moreover, if $\mathbf{z} = P(\mathbf{w}) \in D$ then $\arg(w_1) \in (0, \pi/2)$ and $\arg(w_2) \in (0, \theta)$. Therefore when $\mathbf{z} \in P^{-1}(D)$ we have $\arg(z_1) \in (0, \pi/2)$ and again $\arg(z_2) \in (0, \theta)$. Similarly, I_1 sends z_1 to $-z_1$ and fixes z_2. Hence if $\mathbf{z} \in I_1(D)$ then $\arg(z_1) \in (\pi/2, \pi)$ and if $\mathbf{z} \in I_1P^{-1}(D)$ then $\arg(z_1) \in (-\pi, -\pi/2)$. In both cases the argument of z_2 remains unchanged.

Likewise R_1 maps z_1 to itself and maps z_2 to $e^{i\theta}z_2$. So if $\mathbf{z} \in R_1(D)$ we have $\arg(z_1) \in (-\pi/2, 0)$ and $\arg z_2 \in (\theta, 2\theta)$. Using similar arguments, it is easy to show that if $\mathbf{z}$ is in one of the following images of D then the arguments of z_1 and z_2 lie in the following intervals (compare this with Fig 12):

	$\arg(z_1)$	$\arg(z_2)$
D	$(-\pi/2, 0)$	$(0, \theta)$
$P^{-1}(D)$	$(0, \pi/2)$	$(0, \theta)$
$I_1(D)$	$(\pi/2, \pi)$	$(0, \theta)$
$I_1P^{-1}(D)$	$(-\pi, -\pi/2)$,	$(0, \theta)$
$R_1(D)$	$(-\pi/2, 0)$	$(\theta, 2\theta)$
$R_1P^{-1}(D)$	$(0, \pi/2)$	$(\theta, 2\theta)$
$R_1I_1(D)$	$(\pi/2, \pi)$	$(\theta, 2\theta)$
$R_1I_1P^{-1}(D)$	$(-\pi, -\pi/2)$,	$(\theta, 2\theta)$
$R_1^{-1}(D)$	$(-\pi/2, 0)$	$(-\theta, 0)$
$R_1^{-1}P^{-1}(D)$	$(0, \pi/2)$	$(-\theta, 0)$
$R_1^{-1}I_1(D)$	$(\pi/2, \pi)$	$(-\theta, 0)$
$R_1^{-1}I_1P^{-1}(D)$	$(-\pi, -\pi/2)$,	$(-\theta, 0)$

Proposition 4.8 *The polyhedron D and its images under R_1^{-1}, P^{-1} and $R_1^{-1}P^{-1}$ tessellate around the face $F_{1347} = S_{13} \cap S_{17}$. Moreover, the corresponding cycle transformation is $P^{-1}R_2^{-1}PR_1$ and $l = m = 1$. This gives the cycle relation $P^{-1}R_2^{-1}PR_1 = 1$.*

PROOF: If $\mathbf{z} \in F_{1347}$ then $\arg(z_1) = \arg(z_2) = 0$ and so $\mathrm{Im}\,(z_1) = \mathrm{Im}\,(z_2) = 0$. From the table, we can use the arguments of z_1 and z_2 to read off the sign of their imaginary parts. Thus, if $\mathbf{z} \in D$ then $\mathrm{Im}\,(z_1) < 0$ and $\mathrm{Im}\,(z_2) > 0$; if $\mathbf{z} \in P^{-1}(D)$ then $\mathrm{Im}\,(z_1) > 0$ and $\mathrm{Im}\,(z_2) > 0$; if $\mathbf{z} \in R_1^{-1}D$ then $\mathrm{Im}\,(z_1) < 0$ and $\mathrm{Im}\,(z_2) < 0$ and if $\mathbf{z} \in R_1^{-1}P^{-1}(D)$ then $\mathrm{Im}\,(z_1) < 0$ and $\mathrm{Im}\,(z_2) < 0$. Thus D, $P^{-1}(D)$, $R_1^{-1}(D)$ and $R_1^{-1}P^{-1}(D)$ are all disjoint. Furthermore, arguing as in Proposition 4.5, $\overline{D}$, $P^{-1}(\overline{D})$, $R_1^{-1}(\overline{D})$ and $R_1^{-1}P^{-1}(\overline{D})$ cover a suitably chosen neighbourhood of the interior of F_{1347}.

The cycle transformation follows by observing that

$$S_{17} \cap S_{13} \xrightarrow{R_1} S_{13} \cap S_{18} \xrightarrow{P} S_{26} \cap S_{24} \xrightarrow{R_2^{-1}} S_{24} \cap S_{28}. \xrightarrow{P^{-1}} S_{17} \cap S_{13}.$$

□

By applying R_1, PR_1, $R_2^{-1}PR_1 = P$ to Proposition 4.8 we see that D and its images tessellate around the faces F_{1358}, F_{2436} and F_{2458} respectively. In each case the cycle relation is a cyclic permutation of $P^{-1}R_2^{-1}PR_1 = I$.

Arguing similarly we have

Proposition 4.9 *The polyhedron D and its images under R_1^{-1}, $I_1P^{-1} = J^{-1}$ and $R_1^{-1}I_1P^{-1}$ tessellate around the face $F_{167} = S_{16} \cap S_{17}$. Moreover, the corresponding cycle transformation is $J^{-1}R_2^{-1}JR_1$ and $l = m = 1$. This gives the cycle relation $J^{-1}R_2^{-1}JR_1 = 1$.*

Proposition 4.10 *The polyhedron D and its images under P^{-1}, I_1 and I_1P^{-1} tessellate around the face $F_{178} = S_{13} \cap S_{16}$. Moreover, the corresponding cycle transformation is $P^{-1}J$ and $l = 1$, $m = 2$. This gives the cycle relation $(P^{-1}J)^2 = 1$.*

As above, we can use these results to show that D and its images tessellate around F_{168}, F_{267}, F_{278} and F_{268}. The cycle transformations are cyclic permutations of relations we have already obtained.

Now consider $F_{136} = S_{17} \cap S_{18}$. This comprises points of ∂D for which $z_2 = 0$. Hence this face is fixed by R_1. Since R_1 just multiplies z_2 by $e^{i\theta} = e^{2\pi i/n}$, the following result is easy to prove.

Proposition 4.11 *The polyhedron D and its images under powers of R_1 tessellate around the face $F_{136} = S_{17} \cap S_{18}$. Moreover, the corresponding cycle transformation is R_1 and $l = 1$, $m = n$. This gives the cycle relation $R_1^n = 1$.*

Applying ι we obtain

Proposition 4.12 *The polyhedron D and its images under powers of R_2 tessellate around the face $F_{247} = S_{26} \cap S_{28}$. Moreover, the corresponding cycle transformation is R_2 and $l = 1$, $m = n$. This gives the cycle relation $R_2^n = 1$.*

4.5 Tessellation around the face $F_{345} = S_{13} \cap S_{24}$

When $n \geq 7$ there is a face F_{345} contained in the complex line L_{345} given by $z_1 = (1-\cos\theta)/\cos\theta$ and containing $\mathbf{z}_3$, $\mathbf{z}_4$ and $\mathbf{z}_5$. The map P cyclically permutes these three points and so maps L_{345} to itself. Moreover, P^3 fixes each of these three points and so fixes L_{345} pointwise. A short computation shows that P^3 rotates a normal vector to L_{345} through an angle $-e^{3i\theta}$. We write $-e^{-3i\theta} = e^{i\psi}$. When $\theta = 2\pi/n$ for $n = 7$, 8, 9, 10, 12 or 18 then $\psi = 2\pi/d$ where $d = 2n/(n-6)$ is an integer. Note that $(1-\cos\theta + i\sin\theta)e^{-i\theta} = e^{i\psi/2}2\sin(\theta/2)$.

When $n \geq 7$ is not on our list the group Γ does not satisfy the Mostow-Thurston conditions (Theorem 2.2 of [14] or Theorem 0.2 of [21]) and so is not discrete. A more geometrical way of seeing this is to observe that, in this case, P^3 is still a boundary elliptic map but the angle of rotation, which is $(n-6)\pi/n$, is not $2\pi/d$ for any integer d. This means that D intersects its image under some non-trivial power of P. Non-discreteness follows in a similar manner to the non-discreteness of triangle groups in the hyperbolic plane whose internal angles are not submultiples of π; see [16] for a way of making this statement precise. Alternatively, one may use Jørgensen's inequality [10] to show that for such n the group Γ is not discrete.

From now of we assume that n is on our list and so $d = 2n/(n-6)$ is an integer. In this section our goal is to prove the following proposition.

Proposition 4.13 *Suppose that $n = 7, 8, 9, 10, 12, 18$ and $d = 2n/(n-6)$. The polyhedron D and its images under powers of P tessellate around the face $F_{345} = S_{13} \cap S_{24}$. Moreover, the corresponding cycle transformation is is P and $l = 3$, $m = d$. This gives the cycle relation $P^{3d} = 1$.*

It would be very tricky to prove this proposition if we were to use the coordinates $\mathbf{z}$ and $\mathbf{w}$ we have used before. Instead, we adopt new coordinates that reflect the action of P. We could have made this change of coordinates via a matrix in $\mathrm{PU}(2,1)$, as we did in (8), but it turns out to be easier to work directly with new basis vectors. We write $\mathbf{z}$ in terms of a new basis for $\mathbb{C}^{2,1}$ as follows:

$$\begin{bmatrix} z_1 \\ z_2 \\ 1 \end{bmatrix} = \frac{1-\cos\theta - z_1\cos\theta}{2\cos\theta - 1}\begin{bmatrix} -1 \\ 0 \\ -1 \end{bmatrix} + z_2\begin{bmatrix} 0 \\ 1 \\ 0 \end{bmatrix} + \frac{1-z_1}{2\cos\theta-1}\begin{bmatrix} 1-\cos\theta \\ 0 \\ \cos\theta \end{bmatrix}. \tag{25}$$

The first vector is the polar vector of L_{345}; see (21). The last two vectors span the complex linear subspace of $\mathbb{C}^{2,1}$ that projects to L_{345}. Consider the coefficients of these three vectors. We define projective coordinates by dividing the first two coordinates by the last one. To check that this is well defined in $\mathbf{H}^2_{\mathbb{C}}$, observe that from Lemma 3.6 we have $|z_1| < 1$ and so $1 - z_1 \neq 0$. Hence with respect to this new basis, the projective coordinates of $\mathbf{z}$ are:

$$\xi_1 = \frac{1-\cos\theta - z_1\cos\theta}{1-z_1}, \qquad \xi_2 = \frac{z_2(2\cos\theta - 1)}{1-z_1}. \tag{26}$$

This is completely analogous to the definitions of z_1 and z_2 except with our new basis rather than the standard basis. It will be useful to express ξ_1 in terms of w_1 and w_2. For completeness we also give ξ_2. We can either use (11) and (12) to substitute for z_1 and z_2, or else we can resolve $P(\mathbf{w})$ in terms of our basis.

$$\xi_1 = e^{i\psi/2}2\sin(\theta/2)\frac{1-\cos\theta - w_1\cos\theta}{1-w_1-w_2e^{-i\theta}(2\cos\theta-1)}, \tag{27}$$

$$\xi_2 = \frac{(1-w_1-w_2e^{-i\theta})(2\cos\theta-1)}{1-w_1-w_2e^{-i\theta}(2\cos\theta-1)}. \tag{28}$$

The coordinate ξ_1 is a complex coordinate on a complex line orthogonal to L_{345} and ξ_2 is a complex coordinate on L_{345}. There is a complex line orthogonal to L_{345} through each point of L_{345}. The coordinate ξ_1 parametrises a line intersecting L_{345} in $\mathbf{z}_3$. Thus these coordinates are well adapted to the geometry of the action of P. We remark that P^3 sends (ξ_1, ξ_2) to $(\xi_1 e^{i\psi}, \xi_2)$.

Similarly we may write $\mathbf{w} = P^{-1}(\mathbf{z})$ in terms of the new basis:

$$\begin{aligned} P^{-1}\begin{bmatrix} z_1 \\ z_2 \\ 1 \end{bmatrix} &= \frac{1-\cos\theta - z_1\cos\theta}{2\cos\theta - 1}\begin{bmatrix} -1 \\ 0 \\ -1 \end{bmatrix} + \frac{1-z_1-z_2}{1-\cos\theta - i\sin\theta}\begin{bmatrix} 0 \\ 1 \\ 0 \end{bmatrix} \\ &\quad + \frac{(1-z_1)e^{-i\theta} - z_2(2\cos\theta-1)e^{-i\theta}}{(2\cos\theta-1)(1-\cos\theta-i\sin\theta)}\begin{bmatrix} 1-\cos\theta \\ 0 \\ \cos\theta \end{bmatrix}. \end{aligned}$$

Thus the projective coordinates of $\mathbf{w} = P^{-1}(\mathbf{z})$ in terms of z_1 and z_2 are

$$\eta_1 = e^{-i\psi/2} 2\sin(\theta/2)\frac{1-\cos\theta - z_1\cos\theta}{1-z_1-z_2(2\cos\theta-1)}, \tag{29}$$

$$\eta_2 = e^{i\theta}\frac{(1-z_1-z_2)(2\cos\theta-1)}{1-z_1-z_2(2\cos\theta-1)}. \tag{30}$$

In terms of w_1 and w_2 these coordinates are

$$\eta_1 = \frac{1-\cos\theta - w_1\cos\theta}{1-w_1}, \qquad \eta_2 = \frac{w_2(2\cos\theta-1)}{1-w_1}. \tag{31}$$

Again η_2 is a complex coordinate on L_{345} and the coordinate η_1 is a complex coordinate on a complex line orthogonal to L_{345}, but which intersects L_{345} in a different point, this time a point through $P^{-1}(\mathbf{z}_3) = \mathbf{z}_5$. Furthermore, P^3 sends (η_1, η_2) to $(\eta_1 e^{i\psi}, \eta_2)$.

Finally we want to write $P(\mathbf{z})$ in the same way. Its projective coordinates are

$$\zeta_1 = e^{i\psi/2} 2\sin(\theta/2)\frac{1-\cos\theta - z_1\cos\theta}{1-z_1-z_2(2\cos\theta-1)e^{-i\theta}}, \tag{32}$$

$$\zeta_2 = \frac{(1-z_1-z_2e^{-i\theta})(2\cos\theta-1)}{1-z_1-z_2(2\cos\theta-1)e^{-i\theta}}. \tag{33}$$

In terms of w_1 and w_2 these coordinates are:

$$\zeta_1 = e^{i\psi/2} 2\sin(\theta/2)\frac{1-\cos\theta - w_1\cos\theta}{1-w_1-w_2(2\cos\theta-1)}, \tag{34}$$

$$\zeta_2 = e^{i\theta}\frac{(1-w_1-w_2)(2\cos\theta-1)}{1-z_1-z_2(2\cos\theta-1)}. \tag{35}$$

These are complex coordinates on a complex line through $\mathbf{z}_4$ orthogonal to L_{345} and on L_{345} respectively. Also, P^3 sends (ζ_1, ζ_2) to $(\zeta_1 e^{i\psi}, \zeta_2)$.

We can write the vertices $\mathbf{z}_j$ for $j = 3, \ldots, 8$ in terms of the new coordinates as follows:

	ξ_1	ξ_2	η_1	η_2	ζ_1	ζ_2
$\mathbf{z}_3$	0	0	0	$e^{i\theta}(2\cos\theta-1)$	0	$2\cos\theta-1$
$\mathbf{z}_4$	0	$2\cos\theta-1$	0	0	0	$e^{i\theta}(2\cos\theta-1)$
$\mathbf{z}_5$	0	$e^{i\theta}(2\cos\theta-1)$	0	$2\cos\theta-1$	0	0
$\mathbf{z}_6$	$e^{i\psi/2}\sin\frac{\theta}{2}$	0	$1-\cos\theta$	$e^{i\theta}(2\cos\theta-1)$	$e^{i\psi}(1-\cos\theta)$	$2\cos\theta-1$
$\mathbf{z}_7$	$1-\cos\theta$	$2\cos\theta-1$	$e^{-i\psi/2}\sin\frac{\theta}{2}$	0	$1-\cos\theta$	$e^{i\theta}(2\cos\theta-1)$
$\mathbf{z}_8$	$1-\cos\theta$	$e^{i\theta}(2\cos\theta-1)$	$1-\cos\theta$	$2\cos\theta-1$	$e^{i\psi/2}\sin\frac{\theta}{2}$	0

Our proof of Proposition 4.13 will depend on studying the arguments of ξ_1, η_1 and ζ_1 for points in D and in its images under powers of P. As P^3 acts on each of these three variables by multiplying them by $e^{i\psi}$, we see that in each case a fundamental domain for the action of $\langle P^3\rangle$ comprises a sector where $\arg(\xi_1)$, $\arg(\eta_1)$ or $\arg(\zeta_1)$ lies in a segment of length ψ. We begin by investigating the ranges of these three arguments for points lying in D.

Lemma 4.14 *If* $\mathbf{z}\in D$ *then* $\arg(\xi_1)\in(0,\psi/2)$*,* $\arg(\eta_1)\in(-\psi/2,0)$*, and* $\arg(\zeta_1)\in(0,\psi)$*.*

PROOF: From (26) we have

$$\begin{aligned}|1-z_1|^2\mathrm{Im}\,(\xi_1) &= |1-z_1|^2\mathrm{Im}\left(\frac{1-\cos\theta-z_1\cos\theta}{1-z_1}\right)\\ &= \mathrm{Im}\big((1-\cos\theta-z_1\cos\theta)(1-\overline{z}_1)\big)\\ &= -(2\cos\theta-1)\mathrm{Im}\,(z_1).\end{aligned}$$

Since $\mathrm{Im}\,(z_1)<0$ for points of D, this is positive and so $\mathrm{Im}\,(\xi_1)>0$.

From (27) we have

$$\begin{aligned}&\frac{\big|1-w_1-w_2e^{-i\theta}(2\cos\theta-1)\big|^2}{2\sin\frac{\theta}{2}}\mathrm{Im}\,(\xi_1e^{-i\psi/2})\\ &\quad= \mathrm{Im}\big((1-\cos\theta-w_1\cos\theta)(1-\overline{w}_1-\overline{w}_2e^{i\theta}(2\cos\theta-1))\big)\\ &\quad= (2\cos\theta-1)\Big(-\mathrm{Im}\,(w_1)\big(1-\mathrm{Re}\,(w_2e^{-i\theta})\cos\theta\big)+\mathrm{Im}\,(w_2e^{-i\theta})\big(1-\cos\theta-\mathrm{Re}\,(w_1)\cos\theta\big)\Big).\end{aligned}$$

For points of D we have $\mathrm{Im}\,(w_1)>0$ and $\mathrm{Im}\,(w_2e^{-i\theta})<0$ and also $\mathrm{Re}\,(w_2e^{-i\theta})\leq|w_2|<1/\cos\theta$ and $\mathrm{Re}\,(w_1)\leq(1-\cos\theta)/\cos\theta$. Therefore $\mathrm{Im}\,(\xi_1e^{-i\psi/2})<0$ as claimed.

This gives the first part. The second part follows by applying ι. For the last part, from (26) and (32) we have:

$$\begin{aligned}\frac{|1-z_1|^2}{(2\cos\theta-1)2\sin\frac{\theta}{2}}\mathrm{Im}\,(\xi_1e^{i\psi/2}/\zeta_1) &= \mathrm{Im}\big(-z_2e^{-i\theta}(1-\overline{z}_1)\big)\\ &= -\mathrm{Im}\,(z_1)\mathrm{Re}\,(z_2e^{-i\theta})-\mathrm{Im}\,(z_2e^{-i\theta})\big(1-\mathrm{Re}\,(z_1)\big).\end{aligned}$$

Since on D we have $\mathrm{Re}\,(z_1)\leq|z_1|<1$, $\mathrm{Im}\,(z_1)<0$, $\mathrm{Re}\,(z_2e^{i\theta})>0$ and $\mathrm{Im}\,(z_2e^{-i\theta})<0$ this expression is positive. Thus $\arg(\xi_1/\zeta_1)>-\psi/2$. Now $\arg(\zeta_1)=\arg(\xi_1)-\arg(\xi_1/\zeta_1)<\psi/2+\psi/2=\psi$.

Likewise from (31) and (34) we have

$$\begin{aligned}\frac{|1-w_1|^2}{(2\cos\theta-1)2\sin\frac{\theta}{2}}\mathrm{Im}\,(\eta_1e^{i\psi/2}/\zeta_1) &= \mathrm{Im}\big(-w_2(1-\overline{w}_1)\big)\\ &= -\mathrm{Im}\,(w_1)\mathrm{Re}\,(w_2)-\mathrm{Im}\,(w_2)\big(1-\mathrm{Re}\,(w_1)\big).\end{aligned}$$

Since on D we have $\mathrm{Re}\,(w_1)<1$, $\mathrm{Im}\,(w_1)>0$, $\mathrm{Re}\,(w_2)>0$ and $\mathrm{Im}\,(w_2)>0$ this expression is negative. Thus $\arg(\eta_1/\zeta_1)<-\psi/2$. Now $\arg(\zeta_1)=\arg(\eta_1)-\arg(\eta_1/\zeta_1)>-\psi/2+\psi/2=0$. □

We now do the same thing for points lying in $P(D)$ or $P^{-1}(D)$.

Lemma 4.15 *If* $\mathbf{z}\in P(D)$ *then* $\arg(\xi_1)\in(0,\psi)$*,* $\arg(\eta_1)\in(0,\psi/2)$*, and* $\arg(\zeta_1)\in(\psi/2,\psi)$*. If* $\mathbf{z}\in P^{-1}(D)$ *then* $\arg(\xi_1)\in(-\psi/2,0)$*,* $\arg(\eta_1)\in(-\psi,0)$ *and* $\arg(\zeta_1)\in(0,\psi/2)$*.*

Proof: If $\mathbf{z} \in P(D)$ then $P^{-1}(\mathbf{z}) \in D$. Thus the result follows along the same lines as the proof of Lemma 4.14 but with η_1 instead of ξ_1; ξ_1 instead of ζ_1 and, since $P^{-1}\big(P^{-1}(\mathbf{z})\big) = P^{-3}\big(P(\mathbf{z})\big)$, $\zeta_1 e^{-i\psi}$ instead of η_1. This proves the first part.

If $\mathbf{z} \in P^{-1}(D)$ then $P(\mathbf{z}) \in D$. The result follows similarly. □

Applying P^3 increases the argument of each of ξ_1, η_1 and ζ_1 by ψ. Hence, using the previous two lemmas, we can find the range for the arguments of ξ_1, ζ_1 and η_1 when $\mathbf{z} \in P^j(D)$ for $j = -1, \ldots, 3d-2$ as follows. In each case $k = 0, \ldots, d-1$

j	$\arg(\xi_1)$	$\arg(\eta_1)$	$\arg(\zeta_1)$
$3k$	$\big(k\psi,\ (k+1/2)\psi\big)$	$\big((k-1/2)\psi,\ k\psi\big)$	$\big(k\psi,\ (k+1)\psi\big)$
$3k+1$	$\big(k\psi,\ (k+1)\psi\big)$	$\big(k\psi,\ (k+1/2)\psi\big)$	$\big((k+1/2)\psi,\ (k+1)\psi\big)$
$3k-1$	$\big((k-1/2)\psi,\ k\psi\big)$	$\big((k-1)\psi,\ k\psi\big)$	$\big(k\psi,\ (k+1/2)\psi\big)$

Proposition 4.16 *The images of D under distinct powers of P are disjoint.*

Proof: Suppose we are given points in the images of D under distinct powers of P (mod $3d$). By inspection from the table above we see that the arguments of at least one of ξ_1, η_1, ζ_1 lie in disjoint intervals. Hence the points are distinct. □

It remains to show that the images of $\overline{D}$ under powers of P cover a neighbourhood of the interior of F_{345}. Let U be a neighbourhood of the interior of F_{345} and, by shrinking U if necessary, assume that on U we have

$$\arg(z_1) \in (-\pi/2, \pi/2), \qquad \arg(z_2) \in (0, \theta), \qquad \arg(w_1) \in (-\pi/2, \pi/2), \qquad \arg(w_2) \in (0, \theta).$$

Proposition 4.17 *Let U be as above. Then the images of $\overline{D}$ under powers of P cover U.*

Proof: A point $\mathbf{z}$ of U is in $\overline{D}$ if and only if both $\mathrm{Im}\,(z_1) \le 0$ and $\mathrm{Im}\,(w_1) \ge 0$. This is equivalent to $\arg(\xi_1) \ge 0$ and $\arg(\eta_1) \le 0$. Likewise, such a point of U is in $P(\overline{D})$ if and only if $\arg(\xi_1) \le \psi$ and $\arg(\eta_1) \ge 0$; and in $P^{-1}(\overline{D})$ if and only if $\arg(\xi_1) \le 0$ and $\arg(\zeta_1) \ge 0$. For all these points $\arg(\zeta_1) \in [0, \psi]$.

Suppose that $\mathbf{z} \in U$ has $\arg(\zeta_1) \in [0, \psi]$. If $\arg(\xi_1) \le 0$ then $\mathbf{z} \in P^{-1}(\overline{D})$; if $\arg(\eta_1) \ge 0$ then $\mathbf{z} \in P(\overline{D})$ and if both $\arg(\xi_1) \ge 0$ and $\arg(\eta_1) \le 0$ then $\mathbf{z} \in \overline{D}$. Hence $\overline{D}$, $P^{-1}(\overline{D})$ and $P(\overline{D})$ cover that part of U comprising points with $\arg(\zeta_1) \in [0, \psi]$.

Applying powers of P^3 we see that for $k = 0, \ldots, d-1$ then $P^{3k}(\overline{D})$, $P^{3k-1}(\overline{D})$ and $P^{3k+1}(\overline{D})$ cover that part of U comprising points with $\arg(\zeta_1) \in \big[k\psi, (k+1)\psi\big]$. This completes the result. □

This completes the proof of Proposition 4.13 and hence also the proof of Theorem 4.1.

5 Other presentations

In this section we show that the geometrical presentation (19) is equivalent to three other presentations that reveal more symmetry. The first presentation will enable us to show that Γ has a (non-faithful) triangle group as a normal subgroup. It is essentially given by Livné in Lemma 3 on page 108 of [12] (see also [11]). The other two are related to Mostow's groups [13]; see also [7].

Theorem 5.1 *The group Γ given by (19) has presentations:*

(i) $\langle I_1,\, P,\, Q \;:\; I_1^2 = P^{3d} = (PI_1)^3 = (P^{-1}Q)^n = 1, \quad P^3 = Q^2, \quad P^{-1}QI_1 = I_1P^{-1}Q \rangle.$

(ii) $\langle J,\, R_1 \;:\; J^3 = R_1^n = (JR_1^{-1}J)^4 = (R_1JR_1)^{3d} = 1, \quad R_1(JR_1^{-1}J)^2 = (JR_1^{-1}J)^2R_1 \rangle.$

(iii)

$$\left\langle R_1,\, R_2,\, R_3 \;:\; \begin{array}{l} R_j^n = (R_jR_k)^{3d} = 1,\;\; R_jR_kR_j = R_kR_jR_k\,;\;\; j,k = 1,\,2,\,3 \\ (R_1R_2R_3)^4 = 1,\;\; (R_1R_2R_3)^{-2}R_1R_2 = (R_2R_3R_1)^{-2}R_2R_3 \end{array} \right\rangle.$$

We remark that in the presentation (iii) above we have the braid relation $R_1R_2R_1 = R_2R_1R_2$, which we predicted by realising R_1 and R_2 as Dehn twists on the sphere with five cone points.

Lemma 5.2 *Writing $I_1 = P^{-1}J$ and $Q = PR_1$, the presentation of Theorem 5.1 (i) follows from Theorem 4.1.*

PROOF: We write $I_1 = P^{-1}J$ and $Q = PR_1$ and then we must show that each relation in the presentation of Theorem 5.1 (i) follows from those in Theorem 4.1. First

$$I_1^2 = (P^{-1}J)^2 = 1, \qquad P^{3d} = 1, \qquad (PI_1)^3 = J^3 = 1, \qquad (P^{-1}Q)^n = R_1^n = 1$$

all follow immediately from the substitutions. Next using $PR_1 = R_2P$ and $R_1R_2 = P$ we have

$$Q^2 = PR_1PR_1 = PR_1R_2P = P^3.$$

Finally, using $R_1P^{-1} = P^{-1}R_2$ and $R_2J = JR_1$ we have

$$P^{-1}QI_1 = R_1P^{-1}J = P^{-1}R_2J = P^{-1}JR_1 = I_1P^{-1}Q.$$

□

Lemma 5.3 *Writing $J = PI_1$ and $R_1 = P^{-1}Q$, the presentation of Theorem 5.1 (ii) follows from Theorem 5.1 (i).*

PROOF: Substituting $J = PI_1$ and $R_1 = P^{-1}Q$ means that the relations $J^3 = (PI_1)^3 = 1$ and $R_1^n = (P^{-1}Q)^{-n} = 1$ follow immediately. Next, using $PI_1PI_1 = I_1P^{-1}$, $I_1Q^{-1}PI_1 = Q^{-1}P$ and $PQ^{-2}P^2 = 1$, we find that

$$\begin{aligned} (JR_1^{-1}J)^2 &= PI_1Q^{-1}PPI_1PI_1Q^{-1}PPI_1 \\ &= PI_1Q^{-1}PI_1P^{-1}Q^{-1}P^2I_1 \\ &= PQ^{-1}PP^{-1}Q^{-1}P^2I_1 \\ &= PQ^{-2}P^2I_1 \\ &= I_1. \end{aligned}$$

Therefore $(JR_1^{-1}J)^4 = I_1^2 = 1$ and

$$R_1(JR_1^{-1}R_1)^2 = P^{-1}QI_1 = I_1P^{-1}Q = (JR_1^{-1}J)^2R_1.$$

Finally, using $I_1P^{-1}Q = P^{-1}QI_1$, $P^{-1}Q^2 = P^2$, $PI_1 = I_1P^{-1}I_1P^{-1}$ and $P^{-3d} = 1$ we obtain:

$$\begin{aligned}
(R_1JR_1)^{3d} &= (P^{-1}QPI_1P^{-1}Q)^{3d} \\
&= (P^{-1}QPP^{-1}QI_1)^{3d} \\
&= (P^{-1}Q^2I_1)^{3d} \\
&= (P^2I_1)^{3d} \\
&= (PI_1P^{-1}I_1P^{-1})^{3d} \\
&= PI_1P^{-3d}I_1P^{-1} \\
&= 1.
\end{aligned}$$

□

Lemma 5.4 *Writing $R_2 = JR_1J^{-1}$ and $R_3 = J^{-1}R_1J$, the presentation from Theorem 5.1 (iii) follows from Theorem 5.1 (ii).*

Proof: Since $R_2 = JR_1J^{-1}$, $R_3 = J^{-1}R_1J$ and $R_1^n = 1$, we immediately get $R_2^n = JR_1^nJ^{-1} = 1$ and $R_3^n = J^{-1}R_1^nJ = 1$. Observe that using $J^{-1} = J^2$ and $(JR_1^{-1}J)^4 = 1$

$$\begin{aligned}
(R_1R_2R_3)^{-2}R_1R_2 &= R_3^{-1}R_2^{-1}R_1^{-1}R_3^{-1} \\
&= J^{-1}R_1^{-1}JJR_1^{-1}J^{-1}R_1^{-1}J^{-1}R_1^{-1}J \\
&= J(JR_1^{-1}J)^4 \\
&= J.
\end{aligned}$$

Thus we may cyclically permute the indices to obtain

$$J = (R_1R_2R_3)^{-2}R_1R_2 = (R_2R_3R_1)^{-2}R_2R_3 = (R_3R_1R_2)^{-2}R_3R_1.$$

Using $J = J^{-2}$ and $(JR_1^{-1}J)^4 = 1$ we have

$$(R_3R_1R_2)^4 = (J^{-1}R_1JR_1JR_1J^{-1})^4 = (JR_1^{-1}J)^{12} = 1.$$

Next, using $J = J^{-2}$ and $(JR_1^{-1}J)^{-2} = (JR_1^{-1}J)^2$ we have

$$\begin{aligned}
R_2R_3 = JR_1J^{-2}R_1J &= J^{-1}(JR_1^{-1}J)^{-2}J^{-1} \\
&= J^{-1}(JR_1^{-1}J)^2J^{-1} \\
&= (R_1JR_1)^{-1}.
\end{aligned}$$

Thus $(R_2R_3)^{3d} = 1$ and cyclically permuting the indices, we have $(R_1R_2)^{3d} = (R_3R_1)^{3d} = 1$ as well. Finally, using $J = J^{-2}$ and $(JR_1^{-1}J)^{-2}R_1 = R_1(JR_1^{-1}J)^{-2}$ we have

$$\begin{aligned}
R_2R_3R_2 &= (JR_1J^{-1})(J^{-1}R_1J)(JR_1J^{-1}) \\
&= J^{-1}(JR_1^{-1}J)^{-2}R_1J^{-1} \\
&= J^{-1}R_1(JR_1^{-1}J)^{-2}J^{-1} \\
&= (J^{-1}R_1J)(JR_1J^{-1})(J^{-1}R_1J) \\
&= R_3R_2R_3.
\end{aligned}$$

Again we cyclically permute the indices to obtain $R_1R_2R_1 = R_2R_1R_2$ and $R_3R_1R_3 = R_1R_3R_1$. □

Lemma 5.5 *Writing $J = R_1^{-1}R_3^{-1}R_2^{-1}R_1^{-1}$ and $P = R_1R_3$, the presentation Theorem 4.1 follows from Theorem 5.1 (iii).*

PROOF: Substituting for J and P we immediately see that

$$R_1^n = R_2^n = 1, \qquad P = R_1R_2, \qquad P^{3d} = (R_1R_2)^{3d} = 1.$$

Using $J = R_1^{-1}R_3^{-1}R_2^{-1}R_1^{-1} = R_3^{-1}R_2^{-1}R_1^{-1}R_3^{-1}$ and $(R_3R_1R_2)^4 = 1$ we have

$$\begin{aligned} (P^{-1}J)^2 &= (R_2^{-1}R_1^{-1}R_3^{-1}R_2^{-1}R_1^{-1}R_3^{-1})^2 \\ &= (R_3R_1R_2)^{-4} \\ &= 1. \end{aligned}$$

Next, using $J = R_1^{-1}R_3^{-1}R_2^{-1}R_1^{-1}$ and $J^{-1} = R_2R_3R_1R_2$ we have

$$JR_1J^{-1} = R_1^{-1}R_3^{-1}R_2^{-1}R_1^{-1}R_1R_2R_3R_1R_2 = R_2.$$

Using $R_1R_2R_1 = R_2R_1R_2$ we have

$$PR_1P^{-1} = R_1R_2R_1R_2^{-1}R_1^{-1} = R_2.$$

Finally, $J = R_1^{-1}R_3^{-1}R_2^{-1}R_1^{-1} = R_2^{-1}R_1^{-1}R_3^{-1}R_2^{-2} = R_3^{-1}R_2^{-1}R_1^{-1}R_3^{-1}$ and $(R_1R_2R_3)^4 = 1$ give

$$\begin{aligned} J^3 &= (R_3^{-1}R_2^{-1}R_1^{-1}R_3^{-1})(R_2^{-1}R_1^{-1}R_3^{-1}R_2^{-2})(R_1^{-1}R_3^{-1}R_2^{-1}R_1^{-1}) \\ &= (R_1R_2R_3)^4 \\ &= 1. \end{aligned}$$

□

The following corollary generalises Corollary 5.13 of [7]. It shows that Γ has a very similar presentation to the Mostow groups [13], [4] with, in Mostow's notation, $\rho = 2$, $\sigma = n$, $t = (n+2)/2n$ and $\mu = -1$. Indeed, in the next section we will show that when $n = 5$ the group Γ actually appears on Mostow's list.

Corollary 5.6 *Suppose R_1, R_2 and R_3 satisfy the relations of Theorem 5.1 (iii). Let $s = n$ if n is not divisible by 3 and let $s = n/3$ if n is divisible by 3. Then $(R_3R_2R_1)^{2s} = 1$.*

PROOF: Using just the braid relations we see that $R_2(R_3R_2R_1)^2 = (R_3R_2R_1)^2R_2$. Thus we have

$$\begin{aligned} (R_3R_2R_1)^{2s} &= R_2^{3s}(R_3R_2R_1)^{2s} \\ &= (R_2^3R_3R_2R_1R_3R_2R_1)^s \\ &= (R_2R_3R_2R_3R_1R_3R_1R_2R_1)^s \\ &= \big(R_1^{-1}R_3^{-1}(R_3R_1R_2R_3)R_2R_3R_1(R_3R_1R_2R_3)R_3^{-1}R_1\big)^s \\ &= R_1^{-1}\big(R_3^{-1}(R_1R_2R_3R_1)R_2R_3R_1(R_2R_3R_1R_2)R_3^{-1}\big)^s R_1 \\ &= R_1^{-1}R_3^{-3s}R_1 \\ &= 1. \end{aligned}$$

The only relations we have used are the braid relations, $R_2^{3s} = R_3^{3s} = 1$, $(R_1R_2R_3)^4 = 1$ and

$$R_1R_2R_3R_1 = R_2R_3R_1R_2 = R_3R_1R_2R_3.$$

□

6 The cases $n = 5$ and $n = 6$

In this section we explain how to modify the construction given in the previous sections to the case where $n = 5$ and $n = 6$. In fact in these cases the construction is easier and we leave the details as an exercise for the reader. Moreover, we show that both these groups are (up to conjugacy) the same as other groups with a known fundamental polyhedron and presentation. Thus, in the cases of $n = 5$ and $n = 6$, an explicit construction of a fundamental domain is not as interesting as the case $n \geq 7$. In both cases we could deduce discreteness from the criteria of Mostow [14] and Thurston [21].

6.1 The case $n = 6$: the Eisenstein-Picard modular group

In this case $\cos\theta = 1/2$ and so it is easy to see that $\mathbf{z}_3$, $\mathbf{z}_4$ and $\mathbf{z}_5$ are all the same point. This point is $\mathbf{z}_0$ given by (21), that is it has coordinates $z_1 = w_1 = 1$ and $z_2 = w_2 = 0$. As the Hermitian form H has now become

$$H = -\sqrt{3}\begin{bmatrix} 1 & 0 & 0 \\ 0 & \frac{1}{2} & 0 \\ 0 & 0 & -1 \end{bmatrix}$$

we see that $\mathbf{z}_3 = \mathbf{z}_4 = \mathbf{z}_5$ is on the ideal boundary of $\mathbf{H}^2_{\mathbb{C}}$. This point is a vertex of D and is fixed by the map P, which is now parabolic. In fact $\mathbf{z}_0$ is a cusp of Γ.

Consider the Cayley transform C where

$$C = \begin{bmatrix} \frac{1}{2} & 0 & \frac{1}{2} \\ 0 & \frac{-1-i\sqrt{3}}{2} & 0 \\ \frac{1}{2} & 0 & -\frac{1}{2} \end{bmatrix}.$$

Then $\frac{-2}{\sqrt{3}}C^*HC$ is the Hermitian form used in [7] and $C^{-1}PC$, $C^{-1}R_1C$ and $-C^{-1}I_1C$ are the generators P, QP^{-1} and R for the Eisenstein-Picard modular group $\mathrm{PU}\big(2,1;\mathbb{Z}\big[\frac{-1+i\sqrt{3}}{2}\big]\big)$ given there. This proves:

Proposition 6.1 *When $n = 6$ the Livné group Γ is conjugate to the Eisenstein-Picard modular group.*

Discreteness of Γ follows immediately from this result. We now give a sketch of how to modify the arguments of Section 4 to construct a fundamental polyhedron. First, we could modify our version of Poincaré's theorem to include the possibility of ideal vertices (by introducing consistent horospheres; see [6]). By doing this we could mimic the construction of Section 4 to show that Γ is discrete and has a presentation (19) but without the relation $P^{3d} = 1$ (since the face F_{345} has now degenerated to an ideal vertex, there is no cycle relation). Omitting this relation corresponds to the fact that d is infinite when $n = 6$. Using (the modified version of) Poincaré's theorem, we can show that Γ has the presentation given in Theorem 5.1 (ii) with $n = 6$ and $d = \infty$. This is the same as the presentation of the Eisenstein-Picard modular group given in Theorem 5.11 of [7]. Thus our construction gives a new fundamental domain for $\mathrm{PU}\big(2,1;\mathbb{Z}\big[\frac{-1+i\sqrt{3}}{2}\big]\big)$. It has more sides than that given in [7], but has the advantage that all sides are contained in bisectors.

6.2 The case $n = 5$: a Mostow group

When $n = 5$ the face $F_{345} = S_{13} \cap S_{24}$ collapses to a vertex inside $\mathbf{H}^2_{\mathbb{C}}$. Thus when $n = 5$ all eight faces are solid tetrahedra. As indicated in Section 3.2 the new vertex corresponds to $\mathbf{z}_0$ given by (21), that is $z_1 = w_1 = 1$ and $z_2 = w_2 = 0$. In particular, we again do not obtain a cycle transformation for $S_{13} \cap S_{24}$ from Poincaré's theorem. This means that the presentation coming from Poincaré's theorem does not contain relation $P^{30} = 1$, as predicted above. We now show that, in fact, this relation follows from the other relations and so may be omitted from the presentation:

Lemma 6.2 *If $R_1^5 = R_2^5 = 1$ and $R_1R_2R_1 = R_2R_1R_2$ then $(R_1R_2)^{30} = 1$.*

PROOF: First observe that use of $R_1^5 = 1$ and the braid relation $R_1R_2R_1 = R_2R_1R_2$ gives

$$\begin{aligned}(R_1^{-2})R_2(R_1^2) &= R_1^3R_2R_1^2R_2R_2^{-1} \\ &= R_1^2R_2R_1R_2R_1R_2R_2^{-1} \\ &= R_1R_2R_1R_2R_1R_2R_1R_2^{-1} \\ &= (R_1R_2)^3(R_1R_2^{-1}).\end{aligned}$$

The braid relation also yields $(R_1R_2)^3(R_1R_2^{-1}) = (R_1R_2^{-1})(R_1R_2)^3$ and $(R_1R_2)^3 = (R_2R_1)^3$. Therefore

$$\begin{aligned}(R_1R_2)^{30} &= (R_1R_2)^{15}(R_1R_2^{-1})^5(R_2R_1^{-1})^5(R_2R_1)^{15} \\ &= \big((R_1R_2)^3(R_1R_2^{-1})\big)^5\big((R_2R_1)^3(R_2R_1^{-1})\big)^5 \\ &= (R_1^{-2}R_2R_1^2)^5(R_2^{-2}R_1R_2^2)^5 \\ &= R_1^{-2}R_2^5R_1^2R_2^{-2}R_1^5R_2^2 \\ &= 1.\end{aligned}$$

□

We now show that Γ is one of the groups constructed by Mostow in [13]. This is a special case of the theorem in Section 4 of [14]. Deraux, Falbel and Paupert [4] have constructed a simple fundamental domain for each of Mostow's groups (and hence for Γ). Their domain is a polyhedron with ten sides, not all of which are contained in bisectors. Using Mostow's notation; see Table 2 on page 248 of [13], we have:

Proposition 6.3 *When $n = 5$ the Livné group Γ is conjugate to the Mostow group with $p = 5$, $\rho = 2$, $\sigma = 5$, $t = 7/10$, $r = 2$, $s = 5$ and $\mu = -1$.*

PROOF: Putting these parameter values into Theorem 20.1 of [13] the group in question satisfies the relations

$$\begin{aligned}\mathcal{R}' &= \big\{R_j^5 = 1, \quad R_jR_kR_j = R_kR_jR_k, \quad (R_1R_2R_3)^4 = 1, \quad (R_3R_2R_1)^{10} = 1 \ : \ j,k = 1,2,3\big\} \\ \mathcal{R}'' &= \big\{(R_1R_2R_3)^{-2}R_1R_2 = (R_2R_3R_1)^{-2}R_2R_3\big\}\end{aligned}$$

The presentation in Theorem 5.1 (iii) has all these relations except $(R_3R_2R_1)^{10} = 1$, which follows from the others by Corollary 5.6. In addition the presentation in Theorem 5.1 (iii) includes the relation $(R_jR_k)^{30} = 1$ which follows from the others by Lemma 6.2.

Thus the two groups have the same presentation. Since this means that they are isomorphic, by Mostow rigidity, they must be conjugate. □

We could give a Cayley transform conjugating our R_1, R_2, R_3 to those given by Mostow on page 214 of [13] (or in [4]). Livné also gives matrices for the case $n = 5$. We could similarly find a Cayley transform conjugating I_1, $Q = R_1R_2R_1$ and R_1 to the matrices A, y and z given in Theorem 10 on page 111 of [12]. We leave both these calculations for the reader.

7 The triangle groups

Define $I_2 = JI_1J^{-1}$, $I_3 = J^{-1}I_1J$ and consider the group Δ generated by I_1, I_2 and I_3. To that end, we consider the presentation Theorem 5.1 (i). Thus, using $P = JI_1$, we have

$$I_2I_3I_1 = (JI_1J^{-1})(J^{-1}I_1J)I_1 = (JI_1)^3 = P^3,$$

compare Lemma 3.1 (3) of [19]. Moreover, we also have the following relations, which are (R4) on page 108 of [12]:

Lemma 7.1 *We have*

$$\begin{array}{lll} PI_1P^{-1} = I_2, & PI_2P^{-1} = I_2I_3I_2, & PI_3P^{-1} = I_2I_1I_2, \\ QI_1Q^{-1} = I_2, & QI_2Q^{-1} = I_2I_3I_1I_3I_2, & QI_3Q^{-1} = I_2I_3I_2. \end{array}$$

PROOF: Using $P = JI_1$ and $JI_kJ^{-1} = I_{k+1}$ for $k = 1, 2, 3 \pmod 3$, we have

$$PI_kP^{-1} = JI_1I_kI_1J^{-1} = (JI_1J^{-1})(JI_kJ^{-1})(JI_1J^{-1}) = I_2I_{k+1}I_2.$$

In particular, when $k = 1$ we have $PI_1P^{-1} = I_2^3 = I_2$.
Using $P^{-1}QI_1 = I_1P^{-1}Q$ we have

$$QI_1Q^{-1} = P(P^{-1}QI_1Q^{-1}P)P^{-1} = PI_1P^{-1} = I_2.$$

Next using $Q^2 = P^3 = I_2I_3I_1$ we have

$$QI_2Q^{-1} = Q^2(Q^{-1}I_2Q)Q^{-2} = (I_2I_3I_1)I_1(I_1I_3I_2) = I_2I_3I_1I_3I_2.$$

Finally using $Q^2 = I_2I_3I_1$, $QI_1 = I_2Q$ and $Q^{-1}I_2I_3I_1I_3I_2Q = I_2$ gives

$$\begin{aligned} QI_3Q^{-1} &= Q^{-1}Q^2I_3QQ^{-2} \\ &= Q^{-1}I_2I_3I_1I_3QI_1I_3I_2 \\ &= Q^{-1}I_2I_3I_1I_3I_2QI_3I_2 = I_2I_3I_2. \end{aligned}$$

□

The relations PI_jP^{-1} should be compared to Lemma 3.1 of [19]. An immediate consequence of Lemma 7.1 is:

Corollary 7.2 *The group $\Delta = \langle I_1, I_2, I_3\rangle$ is a normal subgroup of Γ with quotient group $\Upsilon = \Gamma/\Delta$ given by*

$$\Upsilon = \langle P, Q \ : \ P^3 = Q^2 = (P^{-1}Q)^n = 1\rangle.$$

PROOF: It is clear that Δ is a normal subgroup of Γ. Also $P^3 = Q^2 = I_2I_3I_1 \in \Delta$. Setting $I_1 = 1$ in the presentation of Theorem 5.1 (i) immediately gives the presentation for Υ given above.
□

The following proposition follows from Lemma 7.1. Alternatively, it could be proved from the presentations of Theorem 5.1.

Proposition 7.3 *The maps I_1I_2, I_2I_3 and I_3I_1 are each elliptic of order n.*

Proof: We claim that

$$R_1^j I_2 R_1^{-j} = (I_2I_3)^j I_2, \qquad R_1^j I_3 R_1^{-j} = (I_2I_3)^{j-1} I_2. \tag{36}$$

It is clear that these identities are true when $j = 0$. Using $R_1 = P^{-1}Q$, we have

$$\begin{aligned} R_1 I_2 R_1^{-1} &= P^{-1} Q I_2 Q^{-1} P \\ &= P^{-1} I_2 I_3 I_1 I_3 I_2 P \\ &= (P^{-1} I_2 I_3 I_2 P)(P^{-1} I_2 I_1 I_2 P)(P^{-1} I_2 I_3 I_2 P) \\ &= I_2 I_3 I_2, \\ R_1 I_3 R_1^{-1} &= P^{-1} Q I_3 Q^{-1} P \\ &= P^{-1} I_2 I_3 I_2 P \\ &= I_2. \end{aligned}$$

In particular, $R_1 I_2 I_3 R_1^{-1} = I_2 I_3$.

Therefore, by induction we have

$$\begin{aligned} R_1^{j+1} I_2 R_1^{-j-1} &= R_1 (I_2I_3)^j I_2 R_1^{-1} = (I_2I_3)^j I_2 I_3 I_2 = (I_2I_3)^{j+1} I_2, \\ R_1^{j+1} I_3 R_1^{-j-1} &= R_1 (I_2I_3)^{j-1} I_2 R_1^{-1} = (I_2I_3)^{j-1} I_2 I_3 I_2 = (I_2I_3)^j I_2. \end{aligned}$$

This proves (36). Putting $j = n$ in (36) and using $R_1^n = 1$ we have $I_2 = R_1^n I_2 R_1^{-n} = (I_2I_3)^n I_2$. Thus $(I_2I_3)^n = 1$. Conjugating by J we find $(I_1I_2)^n = (I_3I_1)^n = 1$. □

An immediate consequence of Proposition 7.3 is that, since $I_j^2 = (I_jI_k)^n = 1$, the group $\Delta = \langle I_1, I_2, I_3 \rangle$ is a representation of an (n, n, n) reflection triangle group; see [17] or [20] for example. As explained in Proposition 1 of [17] (see also [2]) there is a one real parameter family of such representations. In fact, since $QI_3I_1Q^{-1} = I_2I_3I_2I_1$ we see that $(I_jI_kI_jI_l)^n = 1$ and so, using the language of [20], Δ is a representation of type $\rho_n\big(\Gamma(n, n, n)\big)$, compare Theorem 4.7 of [20] for example. In order to see the geometry of triangle group Δ observe that I_1 fixes the complex line with $z_1 = 0$. This is the complex line spanned by $\mathbf{z}_7$ and $\mathbf{z}_8$ (and containing $\mathbf{z}_1$); see Figure 11. Then I_2 fixes the image of this complex line under J, that is the complex line spanned by $\mathbf{z}_6$ and $\mathbf{z}_8$ (and containing $\mathbf{z}_2$). This complex line is given by $w_1 = 0$. Finally, I_3 fixes the complex line spanned by $\mathbf{z}_6$ and $\mathbf{z}_7$. Thus these three complex lines may be thought of as the complexification of the boundary of $F_{678} = S_{16} \cap S_{27}$.

The following corollary follows immediately from the fact that Υ is finite when $n = 5$ and infinite when $n \geq 6$. It should be viewed in the context of representations of reflection triangle groups considered in [20]. We use Bowditch's criteria for geometrical finiteness in variable negative curvature [1], in particular F5 that says that a group is geometrically finite if and only if there is a bound on the orders of finite subgroups and the volume of the compact core of the quotient manifold is finite.

Corollary 7.4 *(i) When $n = 5$ the group $\Delta = \rho_5\big(\Gamma(5, 5, 5)\big)$ is a lattice.*

(ii) When $n = 6, 7, 8, 9, 10, 12, 18$ the group $\Delta = \rho_n\big(\Gamma(n, n, n)\big)$ is a finitely generated, geometrically infinite, discrete subgroup of PU(1, 2).

PROOF: The group Δ is a subgroup of the discrete group Γ and so is itself discrete.

When $n = 5$ we see that Δ is a subgroup of Γ of index 60 (the order of Υ in this case). Thus Δ is also a lattice.

Since Υ is an infinite group when $n = 6, 7, 8, 9, 10, 12, 18$, we see that in these cases Δ has infinite index in Γ. Moreover, since Δ is normal in Γ they have the same limit set, which is the whole of $\partial\mathbf{H}^2_{\mathbb{C}}$, since Γ is a lattice. A fundamental domain for Δ is the union of all Υ-images of the polyhedron D and so has infinite volume. Since the limit set is the whole of $\partial\mathbf{H}^2_{\mathbb{C}}$, this means the convex hull of the limit set is all of $\mathbf{H}^2_{\mathbb{C}}$. Hence the convex core of $\mathbf{H}^2_{\mathbb{C}}/\Delta$ is just $\mathbf{H}^2_{\mathbb{C}}/\Delta$, which has infinite volume. Using Bowditch's condition F5 we see that Δ is geometrically infinite. □

In fact Corollary 7.4 (ii) appears in Kapovich [11] using an identical proof. Also, Corollary 7.4 (i) should be compared to a recent result of Deraux [5], who considers $\rho_5\big(\Gamma(4, 4, 4)\big)$, that is the representation of the (4, 4, 4) reflection triangle group for which $I_jI_kI_jI_l$ has order 5. Deraux shows that this group is also a lattice.

Following Schwartz, a reflection triangle groups is said to be of *type A* if there are some parameter values where $I_jI_kI_jI_l$ is elliptic and $I_jI_kI_l$ is non-elliptic and of *type B* if there are some parameter values where $I_jI_kI_l$ is elliptic and $I_jI_kI_jI_l$ is non-elliptic. A short calculation from Pratoussevitch's formulae [17] shows that the (n, n, n) triangle group is of type A when $n \leq 10$ and type B when $n \geq 11$. Schwartz has conjectured (Conjecture 5.3 of [20]) that the only infinite, discrete representations of triangle groups of type B are faithful. When $n = 12$ or $n = 18$ our groups Δ give counterexamples to this conjecture (and $n = 18$ also seems to contradict Schwartz' computer experiments mentioned in Section 1.2 of [19]):

Proposition 7.5 *When $n = 12$ or $n = 18$ the group Δ is a discrete, non-faithful triangle group of type B.*

A Appendix: Bisector intersections

In this section we find the intersection of each pair of bisectors of the form B_{1j} and B_{2k}.

Proposition A.1 *Suppose that $\mathbf{z} \in B_{13} \cap B_{24}$. Then writing $z_1 = x$ and $w_1 = u$ we either have*

$$x = u = \frac{1-\cos\theta}{\cos\theta}, \qquad w_2 = e^{i\theta}\,\frac{2\cos\theta - 1 - z_2\cos\theta}{\cos\theta(1 - z_2\cos\theta)}$$

or else

$$\begin{aligned} z_2 &= e^{i\theta}\,\frac{1-\cos\theta - u + xu\cos\theta - (x-u)i\sin\theta}{1-\cos\theta - u\cos\theta}, \\ w_2 &= \frac{1-\cos\theta - x + xu\cos\theta - (x-u)i\sin\theta}{1-\cos\theta - x\cos\theta}. \end{aligned}$$

PROOF: Substituting $z_1 = x$ and $w_1 = u$ in (9) gives

$$u = \frac{-xi\sin\theta - z_2e^{-i\theta}(1-\cos\theta) + 1 - \cos\theta}{-x\cos\theta - z_2e^{-i\theta}\cos\theta + 1 - i\sin\theta}.$$

It is easy to see that if $x = (1-\cos\theta)/\cos\theta$ then $u = (1-\cos\theta)/\cos\theta$ independent of z_2. In which case we obtain w_2 from (10). Otherwise, solving for z_2 gives

$$z_2 = e^{i\theta}\,\frac{1-\cos\theta - u + xu\cos\theta - (x-u)i\sin\theta}{1-\cos\theta - u\cos\theta}.$$

Similarly, substituting $z_1 = x$ and $w_1 = u$ in (11) and solving for w_2 gives

$$w_2 = \frac{1 - \cos\theta - x + xu\cos\theta - (x-u)i\sin\theta}{1 - \cos\theta - x\cos\theta}.$$

□

A similar argument yields:

Proposition A.2 *Suppose that* $\mathbf{z} \in B_{13} \cap B_{27}$*. Then writing* $z_1 = x$ *and* $w_1 = iv$ *we have*

$$\begin{aligned} z_2 &= e^{i\theta}\frac{1 - \cos\theta - v\sin\theta - iv - xi\sin\theta + xvi\cos\theta}{1 - \cos\theta - iv\cos\theta}, \\ w_2 &= \frac{1 - \cos\theta - x - v\sin\theta - xi\sin\theta + xvi\cos\theta}{1 - \cos\theta - x\cos\theta}. \end{aligned}$$

Applying ι to Proposition A.2 gives:

Proposition A.3 *Suppose that* $\mathbf{z} \in B_{16} \cap B_{24}$*. Then writing* $z_1 = iy$ *and* $w_1 = u$ *we have*

$$\begin{aligned} z_2 &= e^{i\theta}\frac{1 - \cos\theta - u + y\sin\theta + iu\sin\theta + iyu\cos\theta}{1 - \cos\theta - u\cos\theta}, \\ w_2 &= \frac{1 - \cos\theta + y\sin\theta - yi + ui\sin\theta + uyi\cos\theta}{1 - \cos\theta - iy\cos\theta}. \end{aligned}$$

Proposition A.4 *Suppose that* $\mathbf{z} \in B_{16} \cap B_{27}$*. Then writing* $z_1 = iy$ *and* $w_1 = iv$*, we have*

$$\begin{aligned} z_2 &= e^{i\theta}\frac{1 - \cos\theta + y\sin\theta - v\sin\theta - yv\cos\theta - iv}{1 - \cos\theta - iv\cos\theta}, \\ w_2 &= \frac{1 - \cos\theta + y\sin\theta - v\sin\theta - yv\cos\theta - iy}{1 - \cos\theta - iy\cos\theta}. \end{aligned}$$

Performing similar arguments but using (10) gives:

Proposition A.5 *Suppose that* $\mathbf{z} \in B_{13} \cap B_{26}$*. Then writing* $z_1 = x$ *and* $w_2 = ue^{i\theta}$*, we have*

$$\begin{aligned} z_2 &= e^{i\theta}\frac{\cos\theta - x\cos\theta - u + xu\cos\theta - i\sin\theta(1 - x - u)}{1 - u\cos\theta}, \\ w_1 &= \frac{1 - \cos\theta - x - ue^{i\theta}(1 - \cos\theta) + uxe^{i\theta}\cos\theta - xi\sin\theta}{-i\sin\theta - x\cos\theta}. \end{aligned}$$

Proposition A.6 *Suppose that* $\mathbf{z} \in B_{13} \cap B_{28}$*. Then writing* $z_1 = x$ *and* $w_2 = u$*, we have*

$$\begin{aligned} z_2 &= e^{i\theta}\frac{1 - x - u + xu\cos\theta + ui\sin\theta}{\cos\theta - u\cos\theta + i\sin\theta}, \\ w_1 &= \frac{1 - \cos\theta - x - u(1 - \cos\theta) + xu\cos\theta - xi\sin\theta}{-i\sin\theta - x\cos\theta}. \end{aligned}$$

Proposition A.7 *Suppose that* $\mathbf{z} \in B_{16} \cap B_{26}$*. Then writing* $z_1 = iy$ *and* $w_2 = ue^{i\theta}$*, we have*

$$\begin{aligned} z_2 &= e^{i\theta}\frac{\cos\theta - y\sin\theta - u - i\sin\theta - iy\cos\theta + iu\sin\theta + iyu\cos\theta}{1 - u\cos\theta}, \\ w_1 &= \frac{1 - \cos\theta + y\sin\theta - ue^{i\theta}(1 - \cos\theta) - iy + iyue^{i\theta}\cos\theta}{-i\sin\theta - iy\cos\theta}. \end{aligned}$$

Proposition A.8 *Suppose that* $\mathbf{z} \in B_{16} \cap B_{28}$*. Then writing* $z_1 = iy$ *and* $w_2 = u$*, we have*

$$\begin{aligned} z_2 &= e^{i\theta}\frac{1-u-iy+iu\sin\theta+iyu\cos\theta}{\cos\theta-u\cos\theta+i\sin\theta}, \\ w_1 &= \frac{1-\cos\theta+y\sin\theta-u(1-\cos\theta)-iy+iyu\cos\theta}{-i\sin\theta-iy\cos\theta}. \end{aligned}$$

Applying ι to the previous four propositions gives:

Proposition A.9 *Suppose that* $\mathbf{z} \in B_{17} \cap B_{24}$*. Then writing* $z_2 = x$ *and* $w_1 = u$*, we have*

$$\begin{aligned} z_1 &= \frac{1-\cos\theta-xe^{-i\theta}(1-\cos\theta)-u+xue^{-i\theta}\cos\theta+ui\sin\theta}{i\sin\theta-u\cos\theta}, \\ w_2 &= \frac{\cos\theta-x-u\cos\theta+xu\cos\theta+i\sin\theta(1-x-u)}{1-x\cos\theta}. \end{aligned}$$

Proposition A.10 *Suppose that* $\mathbf{z} \in B_{18} \cap B_{24}$*. Then writing* $z_2 = xe^{i\theta}$ *and* $w_1 = u$*, we have*

$$\begin{aligned} z_1 &= \frac{1-\cos\theta-x(1-\cos\theta)-u+xu\cos\theta+ui\sin\theta}{i\sin\theta-u\cos\theta}, \\ w_2 &= \frac{1-x-u+xu\cos\theta-xi\sin\theta}{\cos\theta-x\cos\theta-i\sin\theta}. \end{aligned}$$

Proposition A.11 *Suppose that* $\mathbf{z} \in B_{17} \cap B_{27}$*. Then writing* $z_2 = x$ *and* $w_1 = iv$*, we have*

$$\begin{aligned} z_1 &= \frac{1-\cos\theta-xe^{-i\theta}(1-\cos\theta)-v\sin\theta-iv-ixve^{-i\theta}\cos\theta}{i\sin\theta-iv\cos\theta}, \\ w_2 &= \frac{e^{i\theta}-x-ix\sin\theta-ive^{i\theta}+ixv\cos\theta}{1-x\cos\theta}. \end{aligned}$$

Proposition A.12 *Suppose that* $\mathbf{z} \in B_{18} \cap B_{27}$*. Then writing* $z_2 = xe^{i\theta}$ *and* $w_1 = iv$*, we have*

$$\begin{aligned} z_1 &= \frac{1-\cos\theta-x(1-\cos\theta)-v\sin\theta-iv+ixv\cos\theta}{i\sin\theta-iv\cos\theta}, \\ w_2 &= \frac{1-x-ix\sin\theta-iv+ixv\cos\theta}{\cos\theta-x\cos\theta-i\sin\theta}. \end{aligned}$$

Likewise:

Proposition A.13 *Suppose that* $\mathbf{z} \in B_{17} \cap B_{26}$*. Then writing* $z_2 = x$ *and* $w_2 = ue^{i\theta}$*, we have*

$$\begin{aligned} z_1 &= \frac{1-x-ue^{i\theta}+xu\cos\theta+iue^{i\theta}\sin\theta}{1-ue^{i\theta}\cos\theta}, \\ w_1 &= \frac{1-u-xe^{-i\theta}+xu\cos\theta-ixe^{-i\theta}\sin\theta}{1-xe^{-i\theta}\cos\theta}. \end{aligned}$$

Proposition A.14 *Suppose that* $\mathbf{z} \in B_{17} \cap B_{28}$*. Then writing* $z_2 = x$ *and* $w_2 = u$*, we have*

$$\begin{aligned} z_1 &= \frac{1-x-u+xue^{-i\theta}\cos\theta+iu\sin\theta}{1-u\cos\theta}, \\ w_1 &= \frac{e^{i\theta}-u-x+xu\cos\theta-ix\sin\theta}{e^{i\theta}-x\cos\theta}. \end{aligned}$$

Proposition A.15 *Suppose that* $\mathbf{z} \in B_{18} \cap B_{26}$*. Then writing* $z_2 = xe^{i\theta}$ *and* $w_2 = ue^{i\theta}$*, we have*

$$\begin{aligned} z_1 &= \frac{e^{-i\theta} - x - u + xu\cos\theta + iu\sin\theta}{\cos\theta - u\cos\theta - i\sin\theta}, \\ w_1 &= \frac{1 - x - u + xuE^{i\theta}\cos\theta - xi\sin\theta}{1 - x\cos\theta}. \end{aligned}$$

Proposition A.16 *Suppose that* $\mathbf{z} \in B_{18} \cap B_{28}$*. Then writing* $z_2 = xe^{i\theta}$ *and* $w_2 = u$*, we have*

$$\begin{aligned} z_1 &= \frac{1 - xe^{i\theta} - u + xu\cos\theta + ui\sin\theta}{1 - u\cos\theta}, \\ w_1 &= \frac{1 - x - ue^{-i\theta} + xu\cos\theta - ix\sin\theta}{1 - x\cos\theta}. \end{aligned}$$

B Appendix: Low dimensional intersection of sides

In this section we show that the intersection of each pair of sides not considered in Section 3.4 is one dimensional, indeed we show that it comprises arcs of the 1-skeleton of D. More precisely, we show that each of these intersections is one or two edges of D. Each edge of D is the intersection of at least three bisectors and is a geodesic segment between a pair of vertices. This section may be omitted by readers who are willing to believe that we enumerated all the faces of D in Section 3.4.

Proposition B.1 *If* $\mathbf{z} \in S_{13} \cap S_{24}$ *and* $z_1 \neq (1-\cos\theta)/\cos\theta$ *then* $\mathbf{z} \in \gamma_{58}$*.*

PROOF: As in Proposition A.1 set $z_1 = x$ and $w_1 = u$ where $0 \leq x,\ u < 1$. Using the expressions from Proposition A.1 we have

$$\begin{aligned} 0 \ \leq\ \mathrm{Im}\,(z_2) &= \frac{\sin\theta(1-u)(1-\cos\theta - x\cos\theta)}{1-\cos\theta - u\cos\theta}, \\ 0 \ \geq\ \mathrm{Im}\,(w_2e^{-i\theta}) &= \frac{-\sin\theta(1-x)(1-\cos\theta-u\cos\theta)}{1-\cos\theta - x\cos\theta}. \end{aligned}$$

Since $x < 1$ and $u < 1$ we see that $1-\cos\theta - x\cos\theta$ and $1 - \cos\theta - u\cos\theta$ have the same sign. Also

$$\begin{aligned} 0 \ \geq\ \mathrm{Im}\,(z_2e^{-i\theta}) &= \frac{-(x-u)\sin\theta}{1-\cos\theta-u\cos\theta}, \\ 0 \ \leq\ \mathrm{Im}\,(w_2) &= \frac{-(x-u)\sin\theta}{1-\cos\theta - x\cos\theta}. \end{aligned}$$

Therefore $x = u$ and $\mathrm{Im}\,(z_2e^{-i\theta}) = \mathrm{Im}\,(w_2) = 0$. Hence $\mathbf{z} \in B_{18} \cap B_{28}$ as well. Using our table of edges we see that $\mathbf{z}$ lies in the geodesic containing γ_{58}. □

Proposition B.2 *If* $\mathbf{z} \in S_{13} \cap S_{26}$ *then* $\mathbf{z} \in \gamma_{34} \cup \gamma_{47}$*.*

PROOF: Put $z_1 = x$ and $w_2 = ue^{i\theta}$ where $0 \leq x < 1$ and $0 \leq u < 1/\cos\theta$. Using the expressions of Proposition A.5 we see that

$$0 \leq \mathrm{Im}\,(w_1) = \frac{\sin\theta(1-\cos\theta - x\cos\theta)(1-x)(1-u\cos\theta)}{\sin^2\theta + x^2\cos^2\theta}.$$

Thus $x \leq (1-\cos\theta)/\cos\theta$. Also

$$0 \leq \mathrm{Im}\,(z_2) = \frac{-u\sin\theta(1-\cos\theta - x\cos\theta)}{1-u\cos\theta}.$$

Since $1-u\cos\theta > 0$ we either have $u=0$ or else $x=(1-\cos\theta)/\cos\theta$.

If $u=0$ we have $\mathbf{z} \in B_{17}\cap B_{28}$ as well. Since $0 \leq x \leq (1-\cos\theta)/\cos\theta$, then from our table of edges we see that $\mathbf{z}\in\gamma_{47}$.

If $x=(1-\cos\theta)/\cos\theta$ then $\mathbf{z}\in B_{17}\cap B_{24}$. Moreover, $z_2 = (2\cos\theta - 1 - u)/(\cos\theta - u\cos^2\theta)$ and so $u \leq 2\cos\theta - 1$. Hence $\mathbf{z}\in\gamma_{34}$. □

Applying ι we immediately have

Proposition B.3 *If* $\mathbf{z}\in S_{17}\cap S_{24}$ *then* $\mathbf{z}\in\gamma_{34}\cup\gamma_{36}$.

Similarly,

Proposition B.4 *If* $\mathbf{z}\in S_{16}\cap S_{24}$ *then* $\mathbf{z}\in\gamma_{68}$.

PROOF: As in Proposition A.3, set $z_1 = iy$ and $w_1 = u$ where $-\sin\theta/\cos\theta < y \leq 0$ and $u \geq 0$. Using Lemma 3.6 we have

$$\frac{1}{\cos\theta} > \mathrm{Re}\,(z_2e^{i\theta}) = \frac{1}{\cos\theta} - \frac{(1-\cos\theta)^2 - y\sin\theta\cos\theta}{\cos\theta(1-\cos\theta-u\cos\theta)}.$$

Since $(1-\cos\theta)^2 - y\sin\theta\cos\theta > 0$ we must have $1-\cos\theta - u\cos\theta > 0$. Because $\mathbf{z}$ is in D we have

$$0 \geq \mathrm{Im}\,(z_2e^{-i\theta}) = \frac{u(\sin\theta + y\cos\theta)}{1-\cos\theta-u\cos\theta}$$

and since $y > -\sin\theta/\cos\theta$ we see that $u=0$.

Substituting $u=0$ into the expression from Proposition A.3 we have

$$\begin{aligned} z_2 &= \frac{e^{i\theta}(1-\cos\theta - y\sin\theta)}{1-\cos\theta}, \\ w_2 &= \frac{1-\cos\theta + y\sin\theta - iy}{1-\cos\theta - iy\cos\theta}. \end{aligned}$$

Thus

$$0 \leq \mathrm{Re}\,(z_2e^{-i\theta}) = \frac{1-\cos\theta+y\sin\theta}{1-\cos\theta}.$$

Hence $-(1-\cos\theta)/\sin\theta \leq y \leq 0$. When $y = -(1-\cos\theta)/\sin\theta$ this point is $\mathbf{z}_6$ and when $y=0$ it is $\mathbf{z}_8$. The result follows. □

Applying ι, we have

Proposition B.5 *If* $\mathbf{z}\in S_{13}\cap S_{27}$ *then* $\mathbf{z}\in\gamma_{78}$.

Proposition B.6 *If* $\mathbf{z}\in S_{16}\cap S_{28}$ *then* $\mathbf{z}\in\gamma_{78}$.

PROOF: As in Proposition A.8 set $z_1 = iy$ and $w_2 = u$ where $-\sin\theta/\cos\theta < y \leq 0$ and $0 \leq u \leq 1/\cos\theta$. Then

$$0 \leq \mathrm{Re}\,(w_1) = \frac{y(1-u\cos\theta)}{\sin\theta + y\cos\theta}.$$

Since $1-u\cos\theta$ and $\sin\theta + y\cos\theta$ are both positive, we must have $y=0$.

Substituting $y=0$ into the expressions for z_2 and w_1 from Proposition A.8 gives

$$\begin{aligned} z_2 &= \frac{e^{i\theta}(1-u+iu\sin\theta)}{\cos\theta - u\cos\theta + i\sin\theta}, \\ w_1 &= \frac{i(1-\cos\theta)(1-u)}{\sin\theta}. \end{aligned}$$

Since $\mathrm{Im}\,(w_1) \geq 0$ we have $u \leq 1$. When $u=0$ this point is $\mathbf{z}_7$ and when $u=1$ it is $\mathbf{z}_8$. □

Applying ι gives

Proposition B.7 *If* $\mathbf{z} \in S_{18} \cap S_{27}$ *then* $\mathbf{z} \in \gamma_{68}$.

Proposition B.8 *If* $\mathbf{z} \in S_{16} \cap S_{26}$ *then* $\mathbf{z} \in \gamma_{67}$.

PROOF: As in Proposition A.7 write $z_1 = iy$ and $w_2 = ue^{i\theta}$ where $-\sin\theta/\cos\theta < y \leq 0$ and $0 \leq u < 1/\cos\theta$. Then

$$\begin{aligned} 0 \ \leq \ \mathrm{Im}\,(z_2) &= \frac{-u(1-\cos\theta)\sin\theta - y(1-u\cos^2\theta)}{1-u\cos\theta}, \\ 0 \ \leq \ \mathrm{Re}\,(w_1) &= \frac{u(1-\cos\theta)\sin\theta + y(1-u\cos^2\theta)}{\sin\theta + y\cos\theta}. \end{aligned}$$

Since $1-u\cos\theta > 0$ and $\sin\theta + y\cos\theta > 0$ we must have

$$y = \frac{-u(1-\cos\theta)\sin\theta}{1-u\cos^2\theta}.$$

Hence $\mathrm{Im}\,(z_2) = \mathrm{Re}\,(z_1) = 0$ so $\mathbf{z} \in B_{17} \cap B_{19}$ as well. Thus the intersection is certainly contained in the geodesic containing γ_{67}.

Substituting in the expression from Proposition A.7 we have

$$w_1 = \frac{i(1-\cos\theta)(1-u)}{\sin\theta}.$$

Since $\mathrm{Im}\,(w_1) \geq 0$ we have $u \leq 1$. When $u=0$ the point is $\mathbf{z}_7$ and when $u=1$ the point is $\mathbf{z}_6$. □

Applying ι gives

Proposition B.9 *If* $\mathbf{z} \in S_{17} \cap S_{27}$ *then* $\mathbf{z} \in \gamma_{67}$.

Proposition B.10 *If* $\mathbf{z} \in S_{17} \cap S_{28}$ *the* $\mathbf{z} \in \gamma_{47}$.

Proof: We write $z_2 = x$ and $w_2 = u$ where $0 \leq x, u < 1/\cos\theta$. Then using the expression from Proposition A.14 we have

$$0 \geq \mathrm{Im}\,(z_1) = \frac{u\sin\theta(1-x\cos\theta)}{1-u\cos\theta}.$$

Since $1-x\cos\theta > 0$ and $1-u\cos\theta > 0$ we must have $u=0$. Thus $\mathbf{z} \in B_{13} \cap B_{26}$ as well. Moreover, putting $u=0$ gives $z_1 = 1-x$ and so $x \leq 1$. Hence $\mathbf{z} \in \gamma_{47}$ as claimed. □

Applying ι gives

Proposition B.11 *If* $\mathbf{z} \in S_{18} \cap S_{26}$ *the* $\mathbf{z} \in \gamma_{36}$.

Finally,

Proposition B.12 *If* $\mathbf{z} \in S_{18} \cap S_{28}$ *the* $\mathbf{z} \in \gamma_{58}$.

Proof: We write $z_2 = xe^{i\theta}$ and $w_2 = u$ where $0 \leq x, u < 1/\cos\theta$. Using the formulae from Proposition A.16 we have

$$\begin{aligned} 0 &\geq \mathrm{Im}\,(z_1) = \frac{-(x-u)\sin\theta}{1-u\cos\theta}, \\ 0 &\leq \mathrm{Im}\,(w_1) = \frac{-(x-u)\sin\theta}{1-x\cos\theta}. \end{aligned}$$

Since $1-x\cos\theta > 0$ and $1-u\cos\theta > 0$ we must have $u = x$. Thus $\mathbf{z} \in B_{13} \cap B_{24}$. This gives $z_1 = w_1 = 1-x$ and so the result follows from Proposition A.1. □

References

[1] B.H. Bowditch; *Geometrical finiteness with variable negative curvature*. Duke Math. J **77** (1995), 229–274.

[2] U. Brehm; *The shape invariant of triangles and trigonometry in two-point homogeneous spaces*. Geometriae Dedicata **33** (1990) 59–76.

[3] P. Deligne & G.D. Mostow; Commensurability Among Lattices in PU$(1, n)$. Annals of Maths. Studies **132**, Princeton University Press (1993).

[4] M. Deraux, E. Falbel & J. Paupert; *New constructions of fundamental polyhedra in complex hyperbolic space*. Acta Mathematica **194** (2005), 155–201.

[5] M. Deraux; *Deforming the* $\mathbb{R}$*-Fuchsian* $(4, 4, 4)$*-triangle group into a lattice*. Preprint, 2005.

[6] D.B.A. Epstein, C. Petronio; *An exposition of Poincaré's polyhedron theorem.* L'Enseignement Mathématique, **40** (1994), 113–170.

[7] E. Falbel & J.R. Parker; *The geometry of the Eisenstein-Picard modular group*. To appear in Duke Math. J.

[8] W.M. Goldman; Complex Hyperbolic Geometry. Oxford Mathematical Monographs. Oxford University Press (1999).

[9] F. Hirzebruch; *Arrangements of lines and algebraic surfaces*. Arithmetic and Geometry Vol II, 113–140, ed: M. Artin & J. Tate, Birkhäuser, 1983.

[10] Y. Jiang, S. Kamiya & J.R. Parker; *Jørgensen's inequality for complex hyperbolic space*. Geometriae Dedicata **97** (2003) 55–80.

[11] M. Kapovich; *On normal subgroups in the fundamental groups of complex surfaces*. Preprint, 1998.

[12] R.A. Livné; On Certain Covers of the Universal Elliptic Curve, Ph.D. Thesis, Harvard University, 1981.

[13] G.D. Mostow; *On a remarkable class of polyhedra in complex hyperbolic space*. Pacific J. Maths. **86** (1980), 171–276.

[14] G.D. Mostow; *Generalized Picard lattices arising from half-integral conditions*. Publ. Math. I.H.E.S. **63** (1986), 91–106.

[15] G.D. Mostow; *On discontinuous action of monodromy groups on the complex n-ball*. Journal of the A.M.S. **1** (1988), 555–586.

[16] J.R. Parker; *Unfaithful complex hyperbolic triangle groups*. Preprint, 2005.

[17] A. Pratoussevitch; *Traces in complex hyperbolic triangle groups*. Geometriae Dedicata **111** (2005), 159–185.

[18] J.K. Sauter; *Isomorphisms among monodromy groups and applications to lattices in* $\mathrm{PU}(1,2)$. Pacific J. Maths. **146** (1990), 331–384.

[19] R.E. Schwartz; *Real hyperbolic on the outside, complex hyperbolic on the inside*. Inventiones Math. **151** (2003), 221–295.

[20] R.E. Schwartz; *Complex hyperbolic triangle groups*. Proceedings of the International Congress of Mathematicians Vol II, 339–349, ed: T. Li, Beijing, 2002,

[21] W.P. Thurston; *Shapes of polyhedra and triangulations of the sphere*. Geometry and Topology Monographs **1** (1998), The Epstein Birthday Schrift, 511–549, ed: I. Rivin, C. Rourke & C. Series.

[22] M. Weber; *Fundamentalbereiche komplex hyperbolische Flächen*. Bonner Mathematische Schriften **254**, 1993.